R. & M. No. 2652
(11,036, 11,037, 11,038)
A.R.C. Technical Report

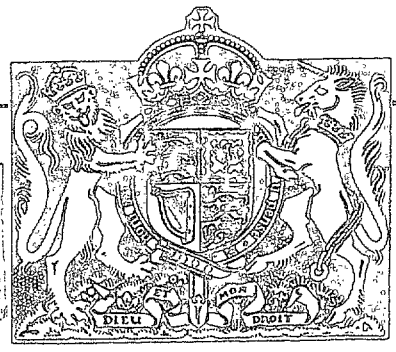

MINISTRY OF SUPPLY

AERONAUTICAL RESEARCH COUNCIL
REPORTS AND MEMORANDA

Investigation of Skin Buckling

By

D. J. FARRAR, M.A.,
of the Bristol Aeroplane Company, Limited

LONDON: HER MAJESTY'S STATIONERY OFFICE
1953
PRICE 17*s* 6*d* NET

Investigation of Skin Buckling

By

D. J. FARRAR, M.A.,
of the Bristol Aeroplane Company, Limited

COMMUNICATED BY THE PRINCIPAL DIRECTOR OF SCIENTIFIC RESEARCH (AIR),
MINISTRY OF SUPPLY

*Reports and Memoranda No. 2652**
October, 1947

This report on an Investigation of Skin Buckling was originally prepared by the Bristol Aeroplane Co. Ltd., as Report No. C.R.434 in October, 1945.

With their permission it is now reproduced in condensed form.

The test results are given in detail in S. & T. M. 12/47.

Summary.—(a) *Purpose of Investigation.*—The present tests were conducted on aluminium alloy plates in endwise compression, with varying conditions of edge support, to provide data on the buckling stress and post-buckling behaviour of aircraft skins.

(b) *Range of Investigation.*—All the plates tested were 35 in. long and nominally 0·064 in. thick. The plate width between the supports was varied between 35 and 120 times its thickness. Both clad (D.T.D. 546) and unclad (D.T.D. 646) material were tested. Three types of edge support were used: rows of steel balls in vee-grooved blocks, intended to imitate pin-edged conditions; rows of steel rollers in recessed blocks, intended to imitate clamp-edged conditions; and a single type of stringer used in previous panel tests.

Measurements were made of the plate load and mean strain, and of the shape of the skin buckles. The test technique is discussed and the experimental results compared with theory.

(c) *Conclusions.*—The ball edge supports did not accurately represent pin-edged conditions, neither did the roller edge supports accurately represent clamped-edged conditions. The tests provided some data on the effect of plasticity in seriously reducing the load carried by the plate after buckling, and on the effect of cladding in reducing the buckling stress.

The buckling stresses measured for the panels with stringer edge supports were in good agreement with theory. The load carried by the plate after buckling in this case was further reduced by the effect of plasticity in the stringers: a simplified theory is developed whose results are in agreement with the experimental observations.

(d) *Further Developments.*—The testing technique used is applicable to further investigations of the buckling of plates as part of a panel.

The information obtained on the effect of plasticity has an important bearing on the load-carrying capacity of panels, and while the present results may form the basis of design data sheets, it is desirable that the range of investigation be extended to cover other material specifications.

1. *Introduction.*—The present series of tests arose from some previous work (unpublished) which deals with tests on flat panels with Z-section stringers. The compressive stress at failure of these panels was lower than that predicted by theory, and one possible explanation was that the tangent stiffness of the skin was lower than expected. The main arguments developed in the previous report may be summarised as follows:—

(a) In the case of flexural instability, the tangent flexural stiffness EI is very dependent on the contribution of the skin to the moment of inertia.

* Bristol Aeroplane Report No. C.R.434, received 25th November, 1947. (Parts 1, 2 and 3 condensed into one single report).

(b) The $f_{average}$ vs. f_{edge} curves were deduced from the panel tests by finding the edge stress from the measured strain and material properties, and deducting the load carried by the stringers and edge members at this stress from the total load. The remaining load divided by the skin area yielded the average stress. It was found that the slope of the $f_{average}$ vs. f_{edge} curve fell off rapidly before failure.
This reduction in $\partial f_{average} / \partial f_{edge}$ would explain the premature failure in flexure.
The observation is, however, open to some doubt. If, because of local plasticity or large amplitudes in flexure, the edge stress was lower than that found from the mean strain, then the apparent $f_{average}$ found as above would be fictitiously low, and there would be a reduction in the gradient of the apparent $f_{average}$ vs. f_{edge} curve. To eliminate this doubt, more exact knowledge of the edge stress is necessary.

(c) It was, therefore, proposed that tests should be carried out on flat skins with simply supported and clamped edges and a range of b/t values.
It was decided to imitate simply supported edge conditions by means of steel balls located in vee grooves in a test rig. In order to imitate clamped edge conditions, the edge support was by steel rollers located in slots in the test rig.
The tests are supplemented by tests on panels with stringer edge supports, the stringers being identical with those of the panels previously tested.
All the tests were done in the 50-ton Avery universal hydraulic machine at the Structural Research Laboratory, Filton.

2. *Ball Edged Panels.*—2.1 *Description of Panels.*—All the panels tested were 35 in. long, and nominally 0·064 in. thick. The panels were designed to cover the following range:—

Clad material (D.T.D. 546)

Panel No.	1A	2A	3A	4A	5A	6A	7A	8A	19A*	20A*
b/t	35	40	45	55	65	80	100	120	55	65

Unclad material (D.T.D. 646)

Panel No.	1B	2B	3B	4B	5B	6B	7B	8B
b/t	35	40	45	55	65	80	100	120

The panels were cut from the same sheet of material, in each case, as the further panels 9A to 18A and 9B to 18B. The panels marked * were made from the same batch of material, and were intended for a special investigation of wave shape along the length of the panel.

The panels were cut accurately to the 35 in. length, and the ends filed flat, but the overall width was about $\frac{3}{4}$ in. greater than that corresponding to the specified b/t and the nominal thickness.

The thickness of each plate was measured at a number of points (five down each side of the plate) and the mean thickness determined. The width between ball centres was then chosen to give the correct b/t ratio.

The dimensions of the panels are summarised in Table 1, and the variation of thickness down the length in Table 2.

Before being set up in the testing machine, the panels were marked with grid lines symmetrical about the centre of the panel and extending over the length $3b$. In the case of panels 19A and 20A the grid extended over the whole length of the panel.

2.2. *Description of Test Rig.*—2.2.1. *Edge support.*—The test rig is shown on Sheet (2). The hardened steel balls, $\frac{1}{4}$ in. diameter, were located in 90 deg vee grooves in steel blocks. These blocks were bolted to robust side supports of rolled steel joist section. In order to prevent

the buckled plate from forcing apart the lines of balls on opposite faces, the blocks were bolted together by 2 B.A. bolts perpendicular to the plane of the plate and the points of the attachment to the side support reinforced with steel blocks.

The balls were intended to roll freely in a vertical direction, thus permitting unconstrained contraction of the plate. It was also expected that there would be little lateral constraint in the plane of the plate. The reinforcements were thus intended only to provide the maximum possible constraint normal to the plane of the plate.

The balls were 5/16 in. pitch, being separated by small rubber blocks. The choice of rubber for the blocks was governed by the fact that it was desirable to provide ball support as near the ends of the plate as possible, and if this were so and the panel contraction was considerable the top ball would come into contact with the headplate. In this case the additional load needed to compress the pile of rubber blocks would be negligible.

The method of adjustment was as follows: the side supports were placed some distance apart, and the balls and rubber blocks fed into the vee grooves with 16 S.W.G. Alclad strips in position to separate the two rows of balls. The panel was then inserted, pushing out the 16 S.W.G. strips, and the side supports moved laterally across the base plate until the desired value of b was obtained with the centroid of the panel on the axis of the loading machine. The side supports were then bolted down to the base plate.

The blocks with vee grooves were then adjusted. The bolts attaching them to the side supports were loosened, and the 2 B.A. bolts joining pairs of blocks gradually tightened until all the balls were in contact with the panel. The bolts on to the side supports were then also tightened.

2.2.2. *Loading platens.*—The lower end of the panel under test rested on the base plate of the testing machine. The upper end was loaded through a steel block bolted to the headplate of the machine. The lower side of the loading block was 0·25 in. thick and was machine planed and set up parallel to the baseplate.

This block made it possible to extend the vee grooved blocks and balls to the upper end of the panel, and to allow for 0·3 in. contraction in this condition.

2.2.3. *Measurement of skin buckles.*—The amplitude of buckling was measured by means of a 0·001-in. dial indicator. The indicator was arranged to be free to slide laterally on a cross-frame, which was itself free to slide vertically on edge runners attached to the edge support rig. The weight of the cross-frame and indicator was balanced by lead weights and wires running over pulleys.

The dial indicator being constrained to move in a plane parallel to the plane of the plate, it was possible to measure amplitudes at all nodes of the marked grid.

2.2.4. *Measurement of panel strain.*—The mean panel strain was measured by a special type of averaging contractometer. The simple type of contractometer is unsuitable for this type of panel for two reasons. Firstly, it is designed to pick up on both sides of a stringer web, and owing to the large edge supports it would be impossible to arrange this type of attachment in the present case. Secondly, the large deflections due to buckling would tend to tear out the attachment points of the contractometer if it were placed on the centre-line of the panel.

In the averaging contractometer, the contractometer rod is attached at the top to the mid-point of a lateral rod. This lateral rod has pick-up points at both ends, the distance apart of the pick-up points being adjustable to suit the width of the panel. The points are arranged to lie just inside the edge supports, where the amplitude of buckling is not large. A duplicate bar is arranged on the opposite side of the plate and the two bars are held together by means of a compression spring on a bar passing through a small hole in the plate. A similar lateral rod is attached to the lever at the bottom of the contractometer.

It is seen that the strain measured is the mean of the strains near the two edges of the panel.

2.2.5. *End dials.*—In order to supplement the contractometer readings, which tend to become unreliable at large strains, the relative movement of the headplate and baseplate was measured by dial indicators attached to the baseplate and picking up on the head plate. Two indicators were used, in the plane of the panel, one close to each edge support.

2.3. *Friction Tests.*—2.3.1. *Nature of friction present.*—Two types of friction can occur in tests of this sort. One is friction in the edge supports, in which case the panel at the upper end carries the full indicated load. Down the length of the panel, the balls will exert an upwards frictional force and the load in the panel will be reduced, the remainder of the load being carried by the side supports.

The other type involves friction between the loading ram and cylinder, and implies that the indicated load (measured by the pressure difference inside the cylinder) is not equal to the load on the platen, the difference being the frictional force between the piston and the cylinder.

It must be pointed out that this friction may be of either sign, depending on the nature of the loading (increasing or decreasing). Also, the friction may be expected to attain some maximum value and then remain constant.

2.3.2. *Standard test technique.*—It has been standard practice in all tests to apply a settling load of about 0·2 tons to each panel, reduce the indicated load to zero, and set the dial indicators to zero reading, then loading in increments. Accordingly any friction tests must provide a check on the conditions when this testing technique is used.

2.3.3. *Friction tests.*—A panel (Panel 10A) was set up with its lower surface about 0·1 in. clear of the baseplate. The vee blocks were arranged so that the ball supports were quite loose and free, the bolts joining the blocks being slack. The blocks were then bolted firmly to the side supports.

The contractometer was set to zero, and the rams extended until the headplate was just in contact with the top of the panel. The end dials were then set to zero. The load was increased and readings taken of the contractometer and end dials. At a negligible indicated load the panel began to slip, until the lower surface came into contact with the baseplate. Small increments of load (0·025 tons) were then applied up to 0·7 tons. The indicated load was then reduced to zero, and a second set of readings taken with load increasing up to 0·7 tons. This second loading run was representative of standard panel test conditions.

The friction test was repeated with the bolts normally tightened. Once again, slip occurred at a negligible indicated load.

2.3.4. *Discussion of results.*—From the contractometer reading the mean load in the panel has been deduced, assuming $E = 10{\cdot}7 \times 10^6$.

It is seen that on the initial loading the graph is very closely a straight line, of unit gradient, passing through the origin. It is concluded therefore that no friction was present either in the edge supports or the rams. On reducing to zero indicated load, there was a mean load in the panel of 0·23 tons in both sets of tests. As this load is independent of the edge support conditions, it follows that the load must be due to ram friction, which maintains the panel load even when the oil pressure difference has been reduced to zero. On increasing the pressure again, the mean load remained constant and there was no relative movement of the platens until an indicated load of 0·2 tons. The graph then followed once more the straight line of unit slope, passing through the origin.

2.3.5. *Conclusions.*—The friction at the ball edge supports is negligible.

When a settling load has been applied, there is a residual load in the panel due to ram friction. (This might be expected, since the ram is designed only for the outgoing stroke and it is quite likely that seals might tend to jam on the return stroke). This results in the initial portion of

the load *vs.* strain curve being vertical; a phenomenon observed many times before in panels tested in this machine.

In order to obtain the corrected strain, the straight line on the load *vs.* strain diagram must be extrapolated backwards and the vertical portion neglected. The friction can then be neglected, no correction to the load being necessary.

Note: As a result of this investigation, it is proposed that in future tests the platen should be taken clear after the settling load, and readings started when the platen just comes into contact again with the panel.

2.4. *Test Results.*—2.4.1. *Procedure.*—A settling load of about 0·2 tons was applied to each panel, the load reduced and the contractometer set to zero. Measurements of panel strain were made at load increments of about 0·1 tons. Measurements of skin buckling were made at increments of deflection of about 0·01 in. Loading was continued until considerable plastic flow took place, at a strain of about 0·006.

2.4.2. *Load* vs. *strain curves.*—The load *vs.* strain curves were plotted for clad panels, and for unclad panels.

2.4.3. *Buckle shape.*—The buckled shape is plotted for clad panels and for unclad panels. The readings were generally of amplitude down the centre-line over a length $3b$, 25 readings being taken over this length, and of amplitude across a section near a wave crest. In the case of Panels 19A and 20A the amplitudes down the centre-line were measured along the entire length of the panel.

No readings were taken of the initial shape of the panel, since this is modified by the supports at the edges. A reading of shape at low load is used instead.

Owing to the size of the edge supports it was not possible to take readings very near the edges of the panel.

2.5. *Analysis of Results.*—2.5.1. *Predicted behaviour with pinned edges.*—In R. & M. 1554, H. L. Cox has analysed the case of a flat plate whose edges are constrained normal to the plate, but are free to move in the plane of the plate. This analysis gives $K = 3{\cdot}62$, and $\partial f_{\text{average}} / \partial f_{\text{edge}} = \frac{1}{3}$ initially, the wave form being a double sine curve. An approximate investigation of the post-buckled state is made, and it is found that $\partial f_{\text{average}} / \partial f_{\text{edge}}$ falls and the cross-section of the wave has a flatter top with increasing strain.

In R. & M. 2178,* an investigation is made including higher order terms. For the case where the plate is free to move laterally at the edges, it is again found that $K = 3{\cdot}62$, but the initial value of $\partial f_{\text{average}} / \partial f_{\text{edge}}$ is found to be $0{\cdot}41$, a value which is exact.

As the edge stress approaches the plastic region, there will tend to be plastic flow in some parts of the panel where the stress resultants are large, and this will involve a change of wave shape and a reduction of $\partial f_{\text{average}} / \partial f_{\text{edge}}$. The onset of this effect can be predicted fairly accurately, but its nature and magnitude have not been determined theoretically.

In both analyses the initial buckling mode has a half wavelength equal to the panel width.

2.5.2. *Predicted behaviour of ball edged panel.*—It was evident from the inception of the tests, that ideal pinned or clamped edges could not be obtained in practice. The ball edges might be expected to offer negligible constraint in the plane of the plate, and their angular constraint at the edges must be small at any rate during the earlier stages of buckling. (During the late stages of buckling, owing to the slope of the plate at the edge, the points of contact with the balls tend to deviate from a straight line and the reaction between the balls and the plate cause a clamping effect.)

* *Theory of Flat Plates Buckled in Compression,* by W. S. Hemp.

Even assuming no constraint from the ball supports, the panel can still not be treated as pin edged at these supports. The perturbation is due to the strips of plate which must be present outside the ball supports. These strips, which for practical reasons are about 0·1 of the panel width, act as elastic angular constraints at the edges, and also provide some lateral constraint. The former affects the buckling stress while both affect the post-buckled behaviour.

In order to estimate the effect of the former on the buckling stress, an energy calculation has been made (*see* Appendix I). The results of this calculation give theoretical values of K which are plotted against the ratio c/b.

The effect of the constraints on the post-buckled behaviour of the plate has not been analysed theoretically.

Two other forms of constraint are present. One is that the panel is of finite length, and the half wavelength can not, in general, be equal to the panel width, but should be some fraction of the total length. This also implies that any tendency for the ends of the panel to be clamped, as would be the case for small amplitudes of a panel whose ends are accurately plane and parallel, will cause perturbation of the buckling stress and wave shape.

The ends of the panel, being in contact with the platens, are constrained against lateral expansion. There will therefore be a further perturbation extending from the panel ends, due to this lateral constraint.

2.5.3. *Experimental buckling stress coefficients.*—The buckling strain has been determined by two methods. One value of the strain is found from the load *vs.* strain diagram, being defined as the strain at which a sudden reduction in slope occurs. The other value of the buckling strain has been determined from the post-buckled amplitude. The square of the mean amplitude was plotted against the strain, and the graphs were substantially linear, the intercept on the strain axis being the buckling strain.

We know $$f_b = KE_T(t/b)^2$$

i.e., $$E_s e_b = KE_T(t/b)^2.$$

Hence, $$K = e_b(b/t)^2 \frac{E_s}{E_T}.$$

The values of K are summarised in Table 3, and are plotted against the theoretical values, defined by the ratio c/b. It is at once apparent that the experimental scatter is severe. The clad panels exhibit values of K about 15 per cent lower than the unclad panels, with the exception of those which buckled below 10,000 lb/sq in. in which there is agreement between the two sets of results. This is consistent with a reduction in buckling stress due to yielding of the cladding at stresses above 10,000 lb/sq in. Apart from this effect, there is fair agreement between the values of K observed and those found theoretically in section 2.5.2 and Appendix I.

2.5.4. *Amplitudes after buckling.*—In N.A.C.A., T.N. 752 a theoretical value is given for the amplitude after buckling

$$a^2 = \frac{4\lambda^2}{\pi^2} \frac{fe - f_b}{E}$$

i.e., $$a^2 = \frac{4\lambda^2}{\pi^2} (e - e_b).$$

This theoretical slope of the a^2 vs. e diagram is compared with the experimental values in Table 4: the values of λ chosen are the mean values observed.

2.5.5. *Wavelengths after buckling.*—The mean wavelength was plotted against the edge strain, and it was apparent that λ/b did not generally assume the value closest to 1·0

2.5.6. $f_{average}$ vs. f_{edge} *curves.*—The value of f_{edge} has been deduced from the strain, using the panel E in the elastic region. In the plastic region the curves have not been plotted out fully. It has been assumed that the strips outside the supports carry the full stress f_{edge}, and hence $f_{average}$ is deduced.

The theoretical value plotted for initial $\partial f_{average} / \partial f_{edge}$

is $$0{\cdot}82 \frac{1 + (\lambda/b)^4}{3 + (\lambda/b)^4}$$

which represents the results of R. & M. 2178 corrected for changes in wavelength.

Note: In order to allow for the variation in the stress at which the second modulus for D.T.D. 546 occurs, the following procedure has been adopted for clad panels between this stress and 45,000 lb/sq in.: if the initial panel modulus is E_1, and the transition stress f_1, then at a strain e we write for the stress

$$f = 0{\cdot}9E_1e + 0{\cdot}1f_1.$$

2.5.7. *Change in buckled shape.*—The cross-sectional shape near a wavecrest is plotted for various values of e/e_b. It is seen that the top of the wave becomes flattened with increasing e/e_b, and the form approximates to

$$w = a \sin \frac{\pi y}{b} + B \sin \frac{3\pi y}{b}.$$

3. *Roller Edged Panels.*—3.1. *Description of Panels.*—The panels were 35 in. long and nominally 0·064 in. thick. They were designed to cover the following range:—

Clad material (D.T.D. 546).

Panel No.	9A†	10A	11A	12A	13A	14A	15A	16A	17A	18A†	21A*
b/t	0	35	40	45	55	65	80	100	120	0	45

Unclad material (D.T.D. 646).

Panel No.	9B†	10B	11B	12B	13B	14B	15B	16B	17B	18B†
b/t	0	35	40	45	55	65	80	100	120	0

Panels marked * were designed for a special investigation of wave shape down the length of the panel.

Panels marked † were designed to provide a direct comparison with compression control tests, and no measurements of buckled shape were made.

The construction of the panels was similar to those with ball edge supports, and the dimensions are summarised in Tables 5 and 6.

3.2. *Description of Test Rig.*—The test rig was identical with that already described with the exception of the edge supports. In this case the hardened steel rollers, $\frac{1}{4}$ in. diameter, were located in slots cut vertically in steel blocks, the blocks being bolted, as before, to the side supports. The rollers were at $\frac{5}{16}$ in. pitch, being separated by small rubber blocks. The axes of the rollers were horizontal, so that one face rolled on the plate and the other on the steel block, thus permitting panel contraction. The edges of the grooves in the steel blocks located the rollers laterally, with a small clearance.

The clamping action of the rollers on the plate involved forces tending to separate the steel blocks on opposite faces of the plate. In trial tests it was discovered that the blocks did in fact

separate suddenly, precipitating failure of the panel by wrinkling at the edges. The blocks were, therefore, tied together by 2 B.A. bolts and the increase in stiffness was sufficient to prevent serious separation of the blocks.

3.3. *Friction Tests.*—Friction tests were performed on a panel, in the same manner as previously. The results are plotted for bolts loose, bolts tight, and for lubricated edge supports.

In the first loading, the panel sustained an appreciable load before slipping occurred (0·08 tons with bolts loose, 0·35 tons with bolts tight). This load increase involved relative movement of the platens, and was due to friction between the plate and the rollers. As loading proceeded after the bottom end of the panel had come into contact with the baseplate, the load indicated by the machine increased at a greater rate than that deduced from the mean panel strain. This did not occur in the case of ball edge supports, and it was, therefore, concluded to be due to increasing friction between the panel and the rollers.

On reloading, the mean load carried by the panel remained constant at 0·15 tons while the indicated load was increased from zero to 0·15 tons. The curve then tended to follow the same course as before, with indicated load increasing at a greater rate than mean load. This phenomenon on reloading may be associated with jamming of the rams on the return stroke, and this is partly confirmed by the fact that the mean load carried at zero indicated load is the same in all cases.

It is known, from an examination of the other test results, that the rate of increase of indicated load becomes equal to that of the mean load after a load of about 1 ton. This shows that the friction at the rollers reaches a limiting value.

3.4. *Interpretation of Load* vs. *Strain Curves**.—It is clear from the foregoing that the indicated load is not equal to the mean load carried by the panel, owing to friction with the rig; and the strain measured from zero indicated load, is not equal to the panel strain, owing to jamming of the rams on the return stroke.

Consider a typical load *vs.* strain curve as under:—

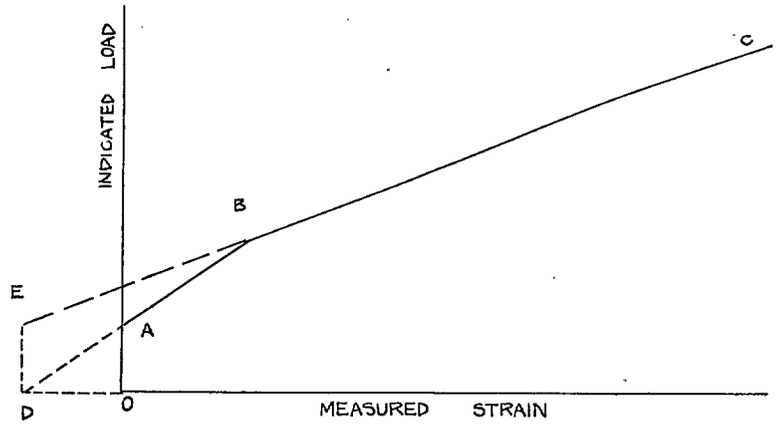

In the portion OA the indicated load is increasing, the load carried by the panel being constant. In the portion AB the friction between the panel and the rollers is increasing, and in the portion BC the friction has reached a limiting value.

It is not known how much of the load AO is carried by friction, but it seems reasonable to assume that the rate of growth is similar to that along AB. This is confirmed by the first loading in the friction tests.

Referring to the diagram above, the corrected strain must therefore be measured from the point D and the corrected load (giving the mean load in the panel) from the point E for all loads past the point B.

* A fuller development of these arguments is made in B.A.C. Ltd. Technical Office Report No. 25 (unpublished).

OD represents the initial mean strain in the panel at zero indicated load. ED represents half the limiting friction between the panel and the rollers (assuming constant friction down the edges), and its deduction gives the mean load in the panel. For the load at the bottom end of the panel, twice the above deduction would then have to be made.

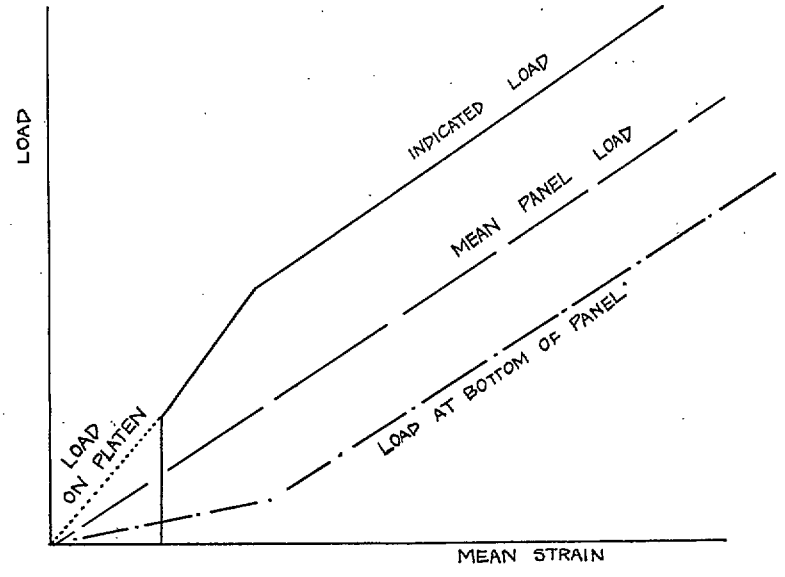

3.5. *Test Results.*—The test procedure and readings taken were the same as for ball supports with the exception that no readings of buckled shape were taken in Panels 9A, 18A, 9B, 18B since these were fully supported. The load *vs.* strain curves and the buckled shapes were plotted.

3.6. *Analysis of Results.*—3.6.1. *Predicted behaviour with clamped edges.*—The case of clamped edges has been treated in R. & M. 1554, in which it is assumed that the edges are unconstrained laterally. It is found that $K = 6{\cdot}32$, and $\partial f_{\text{average}} / \partial f_{\text{edge}} = 0{\cdot}548$ initially, the value of λ/b at buckling being $0{\cdot}66$. The value of $\partial f_{\text{average}} / \partial f_{\text{edge}}$ falls with increasing strain.

In R. & M. 2178, which includes higher order terms, it is found that $K = 632$ as before, and the initial value of $\partial f_{\text{average}} / \partial f_{\text{edge}}$ is $0{\cdot}50$, for a value of λ/b chosen equal to $0{\cdot}7$.

3.6.2. *Effects present in roller edged panel.*—These may be summarised as follows:—

(a) Incomplete clamping owing to the deformability of the rollers, flexibility of the side blocks and initial lack of fit.

(b) Lateral constraint from the strips of metal clamped between the rollers, and also possibly from lateral frictional forces at the rollers.

(c) Lateral constraint at the ends of the panel due to friction with the loading platens.

(d) The panel is of finite length, and the half wavelength should therefore be equal to some fraction of the length, and not to that which gives the minimum K for any infinitely long panel.

(e) The ends of the panel may tend to be clamped at the platens if they are machined accurately plane and the amplitudes are not large.

Theoretical analysis has not been applied to any of these effects.

3.6.3. *Experimental buckling stress coefficients.*—These have been determined as before in two ways; from the load *vs.* strain curves and from plots of the square of the mean amplitude against strain.

The values of K are summarised in Table 3, taking b as the distance between inside faces of the rollers, and are plotted against b/t. Once again the scatter is severe, but the clad panels exhibit values of K lower than the unclad ones. It is apparent that the clamping at the edges of the panels was by no means complete, being sufficient to increase K by only 50 per cent of the amount required for full clamping. The amount of clamping appears to increase with increasing b/t.

3.6.4. *Amplitudes after buckling.*—The slopes of the a^2 vs. e diagrams are summarised in Table 8.

3.6.5. *Wavelengths after buckling.*—It is apparent that λ/b is generally greater than 0·7 and does not assume the value closest to 0·7.

3.6.6. f_{average} vs. f_{edge} *curves.*—The f_{average} vs. f_{edge} curves have been deduced and were plotted. In the case of panels 9A, 18A, 9B, 18B the result yields a stress *vs.* strain curve. In all cases, both the measured load and the measured strain have been corrected for friction as in section 3.4.

The variation in the stress at which the second modulus occurs has been allowed for as follows: if this stress is f_1 and the first panel modulus is E_1 we write for elastic strain e above f_1

$$f = 0{\cdot}9E_1e + 0{\cdot}1f_1.$$

3.6.7. *Change in buckled shape.*—The cross-sectional shape near a wave crest is plotted for various values of e/e_b and compared with the theoretical mode of buckling for a panel with clamped edges.

4. *Stringer Edged Panels.*—4.1. *Introduction.*—The foregoing tests were intended to define the behaviour of a buckled plate under ideal conditions of edge support. These results, though of fundamental importance, do not necessarily apply to a plate supported by stringers, since a number of new variables are introduced. For example, the angular restraint at the edge of the plate depends on the stiffness of the stringer, and this stiffness may be modified by plasticity in the stringer analogous to the plasticity in the plate which caused failure in these tests. Analysis of these effects is postponed until the end of the report.

In order to provide some experimental data on the behaviour of panels with stringer edge supports, the present series of tests was undertaken. The stringers used were identical (except that they were in D.T.D. 646 not D.T.D. 546), with those of the compression box panels previously tested* and were intended to give a check on the results of that report; however, in the current tests there are two stringers per pitch of skin and the conditions are not, therefore, strictly comparable.

The conclusions from all the tests with ball, roller and stringer edge supports are given at the end of this section, together with a summary of the control test results.

4.2. *Description of Panels.*—All the panels tested were 35 in. long. The stringers were 16 S.W.G. D.T.D. 646, of Z section 1·65 × 0·75 in. with 5t inside-bend radius. The stringers were riveted $\frac{1}{8}$ in. diameter D.T.D. 303 rivets at $\frac{3}{4}$ in. pitch to the edges of the plate, with the free flanges facing outwards.

The plate was 5 in. wide, and two panels were made for each plate gauge, *viz.*: 18, 16, 14 and 12 S.W.G.

The panel dimensions are summarised in Table 9. The ends of the panels were cast in Wood's metal and machined plane and parallel before setting up for test.

4.3. *Test Rig.*—The measurements made on test were fundamentally the same as previously, but the portion of the rig for edge support of the panel was omitted, as was also the special loading head. The panel was set up with its centroid on the vertical axis of the testing machine.

* Reported in B.A.C. Report C.R.404 (unpublished).

The skin buckle shape was measured by a universal apparatus similar to that used previously. In order to permit readings of skin buckles near the ends of the panel, a pair of dial indicators was carried on the cross tubes. Of these indicators the upper one gave the buckled shape at the top of the panel, and the lower one the shape at the bottom. The two indicators were set so that they gave identical readings for a point at the centre of the panel.

The panel strain was measured by contractometer of the Mark I type attached to the stringer webs, and the relative movement of the platens was measured by means of two dial indicators attached to the baseplate and registering on the headplate.

4.4. *Test Results.*—4.4.1. *Procedure.*—A settling load of 0·2 tons was applied to each panel, the headplate was then lifted clear of the panel and brought into contact again. The dial indicators were then set to zero and contractometer measurements made at load increments of about 0·1 tons. Measurements were made of skin buckles at increments of 0·01 in. amplitude, the readings giving an amplitude plot down the centre-line of the panel and cross-sections at two or three troughs or crests near the middle of the panel.

Loading was continued until panel failure took place.

4.4.2. *Load* vs. *strain curves.*—The load *vs.* strain curves were plotted, as before.

4.4.3. *Buckle shape.*—The buckled shape was plotted; the amplitude readings were carried to the edges of the panel, in order to determine the effective width of the plate for buckling (*see* section 4.5.2).

4.5. *Analysis of Results.*—4.5.1. *Apparent* $f_{average}$ vs. f_{edge} *curves.*—In order to determine the apparent skin $f_{average}$ vs. f_{edge} curves, the method of analysis used in previous panel tests was applied. For a given edge strain, the edge stress was calculated using the measured panel E. (In these tests the edge stress was sufficiently low for there to be no drop in tangent modulus.) It was assumed that the stringers carried the stress f_{edge} and hence their load was calculated. This load was deducted from the total load to give the load carried by the skin, which divided by the skin area gave $f_{average}$.

The assumption that the stringers carry a uniform stress f_{edge} is open to some question. The buckling involves distortion of both the skin and stringers, and it is possible that the stringer amplitudes may be large enough to cause an appreciable local reduction of stress. Also, the local transverse stresses in the stringer may cause plasticity and a consequent reduction in the compressive stress carried.

4.5.2. *Analysis of buckle readings taken on test.*—The skin contour was measured by two 1/1000-in. dial indicators mounted on a carriage, sliding on two horizontal bars. The horizontal bars were then free to slide in a vertical plane guided by two steel bars which were set perpendicular to the machine baseplate.

On setting up, the panel was placed in position with its centroid on the centre-line of the machine and was then rotated till the skin at its lower end was parallel with the plane of the buckle measuring gear. A very light load (0·05 tons) was then applied to the panel and the dials set to zero at the lower end on the panel, the top end was then moved till the skin there was parallel to the reference plane and the same distance from it as the lower end.

Movement of the panel relative to the reference plane may occur through any of the following effects:—

(a) Headplate lateral movement, causing the top end of the panel to move towards or away from the reference plane.

(b) Flexure of the stringers. The stringers usually move in opposite directions but not by the same distance, giving flexure and twist of the panel.

(c) Curvature of the skin due to fixing moments applied by the stringers.

The objects for which buckle contours were measured are:—

(a) To find from cross-sectional plots, the value b, the effective distance between skin nodal lines down the length of the panel.

(b) To find buckling strain from plots of the square of the amplitude against strain.

(c) To plot λ/b against strain.

(d) To obtain plots of the shape of buckle cross-section eliminating the influence of flexure and skin curvature.

The mean line of the skin at panel centre-line was plotted by taking the observed readings for the amplitude of buckles at each crest and trough, finding the algebraic mean of each pair of adjacent readings then finding the average of each pair of adjacent means. The curve obtained by joining these plots was regarded as the mean flexure of the two stringers, unless curvature of the skin had occurred.

It has been assumed that the difference in mean stringer flexure at two sections is the same as the difference shown by the skin mean line.

Wavelength, λ, has been taken as the intersection of the skin contour lines with the mean line.

To find b, plots of skin contour were taken in horizontal planes across an adjacent crest and trough at several load stations for each panel (except panel B. 4 A). The contour of each peak was plotted as obtained on test, but readings for the troughs were corrected for the difference of flexure at the two sections, by plotting on the buckle centre-line, the difference in ' mean flexure ' of the two sections, given by the skin mean line. Then the base line for each trough was drawn through its respective point and inclined in such a way that the difference between the ordinates of trough and crest was equal at the first and last station.

The value of b has been taken as the distance between intersections of the troughs and crests.

To plot the buckle shape, the difference of corrected crest and trough was found at each station and expressed as a percentage of its maximum value. Thus, the effect of bending in the skin due to stringer twist over a larger wavelength was eliminated. The mean mode on which the buckling was superimposed was found by taking the mean of crest and trough amplitudes. This mean mode is also plotted.

4.5.3. *Experimental buckling stress coefficients.*—The buckling strain has been determined by two methods, from the change of slope of the load *vs.* strain curve and from the post-buckled amplitude. In this second method the square of the amplitude is plotted against the strain, and the intercept on the strain axis is the buckling strain.

The mean value of b has been determined and K evaluated from the relation

$$K = e_b(b/t)^2.$$

The values of K are summarised in Table 10.

4.5.4. *Wavelengths after buckling.*—The wavelengths were determined and were plotted against the strain. The mean value of λ/b is close to $0{\cdot}8$ for most panels.

4.5.5. *Slope of* a^2 vs. *e curve.*—The mean slopes of the (amplitude)^2 *vs.* strain curves are summarised in Table 11.

4.5.6. *Variation of b with strain.*—The values of b are plotted against the ratio e/e_b. It is seen that with increasing edge strain, the value of b increases slowly at first, and then suddenly up to the full panel width of 5 in. This sudden increase may be due to plasticity in the stringer web and flange. The location of the skin nodal line on the stringer flange is shown, where the location is plotted against e/e_b. It is seen that with increasing skin thickness the nodal line tends to be nearer to the stringer web.

4.5.7. *Variation of wave shape.*—The wave cross-sectional shape has been determined as described in section 4.5.2, and is plotted non-dimensionally for values of the strain equal to 1·0, 1·25, 1·5 and 2·0 times the buckling strain. Little change of shape with e/e_b is observable, but considerable clamping is seen to be afforded by the stringers.

4.6. *Comparison with Theoretical Results.*—4.6.1. *Statement of the problem.*—The theory of buckling of panels is not so well-developed as that for plates. This is inevitable, because the addition of (say) a Z-section stringer to a plate adds three new geometrical variables to the problem. Two aspects of the problem require analysis.

(a) The value of the buckling stress coefficient K.

(b) The distribution of stress in the skin and stringers for values of the edge strain greater than the buckling strain.

Some progress has been made with (a), but analysis of (b) is still lacking.

4.6.2. *Buckling stress coefficient.*—In the Royal Aeronautical Society Data Sheet* 02.01.18, the initial buckling stress of a flat panel with Z-section stringers is determined. The panel is assumed to have a large number of stringers which are rigidly attached to the skin.

In the present tests the support from the stringers is greater, since there are two stringers to one skin panel. In order to allow for this a fictitious ' effective stringer ' is found and the results of Data Sheet 02.01.18 applied.

This effective stringer has the same h/t_s ratio as the actual stringer, but the stiffness of its web for rotations about one flange is doubled, *i.e.*, t_s^3/h is doubled. This gives a stringer having twice the dimensions of the actual stringer. (The error due to this assumption is in the wavelength of initial buckling).

The results obtained from Data Sheet 02.01.18 for this effective stringer are plotted and are in good agreement with the experimental points.

4.6.3. *Effect of stringer amplitude on post-buckled behaviour.*—For any longitudinal fibre, whose deflection is w,

$$e = \frac{f}{E} + \frac{1}{2\lambda}\int_0^{\lambda}\left(\frac{\partial w}{\partial x}\right)^2 dx$$

where x is measured along the half-wavelength. Assuming a wave form

$$w = w_0 \sin\frac{\pi x}{\lambda}$$

we have

$$e = \frac{f}{E} + \frac{\pi^2 w_0^2}{4\lambda^2}$$

or

$$f = E\left(e - \frac{\pi^2 w_0^2}{4\lambda^2}\right).$$

Thus the reduction in fibre stress is proportional to the square of the maximum amplitude.

The observed mode of distortion has been considered, and by integration across the stringer the reduction in stringer average stress has been calculated to be about 2 per cent of the reduction in skin average stress. We conclude, therefore, that the apparent skin f_{average} vs. f_{edge} curves are not more than about 2 per cent in error due to this cause.

---

* See Note which appears later.

4.6.4. *Plasticity in stringer web.*—The fixing moment between the skin and stringer causes local stresses which will induce local plasticity in the stringer web and flange. This means that the stiffness at the flange, for providing angular constraint at the edges of the sheet, is reduced.

The maximum stress difference in the stringer (or in the skin where this is thinner than the stringer) has been calculated by an approximate method and is plotted. It is seen that the skin nodal line moves outwards at the same time as the theoretical plastic stress difference is reached.

The sudden decrease of slope of the f_{average} vs. f_{edge} curve appears to be due to the plasticity mentioned above. Consider a panel which buckles at a value of K greater than 3·62. The panel will follow the f_{average} vs. f_{edge} curve appropriate to this value of K. When plasticity in the stringer is fully developed, the skin will become effectively pinned at the edges and will behave as if it had buckled at $K = 3{\cdot}62$.

Further analysis of this effect is developed in B.A.C. Technical Office Report No. 26 (unpublished).

5. *Summary and Conclusions.*—The values of λ/b were plotted against the values of K realised by the panels, and compared with the theoretical curve of N.A.C.A. T.N. 752. It is seen that the experimental values of K corresponding to a given λ/b are less than the theoretical values, and that this is more marked in the case of D.T.D. 546 than in the case of D.T.D. 646.

The experimental points for $\partial f_{\text{average}} / \partial f_{\text{edge}}$ are plotted against f_b and f_{edge} for clad and unclad panels with the various conditions of edge support. Mean contours of $\partial f_{\text{average}} / \partial f_{\text{edge}}$ are drawn through the experimental points, and hence by cross-plotting $\partial f_{\text{average}} / \partial f_{\text{edge}}$ is plotted against f_{edge}/f_b for various values of f_b. In this form the information is suitable for design office use.

It is seen that the value of f_b has a marked effect on $\partial f_{\text{average}} / \partial f_{\text{edge}}$ the reduction being more marked when f_b is large. This reduction for large buckling stresses is associated with plastic flow in the portion of the plate where the local stresses due to buckling are large. As a comparison with the experimental results, the theoretical results of Data Sheet 02.01.i are plotted; the theoretical reduction of $\partial f_{\text{average}} / \partial f_{\text{edge}}$ is in quite good agreement with experiment during the earlier stages of buckling, but the reduction is less than that found experimentally in the later stages. This is as would be expected, since the theory of Data Sheet 02.01.i takes no account of changes of mode due to plasticity. (The results of Data Sheet 02.01.02 are also plotted for comparison.)

Conclusions.—1. Tests with ball edge supports have not imitated pin edged conditions owing to the torsional stiffness of the plate material outside the supports.

2. Tests with roller edge supports have not imitated clamped edge conditions owing to the flexibility of the rollers.

3. The tests are, however, representative of slight edge fixation and heavy edge fixation, corresponding to $K = 4$ and $K = 5$ (approx.) respectively.

4. The tests with stringer edge supports show good agreement with the values of K determined from Data Sheet 02.01.18.

5. The scatter in the observed wavelength is severe, but mean values of λ/b for ball, roller and stringer support are 0·95, 0·7 and 0·8 respectively.

6. The values of $\partial f_{\text{average}} / \partial f_{\text{edge}}$ are dependent on the value of the buckling stress as well as on f_{edge}/f_b. Data Sheets of the type 02.01.02 are therefore inadequate, since account must be taken of plasticity in the plate. Data Sheet 02.01.i represents a better approximation over a limited range.

7. Plastic strain in the stringer modifies the conditions of edge support for the panel when a certain edge stress is reached. This modification is discussed in B.A.C. Technical Office Report No. 26 (unpublished).

8. In tests of the ball and roller support type, the test results must be corrected for initial errors due to friction and contact deformation. These effects are discussed in B.A.C. Technical Office Report No. 25 (unpublished).

Acknowledgement.—The laboratory work, on which this report is based, was undertaken by Mr. C. J. Wilson, Mr. C. H. Jones, Mr. E. E. Fenn and Mr. P. R. V. Walmsley of the Bristol Aeroplane Company.

Note: Since this report was first published by the Bristol Aeroplane Company, the numbering of the Royal Aeronautical Society's Data Sheets on stressed skin structures has been revised.

The data sheets are referred to in this report by their 1947 numbering. The current (April, 1953) changes are given below for those who wish to refer to the Data Sheets.

02.01.18. has now been reissued, with amendments, as 02.01.25. In the new issue the corrected portions of the curves refer to a lower buckling stress than in the original issue, associated with a torsional-cum-local buckling mode of the stringers. The comparisons made in this report are with the upper parts of the curves, which are unaltered, since the geometry of the panels tested here was such that the other type of mode was not critical.

02.01.02. was reissued under the same number in December, 1947, to include the effects of lateral constraint which had previously been neglected. The new issue is appropriate only to conditions immediately after buckling. The well-buckled state is covered by 02.01.03.

02.01.i. was a draft data sheet on the effect of plasticity in buckled plates. This draft was discussed by the Structures Committee of the Royal Aeronautical Society, but was not issued. The only information issued on plasticity is therefore that contained in 02.01.03.

NOTATION

b	Panel width between ball centres or inside ends of rollers
w	Overall panel width
t	Panel thickness
E_T	Tangent modulus
E_S	Secant modulus
λ	Half wavelength of buckles
f_b	Buckling stress
K	Buckling stress coefficient, defined by $f_b = KE(t/b)^2$
f_{edge}	Longitudinal stress at edges of panel
f_{average}	Average stress across width b
e	Mean panel strain
e_b	Buckling strain
a	Amplitude of buckling
B.A.C.	Bristol Aeroplane Company, Ltd.

APPENDIX I

Energy Calculation for Panel with Edge Strips

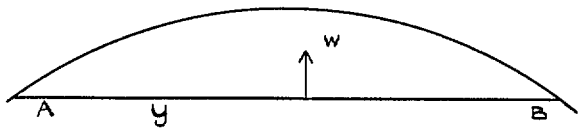

Assume $w = a \sin \frac{\pi x}{b} \sin \frac{\pi y}{b}$ between A and B.

$w = -\frac{\pi}{b} y \sin \frac{\pi x}{b}$ to the left of A, etc.

Then total energy of contraction

$$= \tfrac{1}{2}\int_0^b \int_{-c}^{b+o} \left(\frac{\partial w}{\partial x}\right)^2 ft \, dx \, dy$$

$$= \frac{a^2\pi^2}{8} ft + \frac{\pi^4 c^3}{6b^3} a^2 ft \, .$$

Strain energy of plate

$$= \tfrac{1}{2}\int_0^b \int_0^b \frac{Et^3}{12(1-\sigma^2)} \left\{\left(\frac{\partial^2 w}{\partial x^2}\right)^2 + 2 \frac{\partial^2 w}{\partial x^2} \frac{\partial^2 w}{\partial y^2} + \left(\frac{\partial^2 w}{\partial y^2}\right)^2\right\} dx \, dy$$

$$= \frac{Et^3 a^2}{12(1-\sigma^2)} \left(\frac{\pi^4}{2b^2}\right).$$

Strain energy of strips

$$= 0{\cdot}385E \frac{t^3}{6} \frac{\pi^4 a^2}{b^2} \frac{c}{b}.$$

Equating strain energy to potential energy at buckling,

$$K = \frac{3{\cdot}62 + 5{\cdot}06c/b}{1 + 13{\cdot}33c^3/b^3} \, .$$

TABLE 1

Dimension of Panels. Ball Edge Supports

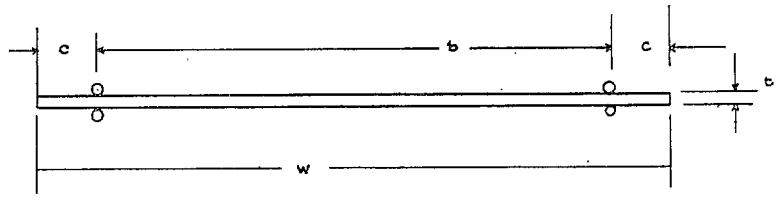

Clad Panels D.T.D. 546

Panel	1A	2A	3A	4A	5A	6A	7A	8A	19A	20A
w	2·922	3·250	3·581	4·425	4·951	5·887	7·190	8·250	4·359	4·733
b	2·160	2·550	2·910	3·600	4·290	5·270	6·520	7·900	3·730	4·460
c/b	0·176	0·136	0·115	0·090	0·077	0·058	0·051	0·039	0·084	0·031
t	0·0618	0·0637	0·0647	0·0656	0·0660	0·0659	0·0652	0·0634	0·0677	0·0687
wt	0·1806	0·2070	0·2316	0·2782	0·3267	0·3878	0·4689	0·5400	0·2954	0·3248

Unclad Panels D.T.D. 646

Panel	1B	2B	3B	4B	5B	6B	7B	8B
w	2·905	3·230	3·575	4·244	4·900	5·890	7·210	8·525
b	2·240	2·630	2·880	3·630	4·350	5·550	6·870	8·010
c/b	0·148	0·114	0·120	0·085	0·063	0·031	0·024	0·031
t	0·0641	0·0658	0·0639	0·0660	0·0669	0·0693	0·0687	0·0668
wt	0·1861	0·2124	0·2285	0·2802	0·3276	0·4084	0·4954	0·5693

TABLE 2

Variation in Thickness down the Length. Panels with Ball Edge Supports

Panel	1A		2A		3A		4A		5A	
Top	0·0622	0·0612	0·0632	0·0640	0·0644	0·0652	0·0658	0·0654	0·0662	0·0660
	0·0622	0·0612	0·0633	0·0640	0·0644	0·0651	0·0657	0·0649	0·0662	0·0663
	0·0622	0·0613	0·0632	0·0640	0·0644	0·0650	0·0657	0·0655	0·0662	0·0662
	0·0624	0·0613	0·0632	0·0639	0·0644	0·0651	0·0658	0·0654	0·0660	0·0657
Bottom	0·0622	0·0612	0·0633	0·0647	0·0642	0·0645	0·0659	0·0652	0·0657	0·0655
Panel	6A		7A		8A		19A		20A	
Top	0·0657	0·0654	0·0652	0·0654	0·0645	0·0627	0·0680	0·0679	0·0683	0·0685
	0·0660	0·0657	0·0650	0·0656	0·0645	0·0625	0·0677	0·0680	0·0694	0·0683
	0·0660	0·0657	0·0652	0·0654	0·0643	0·0622	0·0678	0·0678	0·0688	0·0684
	0·0660	0·0660	0·0650	0·0654	0·0642	0·0622	0·0679	0·0671	0·0683	0·0686
Bottom	0·0660	0·0662	0·0645	0·0654	0·0645	0·0622	0·0680	0·0672	0·0690	0·0688
Panel	1B		2B		3B		4B		5B	
Top	0·0643	0·0652	0·0663	0·0670	0·0632	0·0640	0·0675	0·0668	0·0662	0·0659
	0·0643	0·0649	0·0661	0·0670	0·0633	0·0645	0·0669	0·0660	0·0665	0·0660
	0·0632	0·0645	0·0652	0·0660	0·0634	0·0642	0·0665	0·0651	0·0670	0·0668
	0·0631	0·0642	0·0646	0·0655	0·0636	0·0644	0·0656	0·0651	0·0675	0·0670
Bottom	0·0630	0·0640	0·0645	0·0655	0·0638	0·0648	0·0655	0·0653	0·0683	0·0675
Panel	6B		7B		8B					
Top	0·0705	0·0704	0·0702	0·0693	0·0690	0·0665				
	0·0700	0·0697	0·0696	0·0685	0·0682	0·0660				
	0·0692	0–0692	0·0692	0·0682	0·0685	0·0660				
	0·0688	0·0685	0·0683	0·0675	0·0670	0·0652				
Bottom	0·0687	0·0684	0·0690	0·0673	0·0666	0·0648				

TABLE 3

Value of K. Panels with Ball Edge Supports

Panel	1A	2A	3A	4A	5A	6A	7A	8A	19A	20A
K_1	3·80	3·26	3·35	3·48	3·47	3·53	4·00	3·89	3·47	3·77
K_2	3·68	3·28	3·56	3·48	3·22	3·21	3·30	4·33	4·07	4·18
Panel	1B	2B	3B	4B	5B	6B	7B	8B		
K_1	4·03	3·95	3·95	3·96	4·66	4·10	3·20	4·18		
K_2	3·97	3·77	4·40	4·06	4·23	3·97	3·00	4·18		

K_1 found from load *vs.* strain curve.

K_2 found from post-buckled amplitude.

NOTE: Values of K in Fig. 8 have been corrected for wavelength by multiplying by $\frac{1}{(\lambda/b)^2 + (b/\lambda)^2}$.

TABLE 4

Slope of (amplitude)^2 vs. *strain curves. Panels with Ball Edge Supports*

Panel	1A	2A	3A	4A	5A	6A	7A	8A		
Theoretical	2·50	2·71	3·53	5·09	6·03	14·50	18·0	21·7		
Measured	2·50	3·00	4·20	6·00	6·40	14·50	18·0	23·3		
Panel	1B	2B	3B	4B	5B	6B	7B	8B		
Theoretical	1·76	2·82	3·10	4·55	7·12	9·65	25·0	15·0		
Measured	2·30	2·90	4·30	4·60	7·90	10·80	21·5	17·5		
Panel 19A										
Wave	1	2	3	4	5	6	7	8	9	10
Theoretical	4·08	4·58	4·58	5·1	5·1	5·1	5·65	5·65	4·58	5·10
Measured	5·6	5·9	6·1	6·0	6·7	5·8	6·0	5·2	6·0	3·6
Panel 20A										
Wave	1	2	3	4	5	6	7	8	9	
Theoretical	3·51	5·54	5·54	6·81	7·28	7·28	7·28	7·28	7·3	
Measured	4·6	5·3	7·5	7·4	9·1	9·6	9·0	9·6	6·9	

TABLE 5

Dimensions of Panels. Roller Edge Supports.

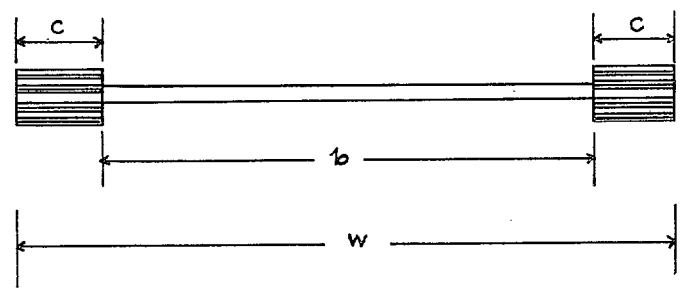

Clad Panels D.T.D. 546

Panel	9A	10A	11A	12A	13A	14A	15A	16A	17A	18A	21A
W	2·505	4·314	4·642	4·980	5·648	6·320	7·280	8·610	9·925	2·510	5·000
b	0	2·18	2·57	2·94	3·645	4·335	5·265	6·388	7·600	0	3·086
t	0·0661	0·0624	0·0643	0·0654	0·0663	0·0667	0·0659	0·0639	0·0633	0·0665	0·0687
wt	0·1655	0·2695	0·2980	0·3260	0·3740	0·4215	0·4800	0·5500	0·6300	0·1670	0·3435

Unclad Panels D.T.D. 646

Panel	9B	10B	11B	12B	13B	14B	15B	16B	17B	18B
W	2·517	4·370	4·730	4·995	5·640	6·300	7·280	8·610	9·925	2·508
b	0	2·207	2·627	3·062	3·590	4·260	5·180	6·300	7·320	0
t	0·0696	0·0631	0·0657	0·0674	0·0653	0·0656	0·0647	0·0630	0·0610	0·0655
wt	0·1752	0·2755	0·3107	0·3364	0·3685	0·4133	0·4713	0·5427	0·6054	0·1643

TABLE 6

Variation in Thickness down Length. Panels with Roller Edge Supports

Panel	9A		10A		11A		12A		13A		14A	
Top	0·0662	0·0664	0·0632	0·0615	0·0650	0·0638	0·0662	0·0650	0·0668	0·0661	0·0670	0·0670
	0·0664	0·0662	0·0630	0·0615	0·0650	0·0638	0·0659	0·0650	0·0668	0·0661	0·0669	0·0669
	0·0662	0·0662	0·0630	0·0620	0·0648	0·0640	0·0660	0·0652	0·0668	0·0663	0·0669	0·0670
	0·0662	0·0655	0·0628	0·0625	0·0645	0·0638	0·0657	0·0652	0·0665	0·0660	0·0665	0·0666
Bottom	0·0656	0·0657	0·0628	0·0615	0·0645	0·0639	0·0654	0·0648	0·0660	0·0660	0·0665	0·0665

Panel	15A		16A		17A		18A		21A	
Top	0·0659	0·0662	0·0630	0·0651	0·0650	0·0622	0·0668	0·0670	0·0687	0·0690
	0·0660	0·0661	0·0625	0·0644	0·0645	0·0618	0·0668	0·0668	0·0684	0·0688
	0·0655	0·0660	0·0630	0·0648	0·0645	0·0620	0·0665	0·0665	0·0688	0·0689
	0·0665	0·0660	0·0632	0·0648	0·0649	0·0620	0·0663	0·0663	0·0686	0·0685
Bottom	0·0650	0·0660	0·0630	0·0650	0·0643	0·0620	0·0661	0·0661	0·0661	0·0684

Panel	9B		10B		11B		12B		13B	
Top	0·0685	0·0691	0·0622	0·0638	0·0661	0·0661	0·0679	0·0667	0·0645	0·0652
	0·0688	0·0695	0·0623	0·0639	0·0649	0·0649	0·0680	0·0669	0·0649	0·0654
	0·0693	0·0692	0·0624	0·0639	0·0649	0·0663	0·0680	0·0672	0·0645	0·0652
	0·0698	0·0705	0·0623	0·0638	0·0650	0·0660	0·0679	0·0669	0·0652	0·0653
Bottom	0·0705	0·0710	0·0623	0·0638	0·0648	0·0648	0·0675	0·0667	0·0654	0·0660

Panel	14B		15B		16B		17B		18B	
Top	0·0660	0·0660	0·0651	0·0641	0·0627	0·0642	0·0597	0·0621	0·0660	0·0659
	0·0660	0·0655	0·0649	0·0641	0·0623	0·0638	0·0598	0·0623	0·0658	0·0657
	0·0655	0·0655	0·0650	0·0644	0·0620	0·0640	0·0598	0·0623	0·0655	0·0652
	0·0655	0·0655	0·0650	0·0648	0·0620	0·0639	0·0598	0·0623	0·0655	0·0655
Bottom	0·0655	0·0655	0·0650	0·0650	0·0619	0·0635	0·0600	0·0627	0·0652	0·0652

TABLE 7

Values of K. Panels with Roller Edge Supports

Panel	9A	10A	11A	12A	13A	14A	15A	16A	17A	18A	21A
K_1	—	3·67	3·80	4·47	4·50	4·31	5·44	4·20	4·76	—	4·65
K_2	—	3·55	3·71	4·29	3·85	4·09	3·75	4·00	4·76	—	5·18
Panel	9B	10B	11B	12B	13B	14B	15B	16B	17B	18B	
K_1	—	4·53	4·08	4·65	4·17	3·73	4·80	4·30	5·33	—	
K_2	—	4·56	4·22	4·76	3·78	3·73	4·80	4·00	4·75	—	

K_1 found from load *vs.* strain curve.

K_2 found from post-buckled amplitude.

TABLE 8

Slope of (amplitude)^2 vs. *strain curves. Panels with Roller Edge Supports*

Panel	10A	11A	12A	13A	14A	15A	16A	17A
$\frac{\partial \lambda^2}{\partial \delta}$	1·6	2·0	2·7	3·7	6·7	12·5	9·5	14·2
Panel	10B	11B	12B	13B	14B	15B	16B	17B
$\frac{\partial a^2}{\partial e}$	2·4	2·4	3·0	4·3	3·2	7·8	8·5	13·0

Panel 21A															
Wave	1	2	3	4	5	6	7	8	9	10	11	12	13	14	15
$\frac{\partial a^2}{\partial e}$	1·6	2·6	2·6	3·0	3·4	2·6	2·5	2·9	3·5	2·5	3·6	2·8	2·9	2·9	3·1

TABLE 9

Panel dimensions. Panels with Stringer Edge Supports

	Mean Width	Mean thickness	Mean Area	Mean Width	Mean thickness	Mean Area
Panel		B. 1 A			B. 1 B	
Skin	5	0·10605	0·53025	5	0·10585	0·52925
Stringer 1 ..	2·684	0·06962	0·18688	2·7092	0·06941	0·18997
Stringer 2 ..	2·694	0·06608	0·17803	2·6992	0·06547	0·17672
Total ..			0·89516			0·89594
Panel		B. 2 A			B. 2 B	
Skin	5	0·08345	0·41725	5	0·08420	0·4210
Stringer 1 ..	2·7058	0·06885	0·1863	2·6975	0·07013	0·18918
Stringer 2 ..	2·6992	0·06992	0·1889	2·6792	0·07017	0·18800
Total ..			0·79225			0·79818
Panel		B. 3 A			B. 3 B	
Skin	5	0·06814	0·3407	5	0·06865	0·34325
Stringer 1 ..	2·6983	0·06683	0·18033	2·6933	0·06818	0·18363
Stringer 2 ..	2·6842	0·06889	0·18490	2·6917	0·06220	0·16742
Total ..			0·70593			0·69430
Panel		B. 4 A			B. 4 B	
Skin	5	0·04918	0·2459	5	0·05001	0·25005
Stringer 1	2·6125	0·06970	0·18210	2·7033	0·06741	0·18233
Stringer 2 ..	2·6908	0·06987	0·1880	2·6733	0·06848	0·18307
Total ..			0·6160			0·61545

TABLE 10

Experimental value of K. Panels with Stringer Edge Supports

Panel	b	b/t	$10^3 e_{b1}$	$10^3 e_{b2}$	K_1	K_2
B. 1 A	4·82	45·5	2·49	2·52	5·15	5·22
B. 1 B	4·78	45·1	2·43	2·52	4·95	5·11
B. 2 A	4·76	57·0	1·675	1·67	5·45	5·43
B. 2 B	4·68	55·7	1·700	1·730	5·28	5·40
B. 3 A	4·38	64·3	1·33	1·30	5·53	5·40
B. 3 B	4·56	66·3	1·375	1·255	6·08	5·55
B. 4 A	4·42	90·0	1·030	0·845	8·30	6·82
B. 4 B	4·42	88·4	1·050	0·845	8·21	6·60

1 from load *vs.* strain curve.

2 from post-buckled amplitude.

TABLE 11

Slope of (amplitude)^2 vs. *strain curve. Panels with Stringer Edge Supports*

Panel	$\partial a^2/\partial e$
B. 1 A	9·75
B. 1 B	9·75
B. 2 A	8·35
B. 2 B	7·12
B. 3 A	7·12
B. 3 B	7·50
B. 4 A	4·50
B. 4 B	5·50

TABLE 12

Summary of Control Tests

Specimen	A.C.382	A.C.383	A.C.384	A.C.394	A.C.395	A.C.396	A.C.422	A.C.429	A.C.436
E or E_1 lb/in.^{2}	$10{\cdot}3 \times 10^6$	$10{\cdot}3 \times 10^6$	$10{\cdot}5 \times 10^6$	$10{\cdot}8 \times 10^6$	$10{\cdot}9 \times 10^6$	$10{\cdot}8 \times 10^6$	$11{\cdot}0 \times 10^6$	$11{\cdot}1 \times 10^6$	$11{\cdot}1 \times 10^6$
E_2 lb/in.^{2}	$9{\cdot}8 \times 10^6$	$9{\cdot}9 \times 10^6$	$9{\cdot}9 \times 10^6$						
L.P. or L.P.$_1$ lb/in.^{2}	18,500	19,100	18,250	47,600	48,500	49,000	50,000	49,500	47,000
L.P.$_2$ lb/in.^{2}	43,500	44,000	41,500						
0·01 P.S. lb/in.^{2}	49,600	50,000	48,800	55,500	56,200	55,750	56,500	55,300	56,100
0·1 P.S. lb/in.^{2}	57,250	57,850	56,750	62,700	63,400	63,000	64,700	64,000	65,000
0·2 P.S. lb/in.^{2}	59,700	60,400	59,400	64,600	65,600	65,000	67,100	66,400	67,250
V.P.H. No.	159	158	159	157	155	154	159	153	159

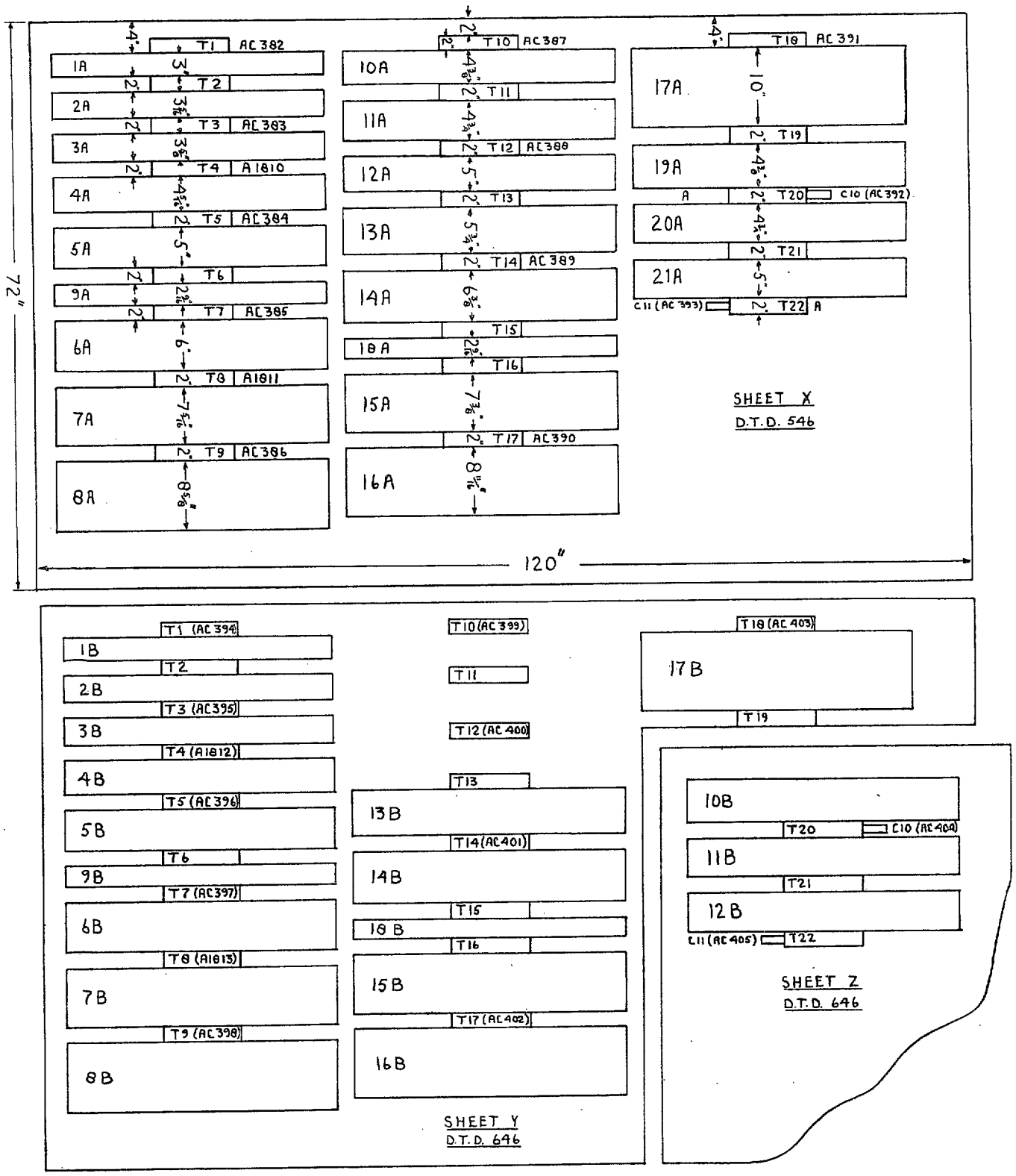

FIG. 1. Layout of sheets for plates and test pieces. Sheets were all 16 s.w.g.

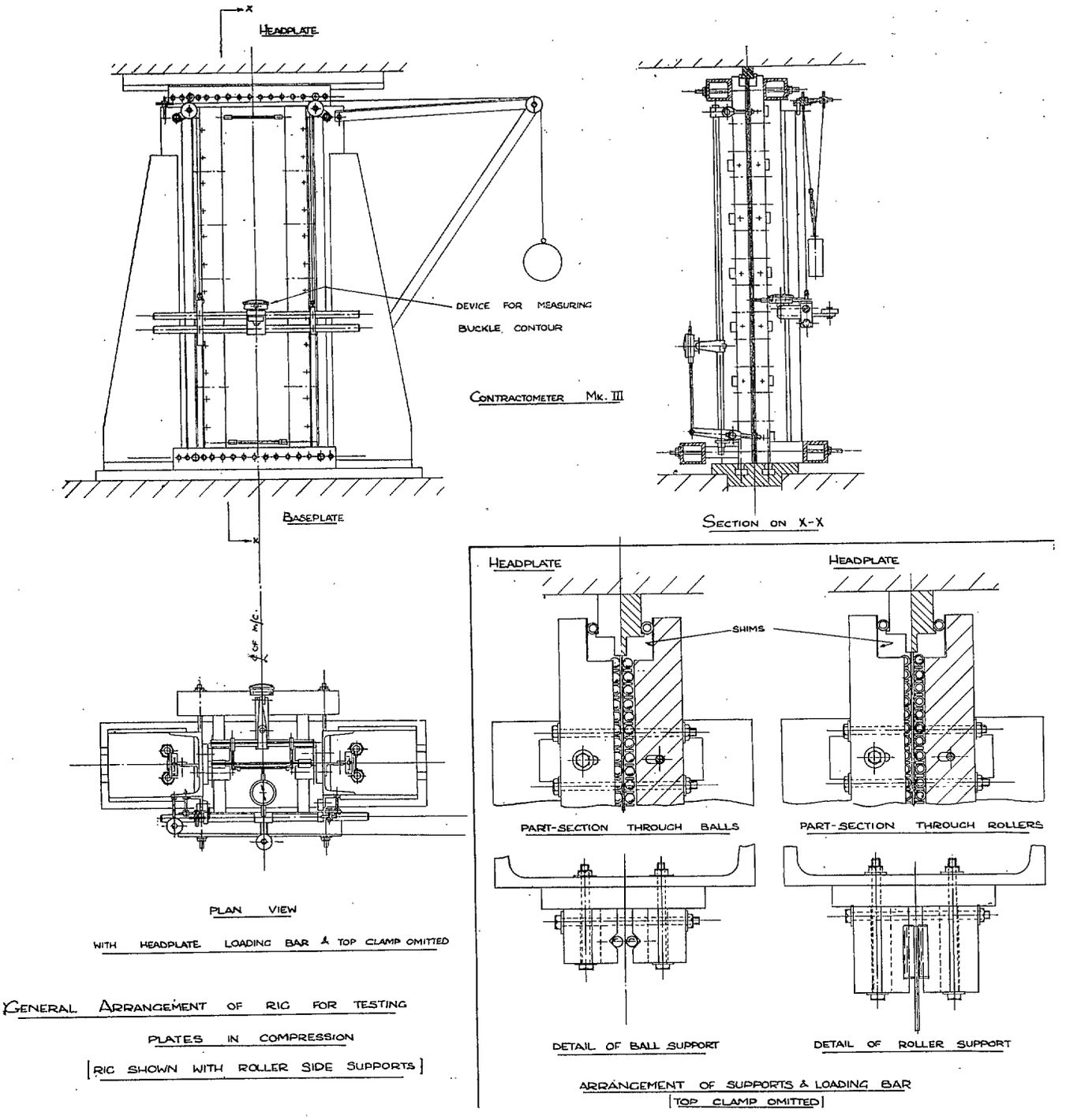

GENERAL ARRANGEMENT OF RIG FOR TESTING PLATES IN COMPRESSION

[RIG SHOWN WITH ROLLER SIDE SUPPORTS]

FIG. 2.

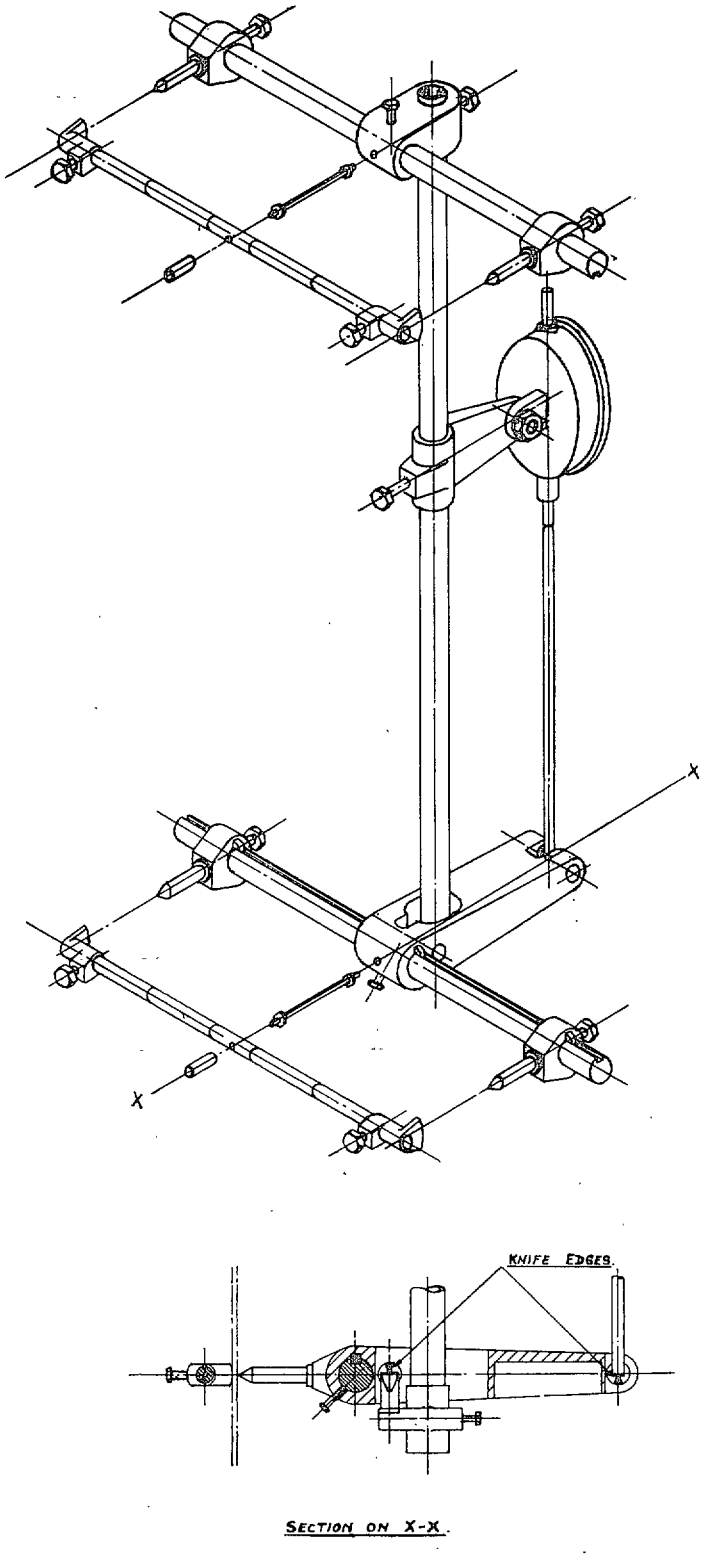

FIG. 3. Sketch of contractometer Mk. III for measuring mean strain across a plate in compression.

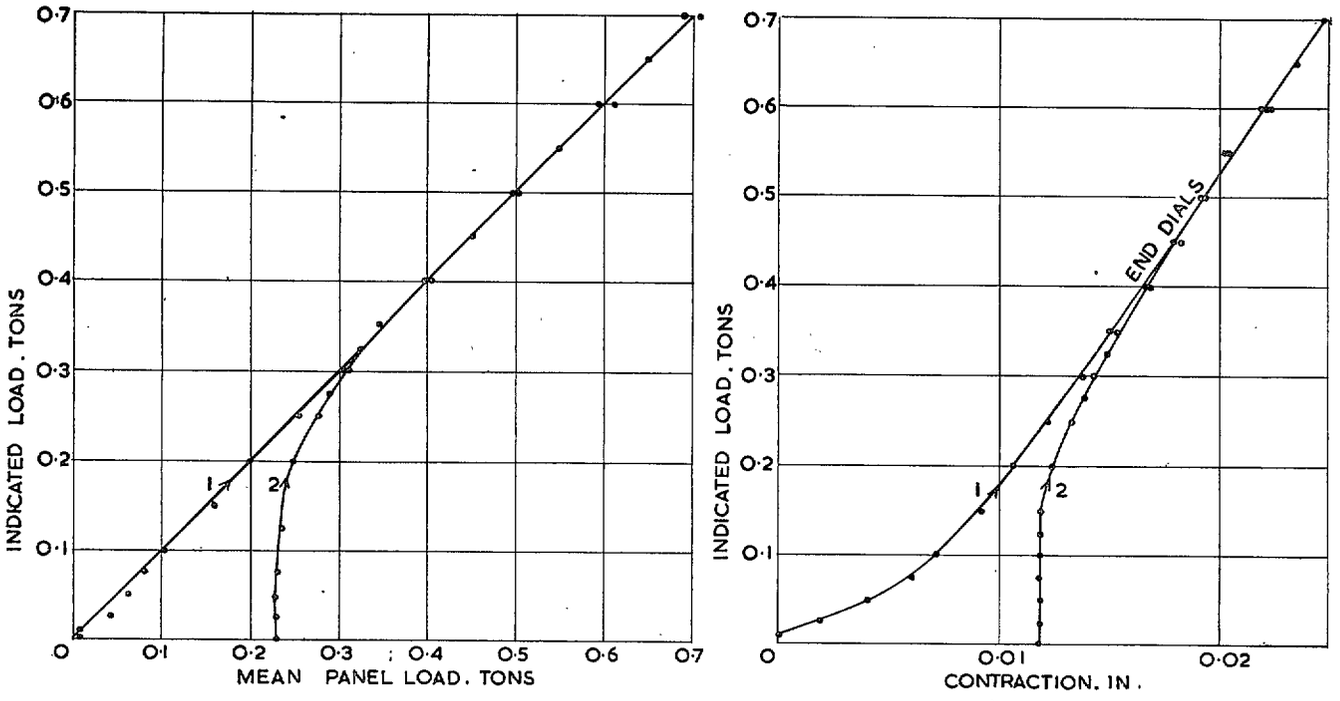

FIG. 4. Ball edge supports. Bolts loose. Friction tests (panel 10A).

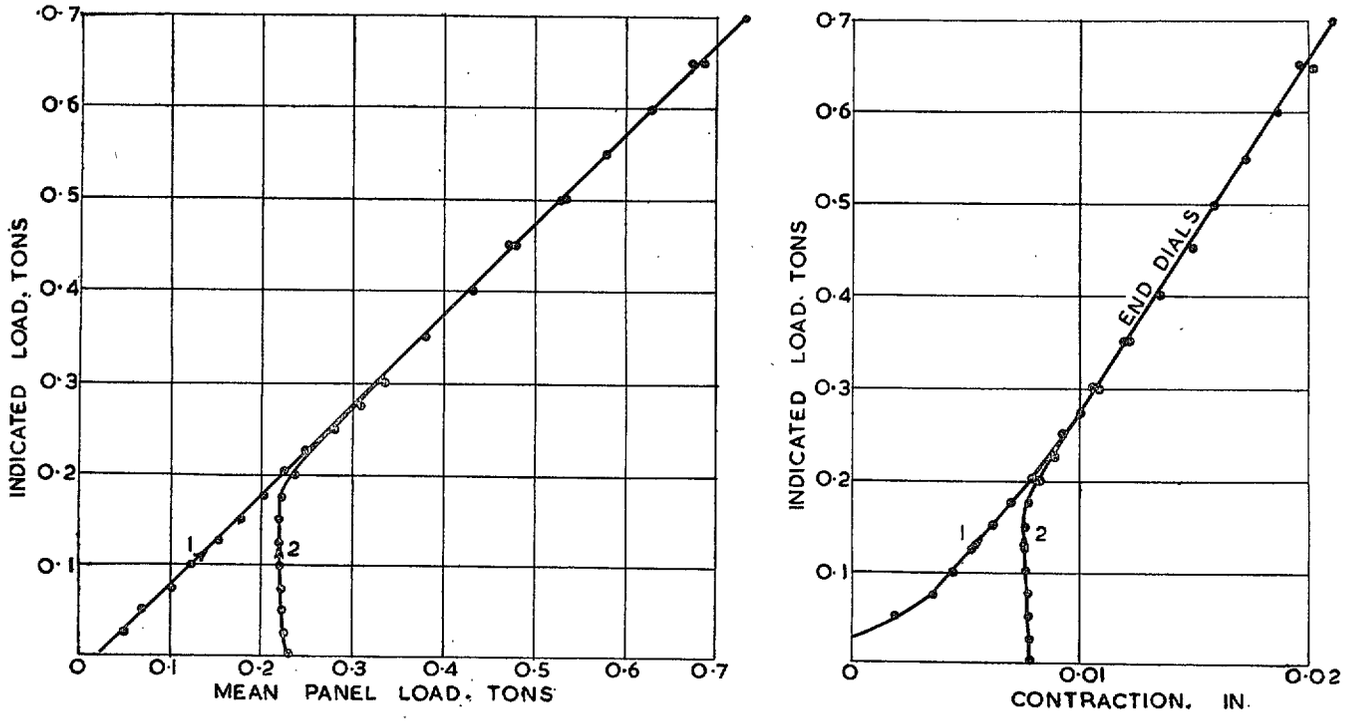

FIG. 5. Ball edge supports. Bolts tight. Friction test (panel 10A).

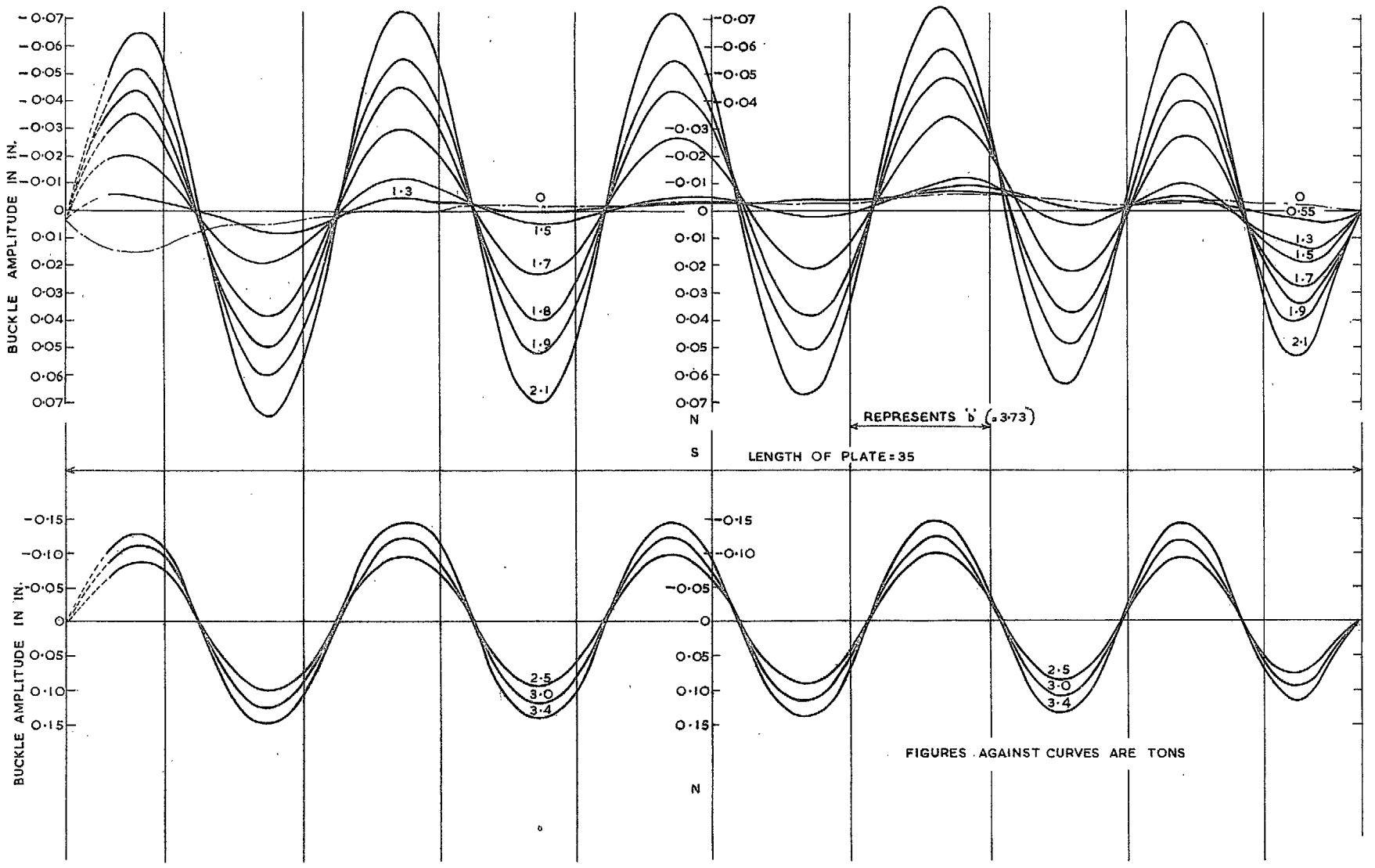

FIG. 6. Plot of Skin Buckle Amplitude. Plate 19A. Mat$\frac{1}{1}$ D.T.D. 546.

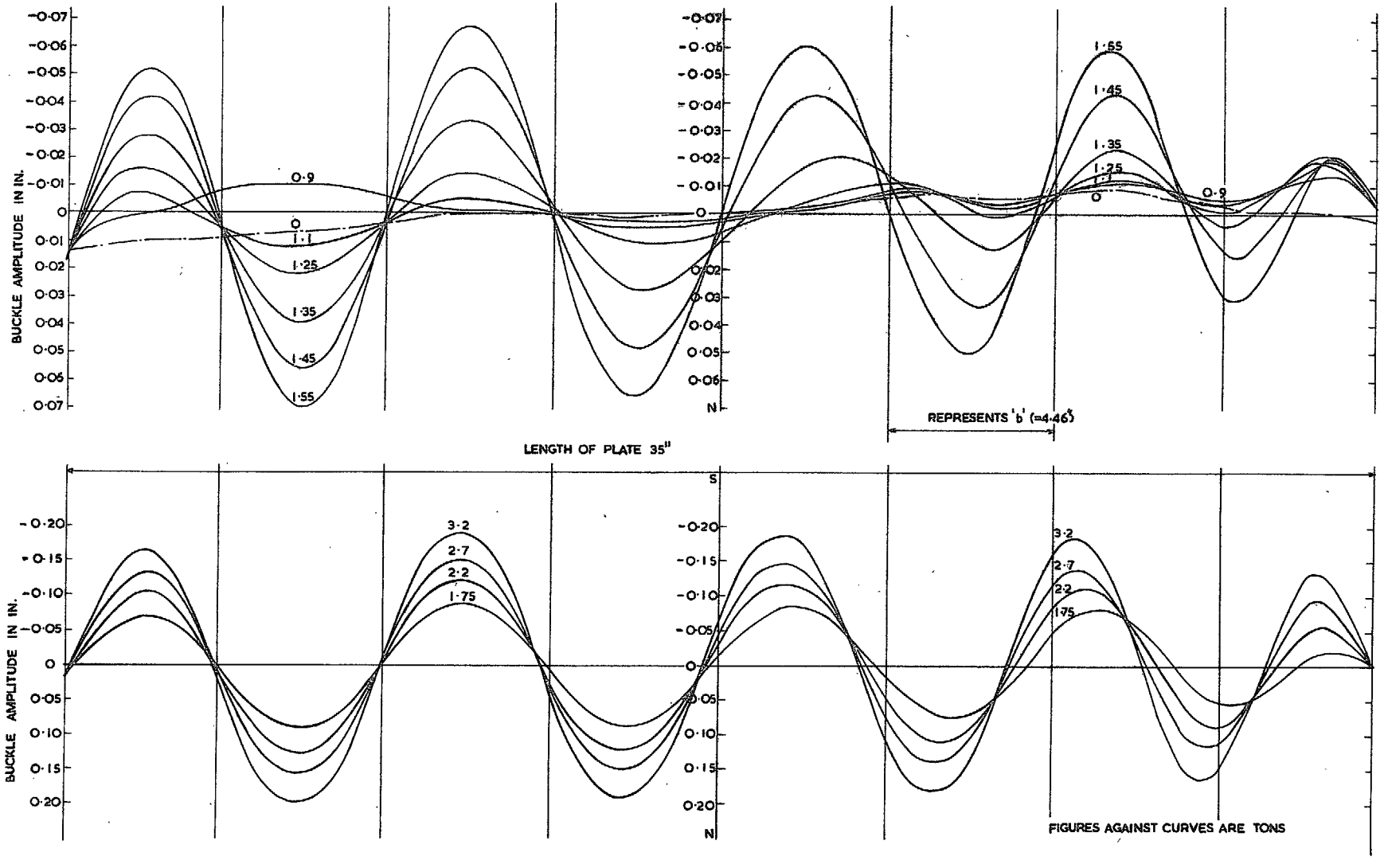

Fig.7. Plot of Skin Buckle Amplitude
Plate. 20A. Mat⊥ DTD 546.

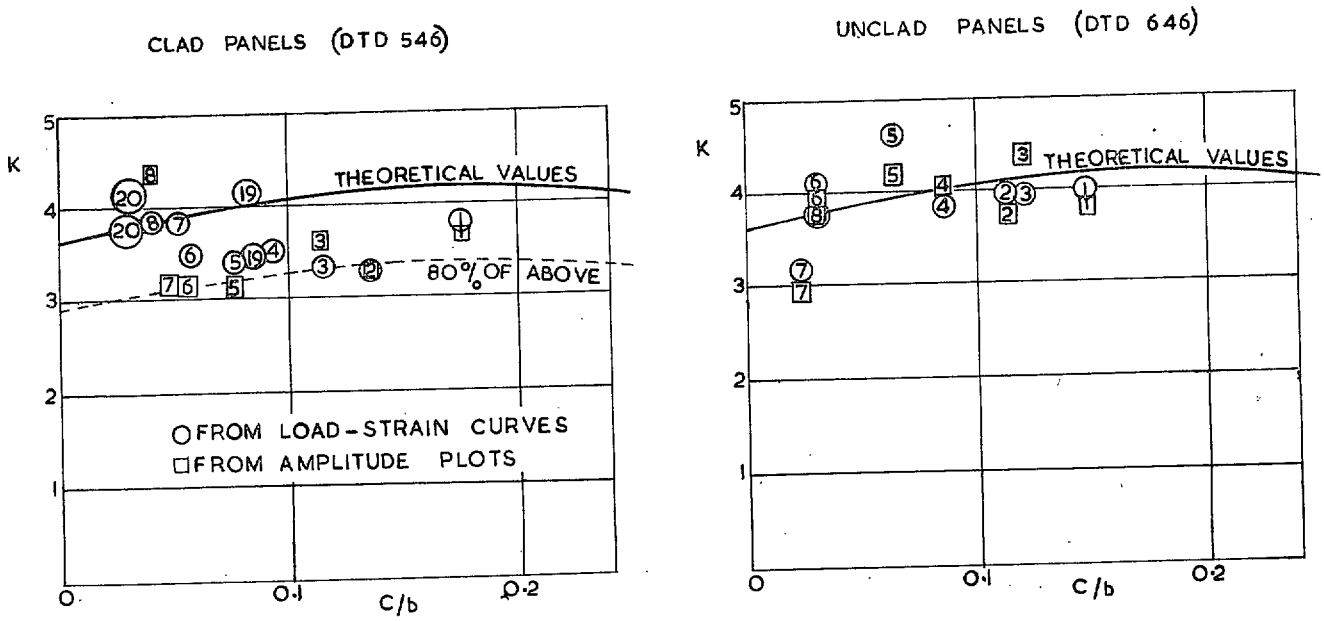

FIG. 8. Ball edge supports.

Note: All experimental points have been corrected for variations in λ/b.

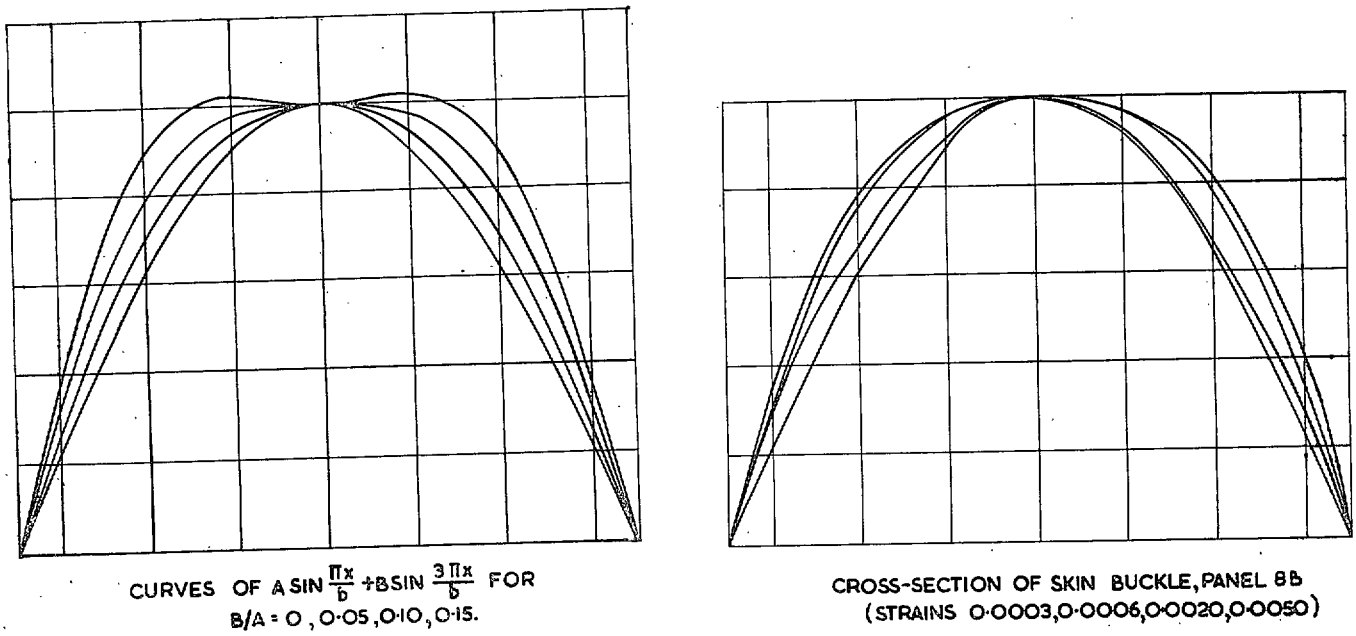

FIG. 9.

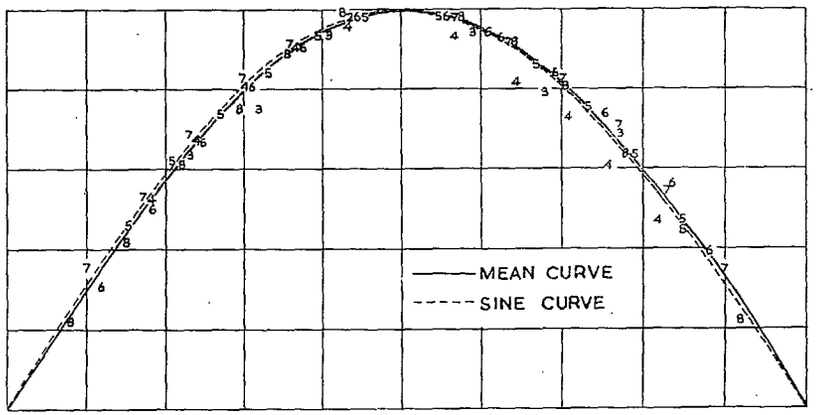

FIG. 10. Buckle cross-section at buckling strain.
D.T.D. 646 panels. Ball edge supports.

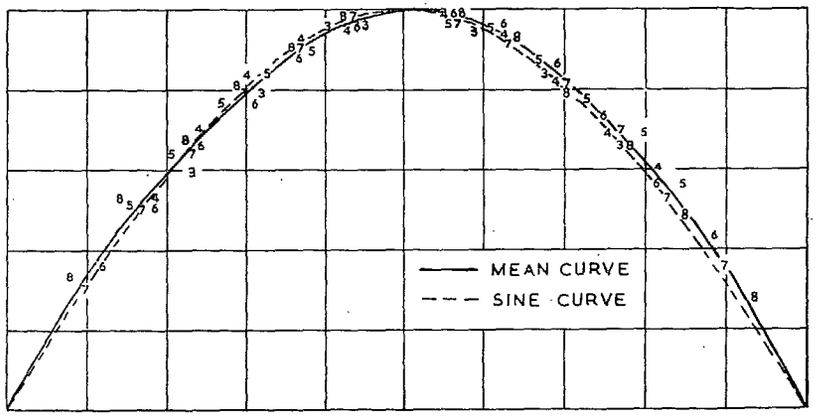

FIG. 11. Buckle cross-section at twice buckle strain.
D.T.D. 646 panels. Ball edge supports.

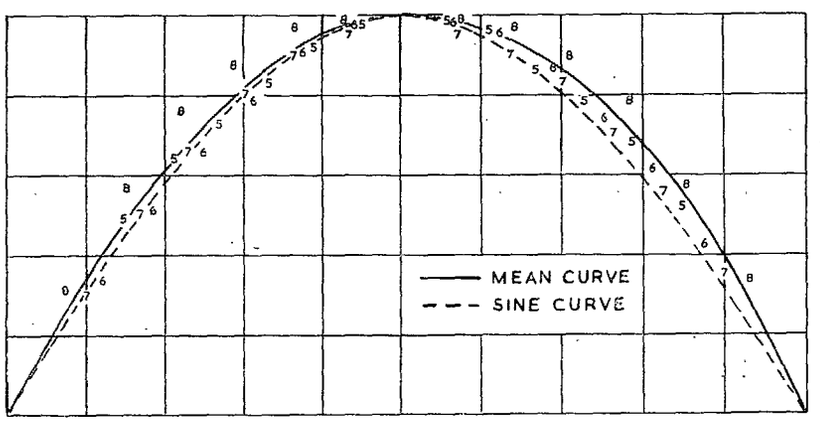

FIG. 12. Buckle cross-section at five times buckling strain.
D.T.D. 646 panels. Ball edge supports.

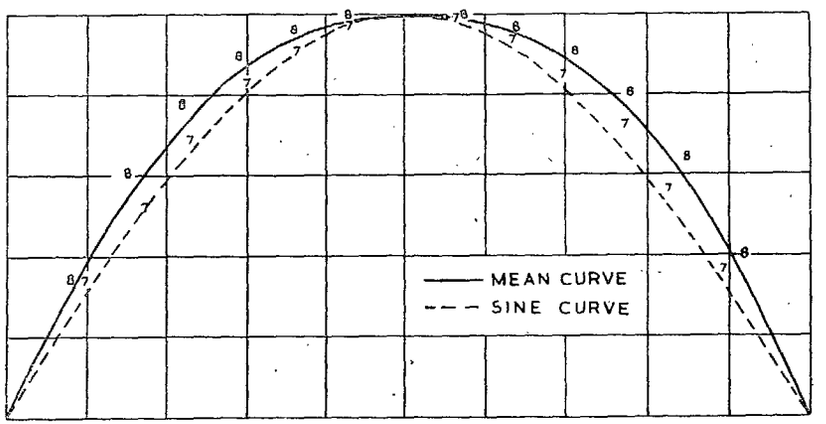

FIG. 13. Buckle cross-section at ten times buckling strain.
D.T.D. 646 panels. Ball edge supports.

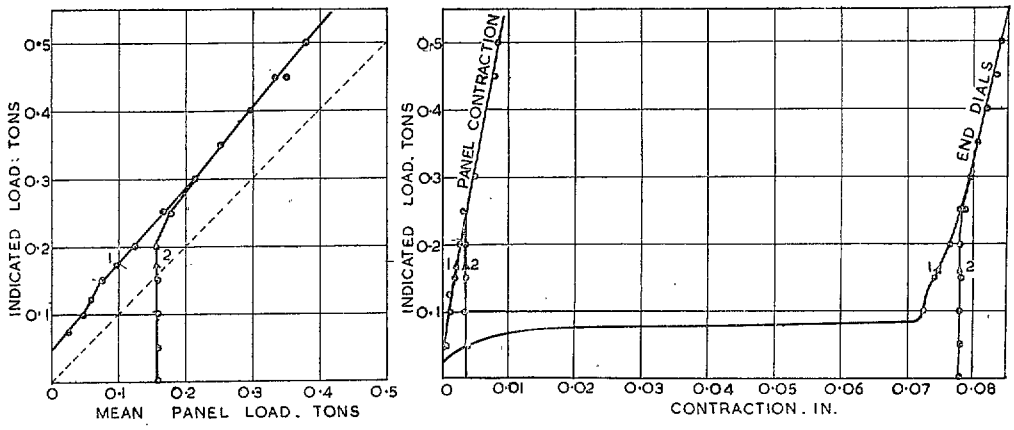

FIG. 14. Roller edge supports. Bolts loose. Friction test (panel 10A).

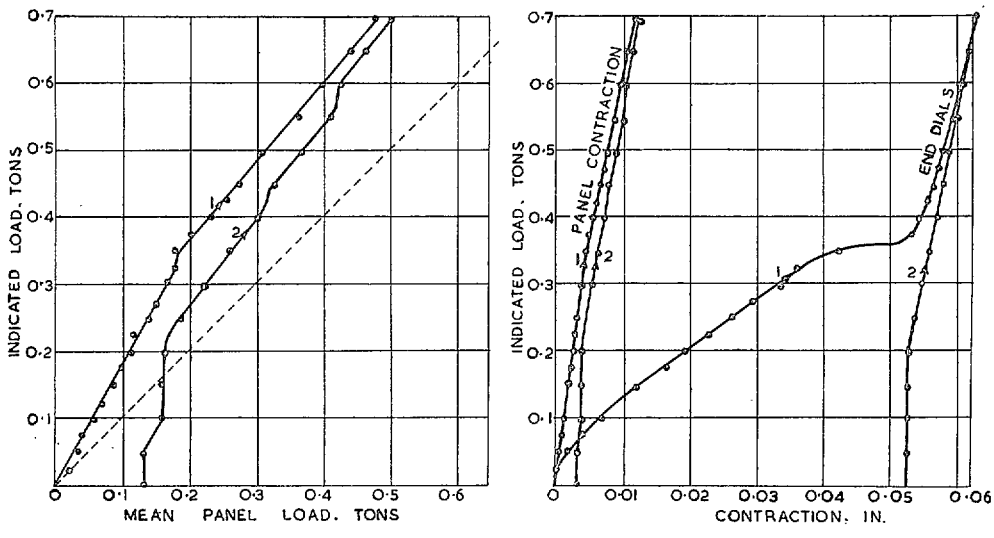

FIG. 15. Roller edge supports. Bolts tight. Friction test (panel 10A).

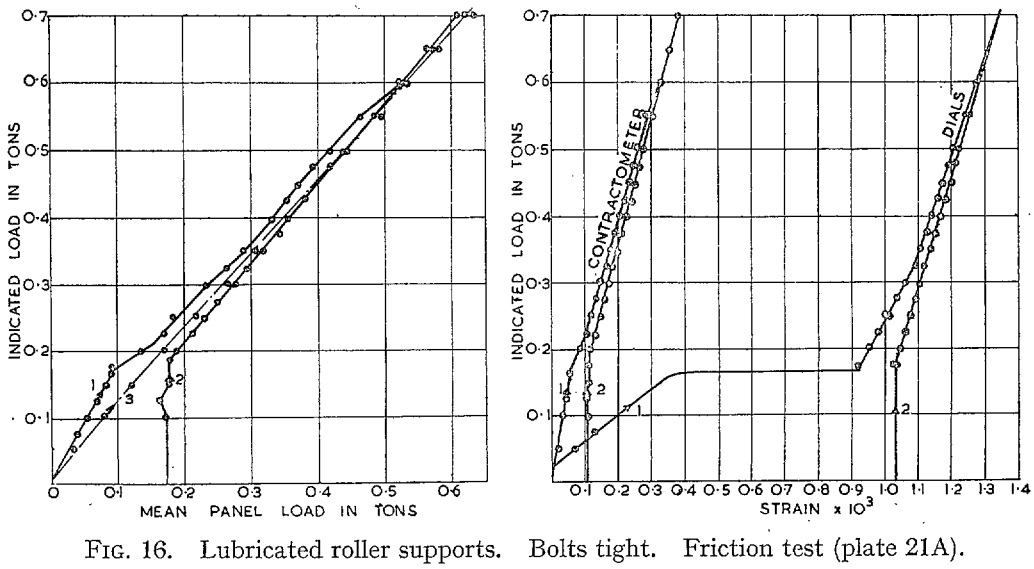

FIG. 16. Lubricated roller supports. Bolts tight. Friction test (plate 21A).

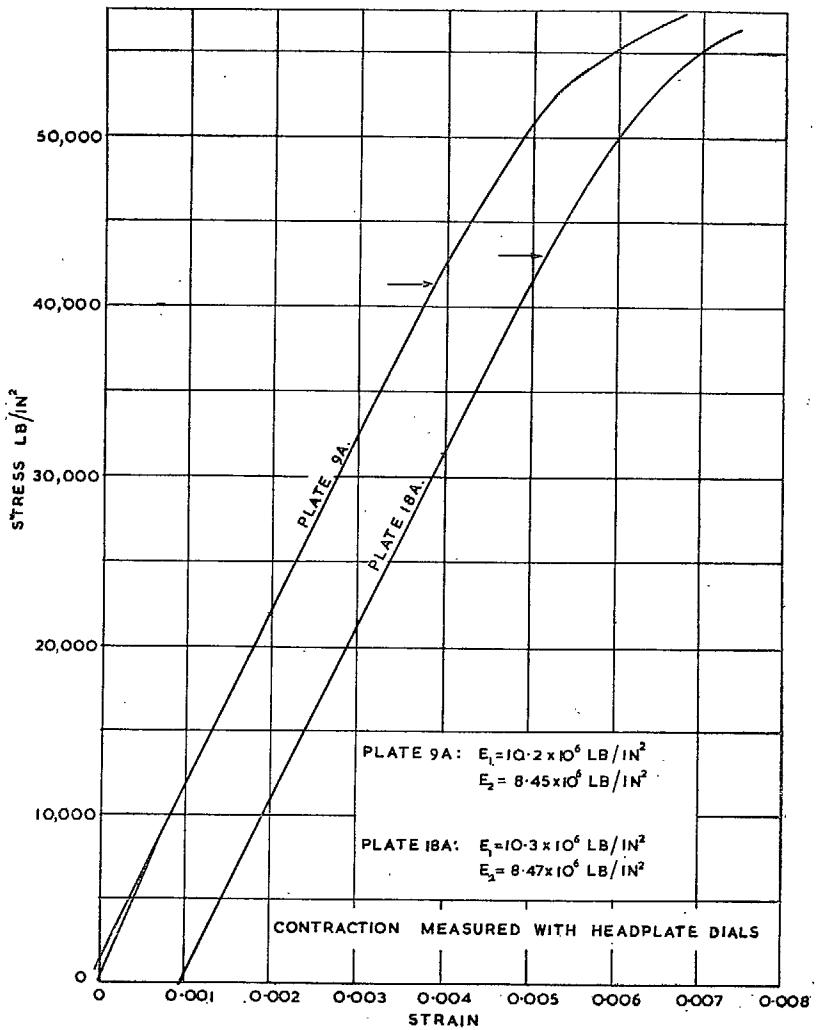

FIG. 17. Stress *vs.* strain curve for plates 9A and 18A.
Material D.T.D. 646.

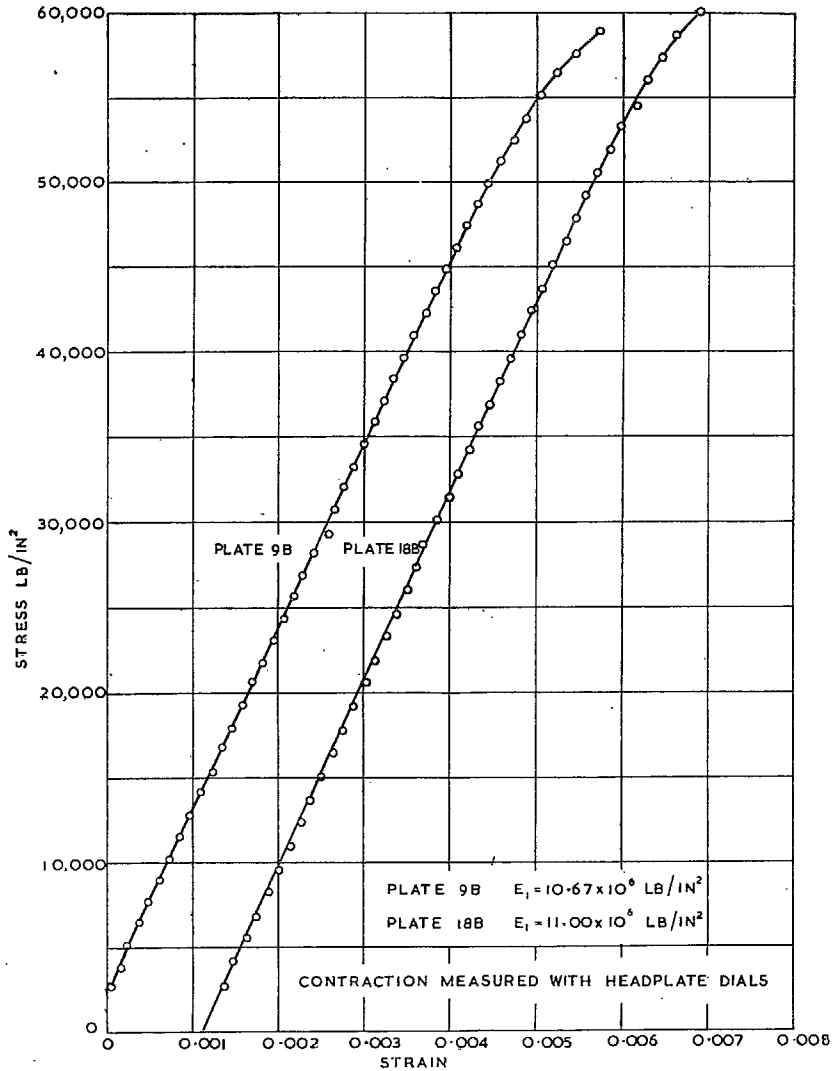

FIG. 18. Strain curve for plates 9B and 18B.
Material D.T.D. 646.

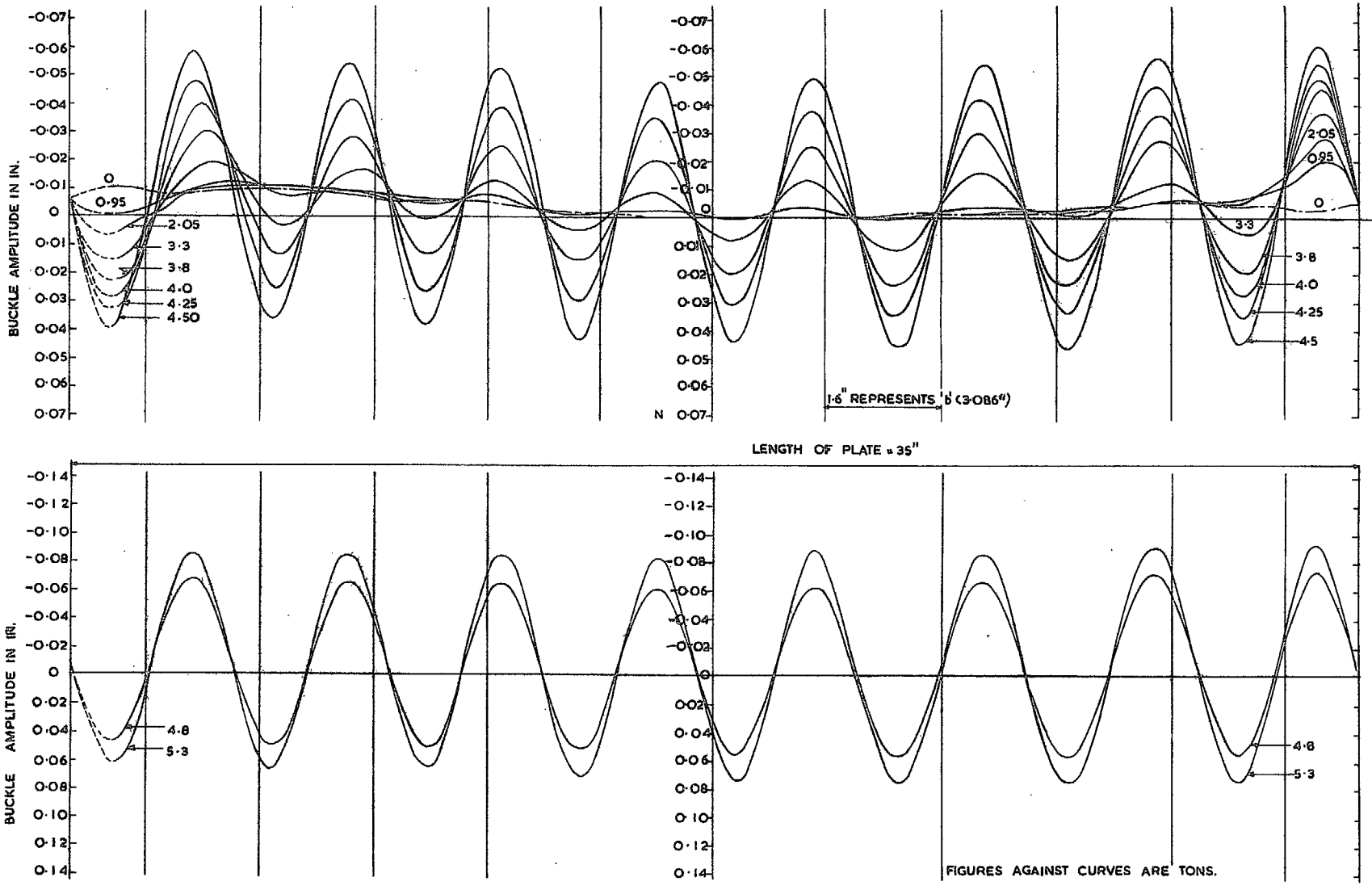

FIG 19. Plot of Buckle Amplitude for Plate. $2'(A \quad {}^{b}/_{t} = 45$.

Mat^{l} D.T.D. 546. Edges Clamped

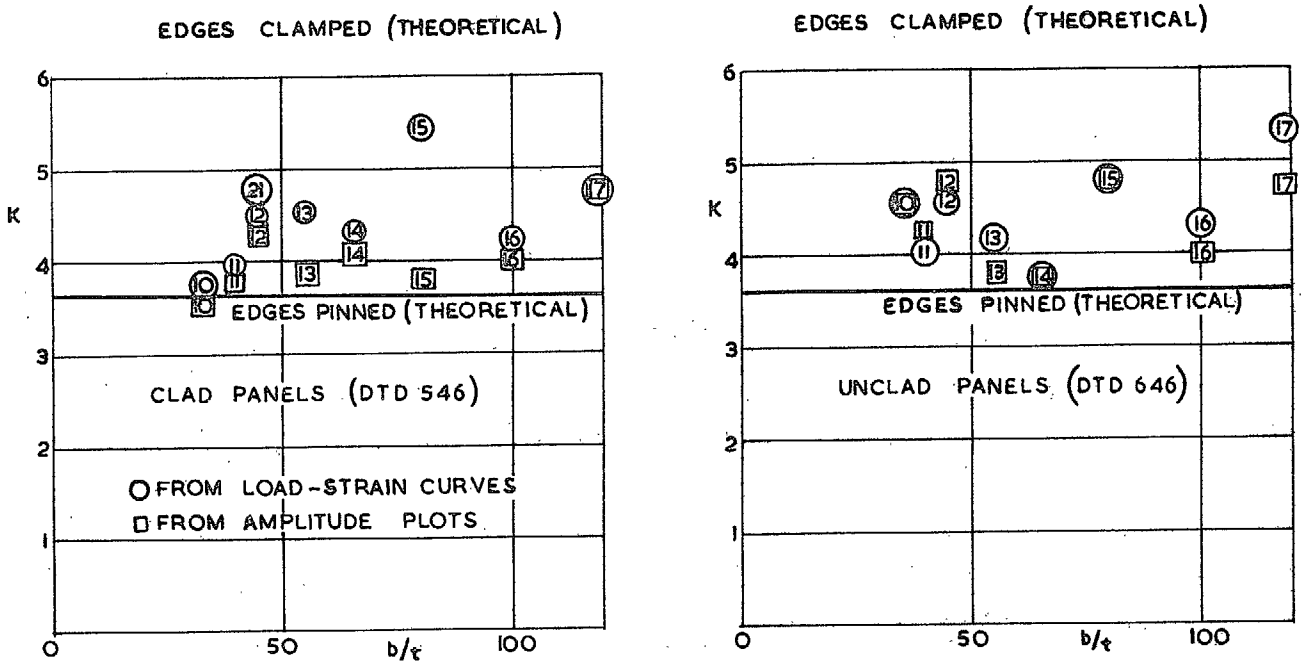

Fig. 20. Roller edge supports.
Note: Experimental points are not corrected for variations in λ/b.

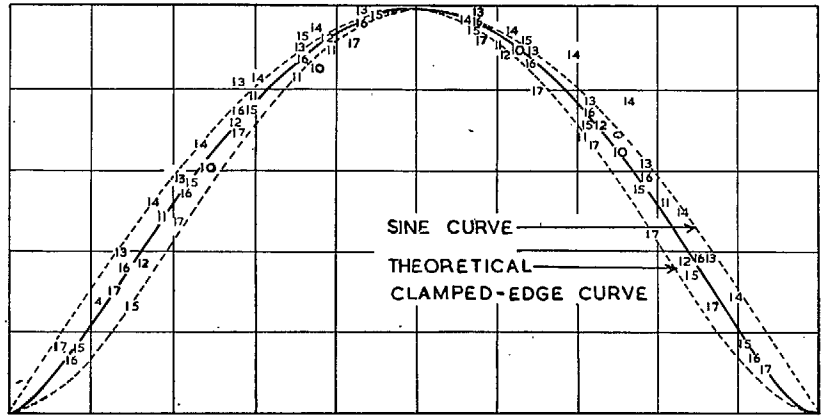

FIG. 21. Buckle cross-section at buckling strain.
D.T.D. 646. Roller edge supports.

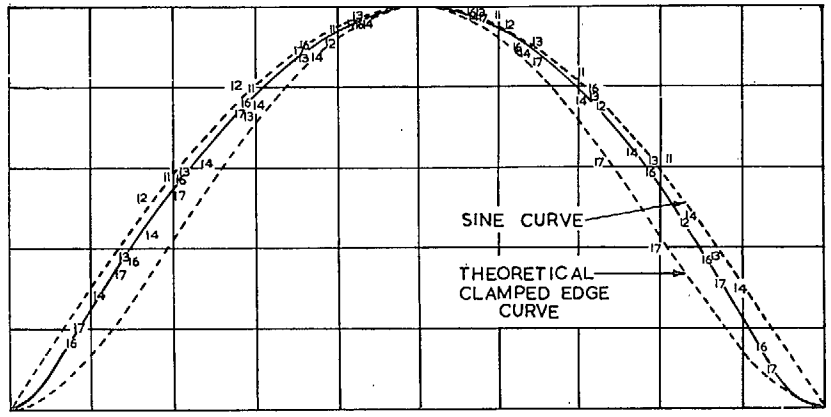

FIG. 22. Buckle cross-section at twice buckling strain.
D.T.D. 646. Roller edge supports.

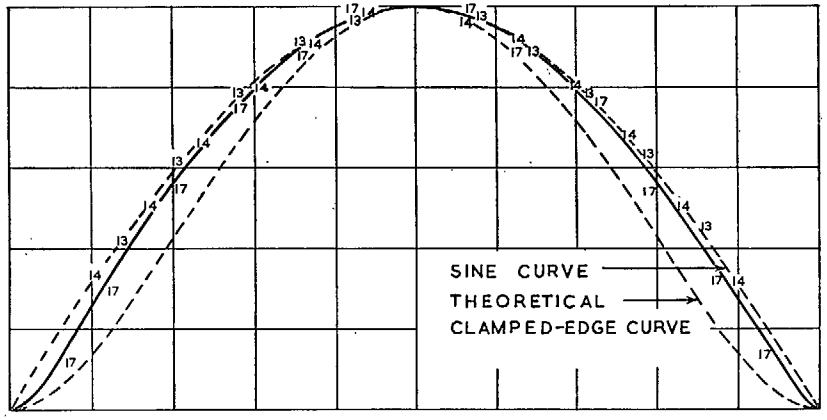

FIG. 23. Buckle cross-section at five times buckling strain.
D.T.D. 646. Roller edge supports.

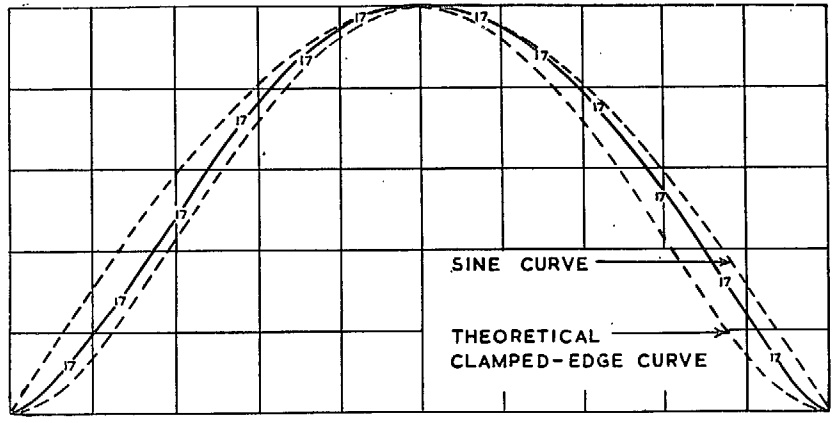

FIG. 24. Buckle cross-section at ten times buckling strain.
D.T.D. 646. Roller edge supports.

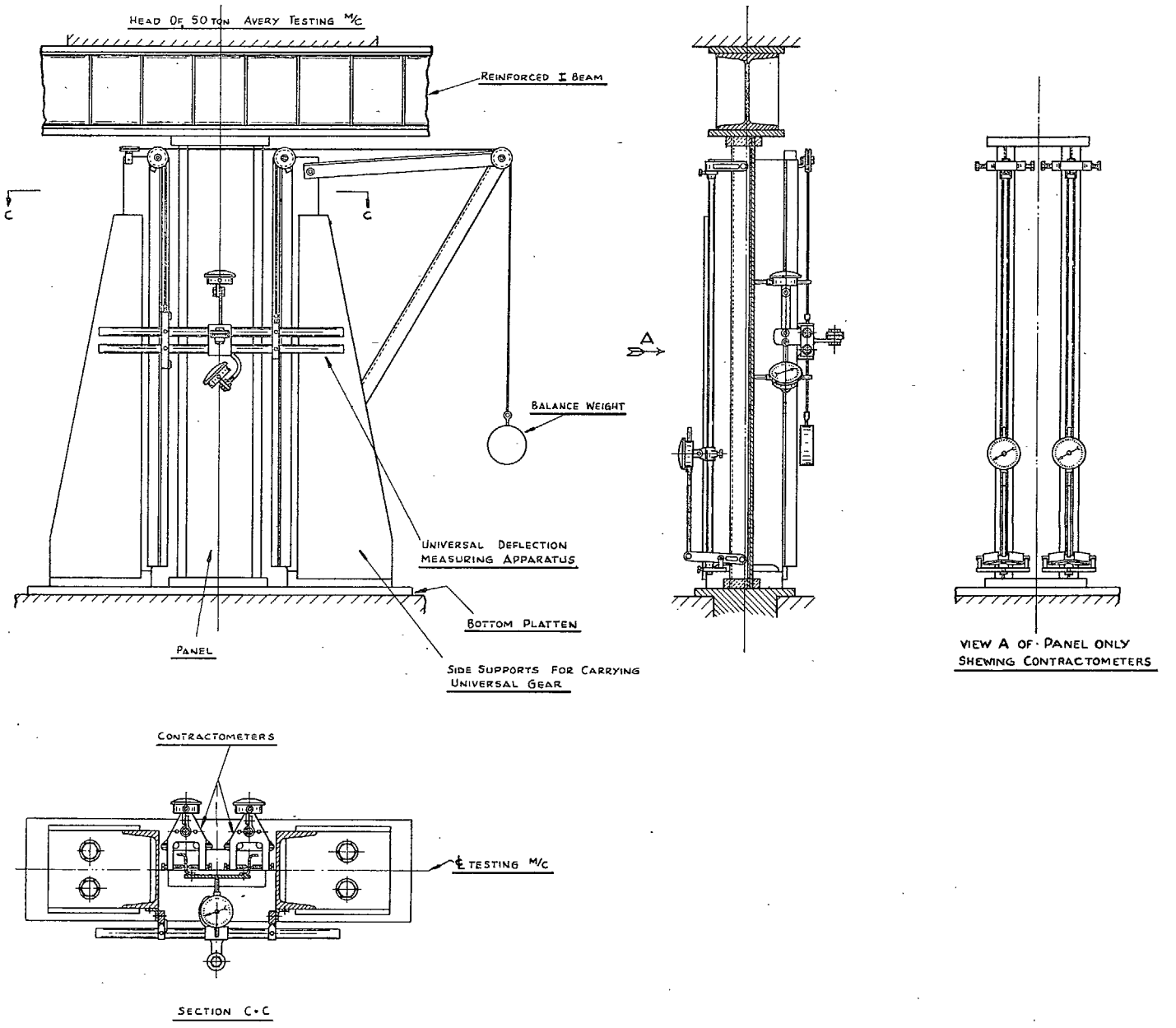
HEAD OF 50 TON AVERY TESTING M/C
REINFORCED I BEAM
C
C
BALANCE WEIGHT
A
UNIVERSAL DEFLECTION MEASURING APPARATUS
BOTTOM PLATTEN
PANEL
SIDE SUPPORTS FOR CARRYING UNIVERSAL GEAR
VIEW A OF PANEL ONLY SHEWING CONTRACTOMETERS
CONTRACTOMETERS
℄ TESTING M/C
SECTION C-C

FIG. 25.

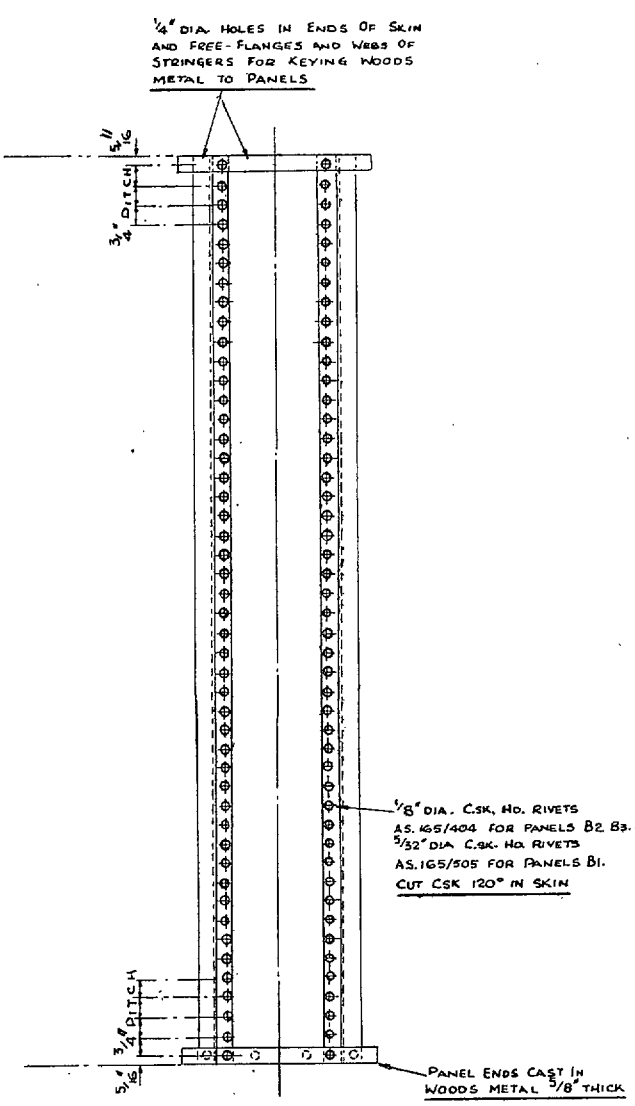

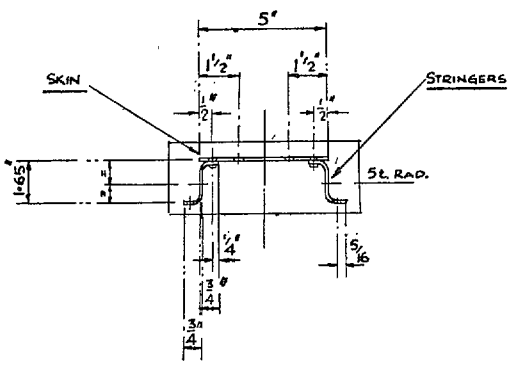

PANEL IDENTIFICATION	NO. OFF	SKIN THICKNESS	STRINGER THICKNESS	SKIN MATERIAL	STRINGER MATERIAL
B.1.	2	12 SWG.	16 SWG	DTD.646	DTD.646
B.2.	2	14 SWG.	16 SWG	DTD.646	DTD.646
B.3.	2	16 SWG	16 SWG	DTD.646	DTD.646
B.4.	2	18 SWG	16 SWG	DTD.646	DTD.646

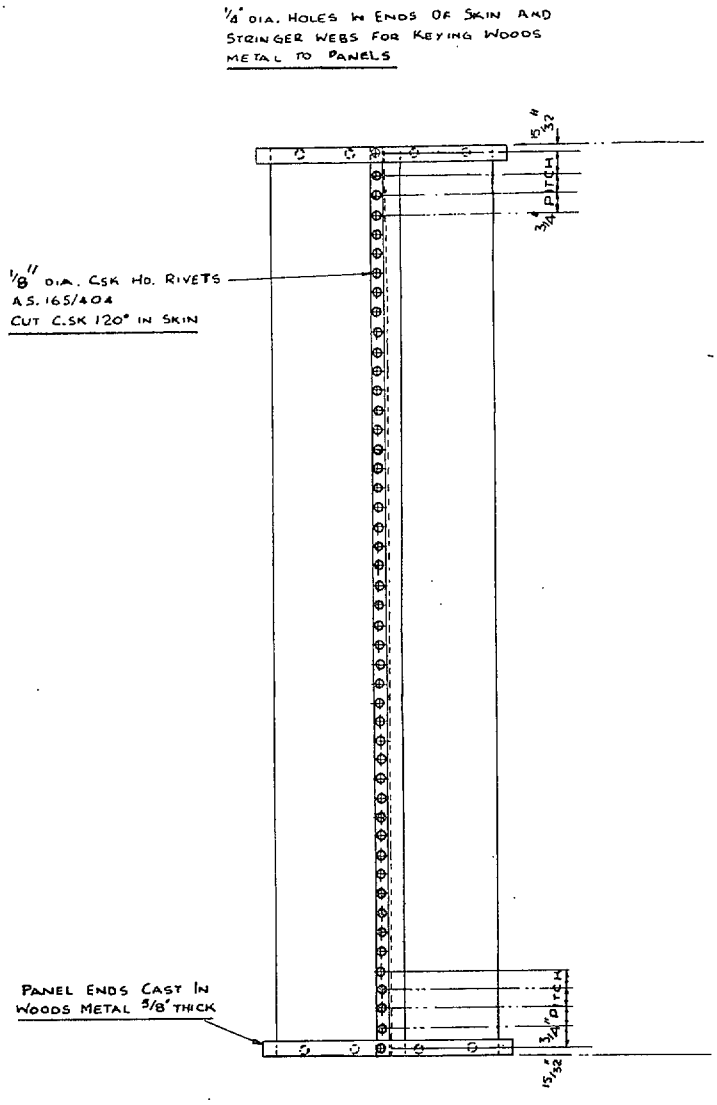

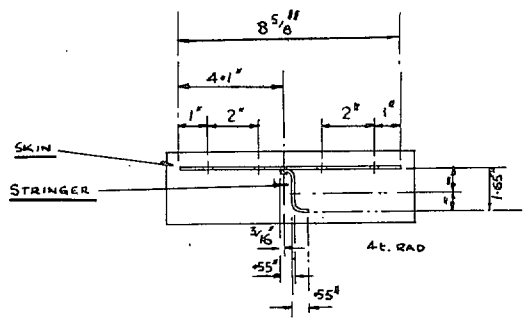

PANEL IDENTIFICATION	NO OFF	SKIN THICKNESS	STRINGER THICKNESS	SKIN MATERIAL	STRINGER MATERIAL
T1	2	14 SWG	16 SWG.	DTD 646	DTD 646
T2	2	16 SWG.	16 SWG.	DTD 646	DTD 646
T3	2	18 SWG.	16 SWG.	DTD 646	DTD 646
T4	2	20 SWG.	16 SWG	DTD 646	DTD646
T5	2	22 SWG	16 SWG	DTD 646	DTD646.

FIG. 26.

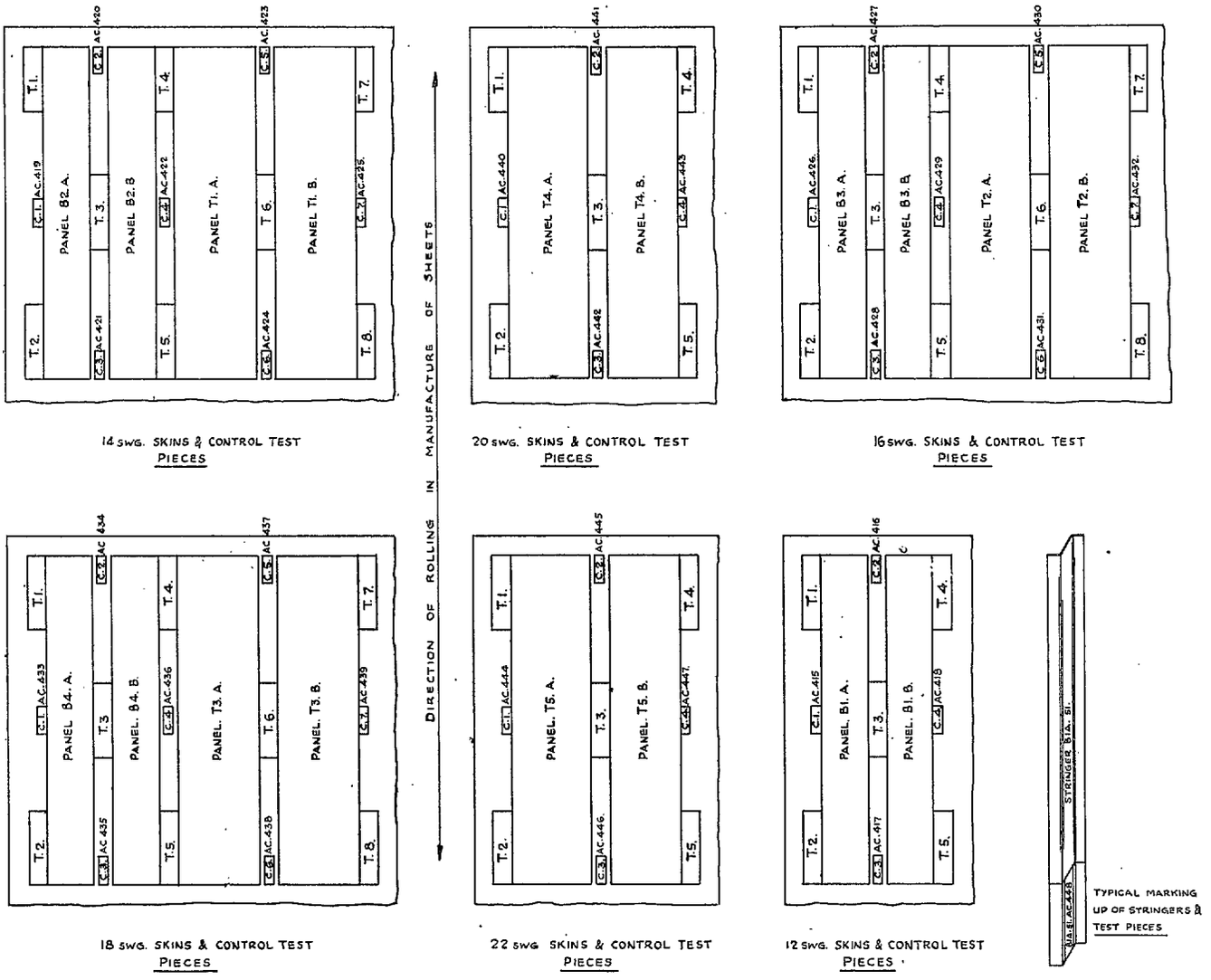

PANEL IDENTIFICATION	STRINGER IDENTIFICATION AND TEST PIECES.
B1. A.	B1A. S1. AC.448 & B1A. S2. AC 449
B1. B	B1B. S1. AC.450 & B1B. S2. AC.451
B2. A.	B2A. S1. AC.452 & B2A. S2. AC.453
B2. B.	B2B. S1. AC.454 & B2B. S2. AC.455
B3. A.	B3A. S1. AC.456 & B3A. S2. AC.457
B3 B.	B3B. S1. AC.458 & B3B. S2. AC.459
B4. A.	B4A. S1 AC.460 & B4A. S2. AC 461
B4. B	B4B. S1 AC.462 & B4B. S2. AC.463
T1. A.	T1A. S1
T1. B.	T1B. S1
T2. A.	T2A. S1.
T2. B	T2B S1
T3. A.	T3A. S1
T3. B.	T3B. S1.
T4. A.	T4A. S1.
T4. B.	T4B. S1
T5. A.	T5A. S1.
T5. B.	T5B. S1.

STRINGER COMPRESSION TEST PIECES.

EACH PANEL SKIN IS MARKED WITH THE PANEL IDENTIFICATION TOGETHER WITH THE BATCH & SHEET Nos. FROM WHICH IT WAS MADE.
EACH STRINGER IS MARKED WITH THE PANEL IDENTIFICATION TO WHICH IT BELONGS TOGETHER WITH THE BATCH & SHEET Nos. FROM WHICH IT WAS MADE. STRINGERS ON B PANELS SUFFIXED 1 & 2 RESPECTIVELY ADDITIONALLY.
BLANKS FOR CONTROL TEST SPECIMENS:- 10" x 2" FOR TENSILE TESTS & 3" x 1" FOR COMPRESSION TESTS
EACH TEST PIECE IS MARKED WITH ITS IDENTIFICATION (AS SHEWN ABOVE) TOGETHER WITH THE BATCH & SHEET Nos. FROM WHICH IT WAS CUT. FOR SKINS.
FOR STRINGER TEST PIECES A BLANK 3½" LONG WAS CUT FROM THE EXCESS LENGTH OF EACH STRINGER AFTER FORMING.
TEST PIECES MARKED WITH THE BATCH & SHEET Nos. OF THE SHEET FROM WHICH THEY WERE CUT TOGETHER WITH THE IDENTIFICATION OF THEIR RESPECTIVE STRINGERS.

FIG. 27.

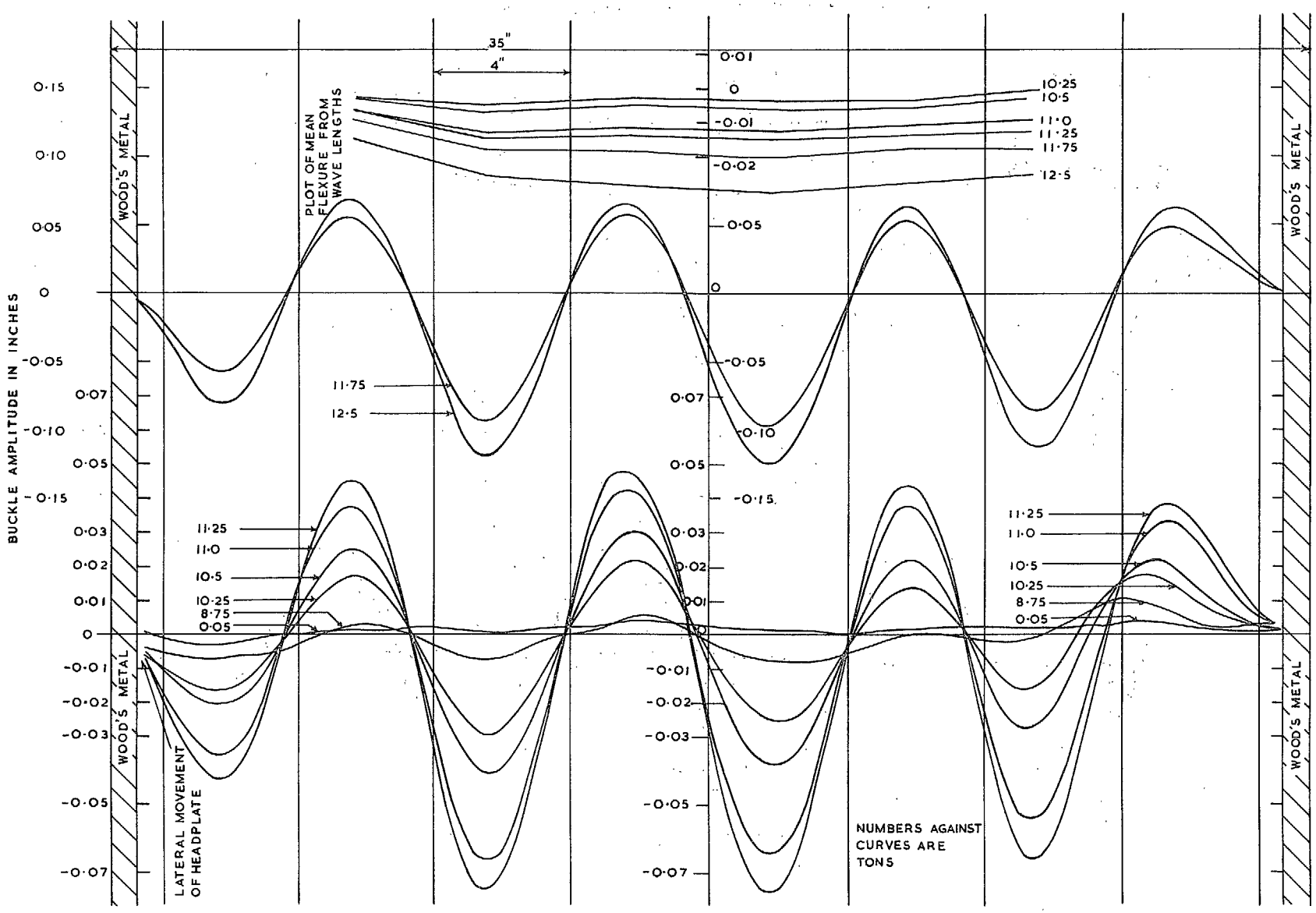

FIG. 28. Panel B1A. Mat[1] DTD 646. Plot of Wave Amplitude on Centre Line of Panel.

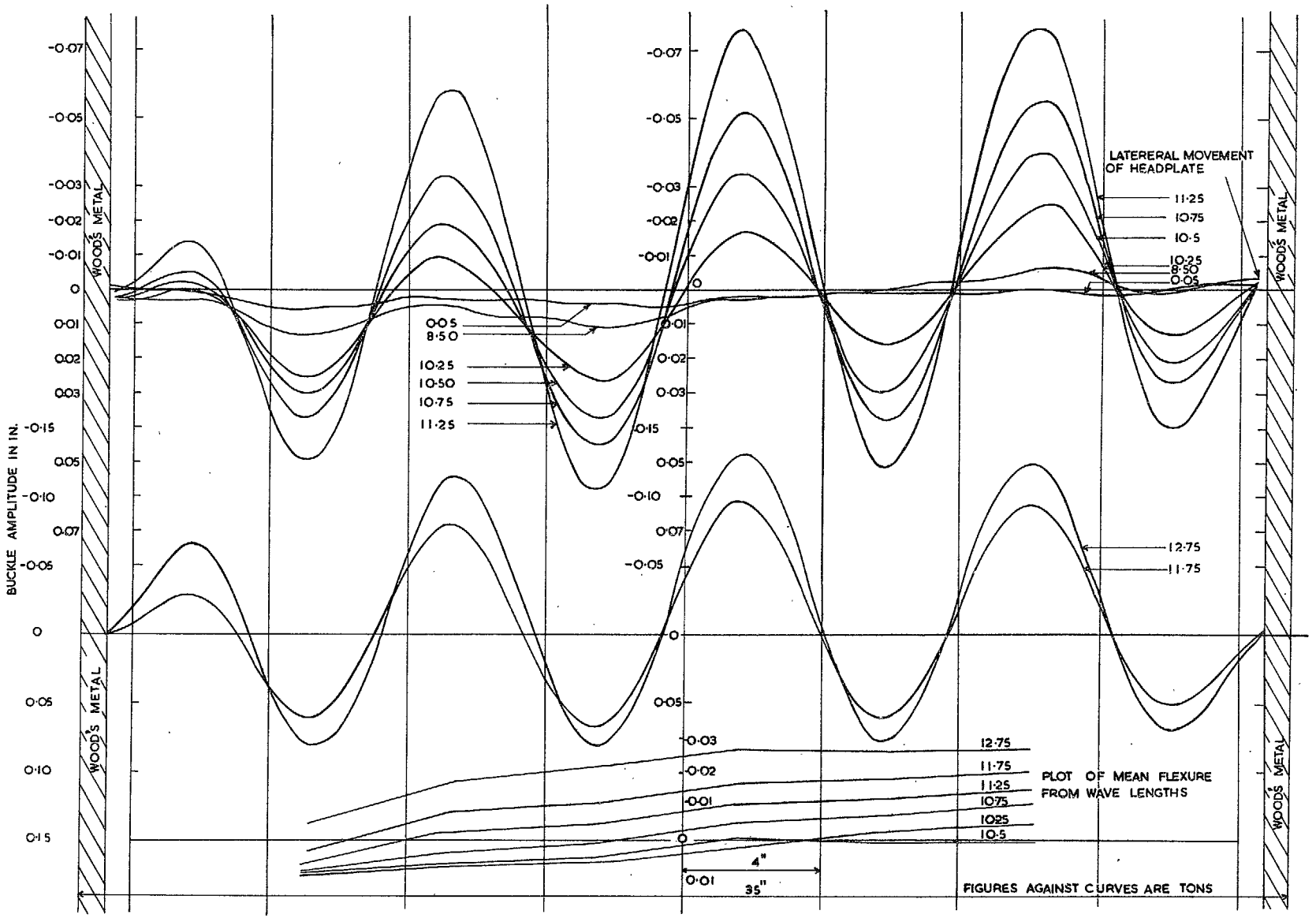

FIG. 29. Panel B.I.B. Mat[1] DTD 646. Plot of Wave Amplitude on Centre Line of Panel.

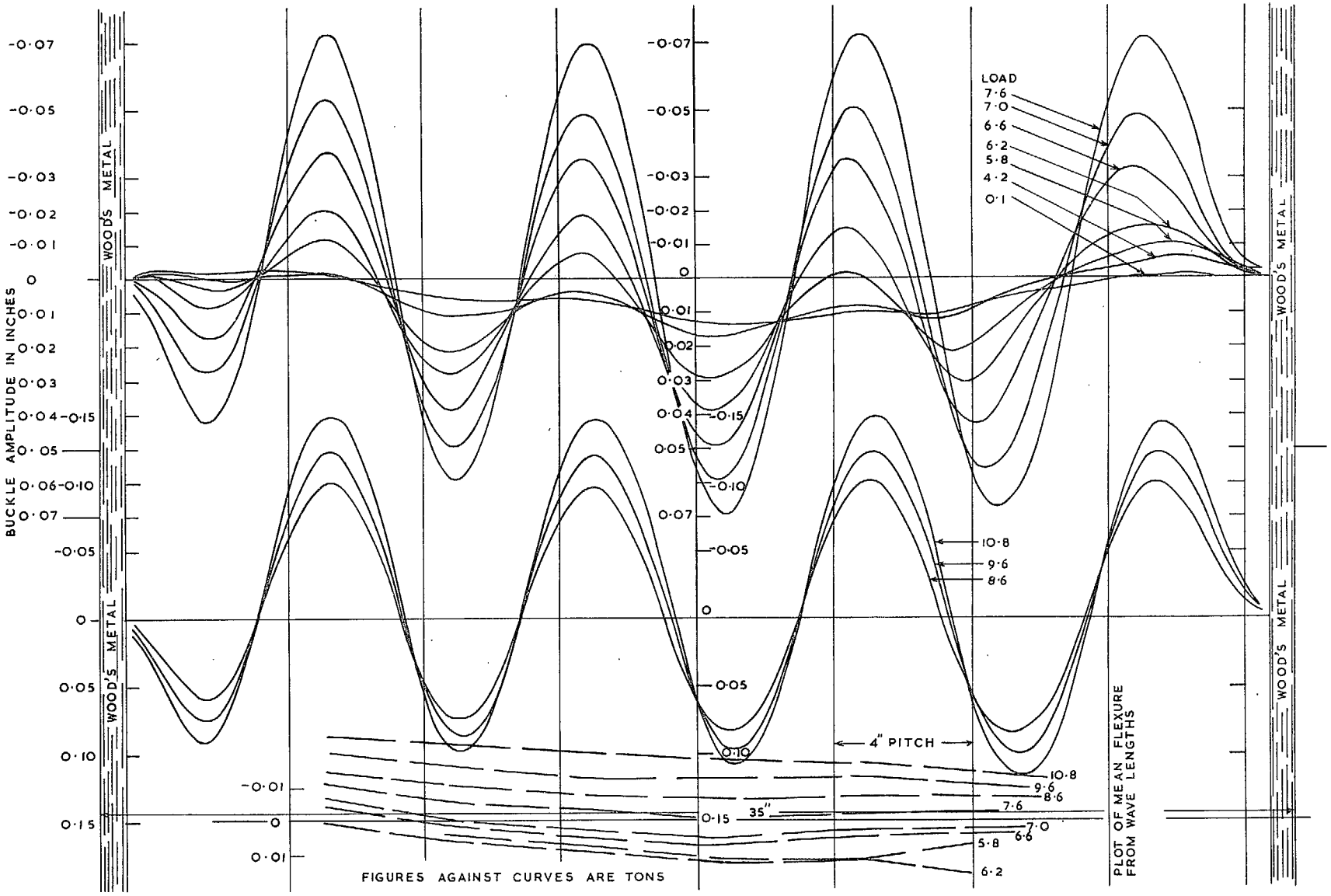

FIG. 30. Panel B2A: Plot of Buckle Amplitude down ℄ of Panel.

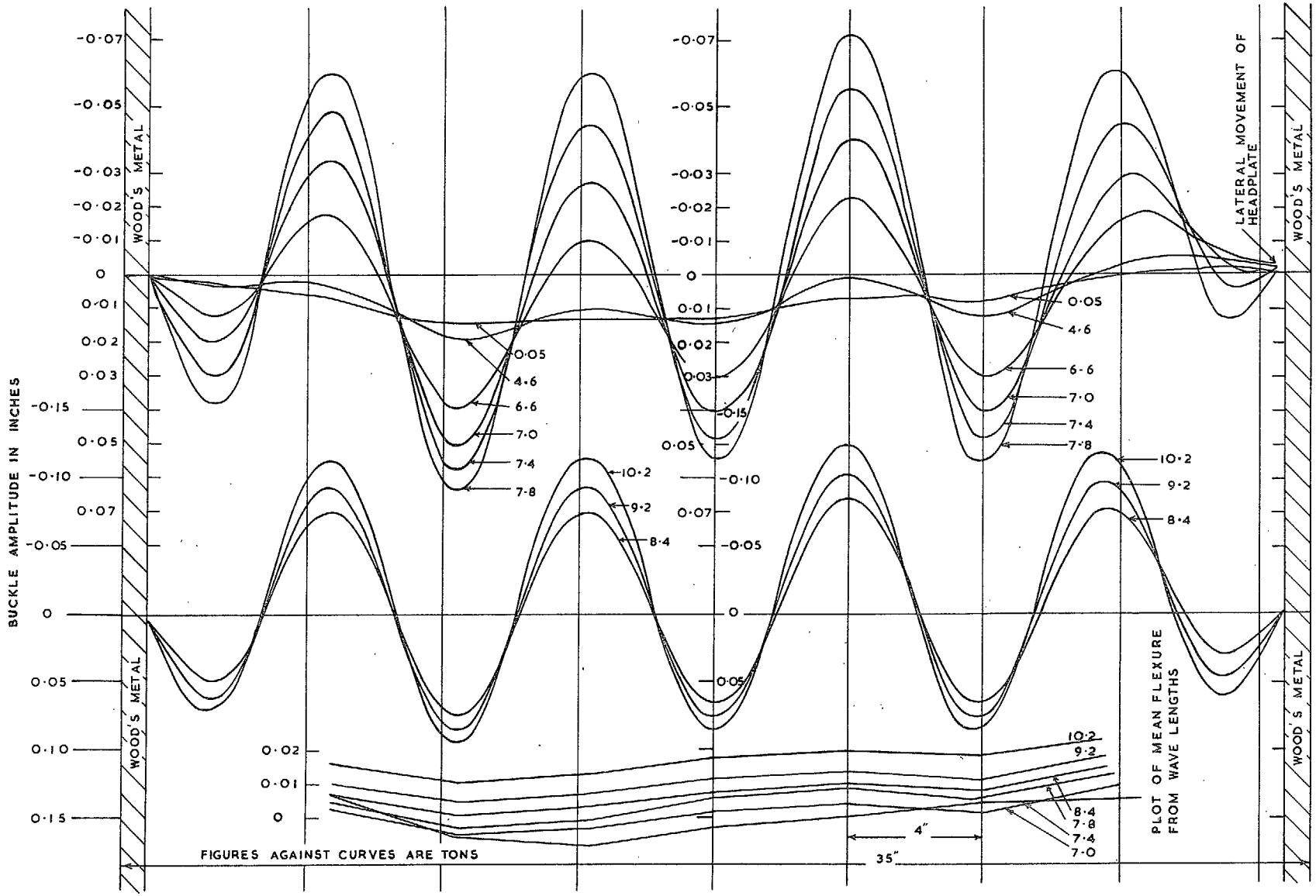

FIG.31. Panel B2B. Mat^{l} DTD 646. Plot of Wave Amplitude on Centre Line of Panel.

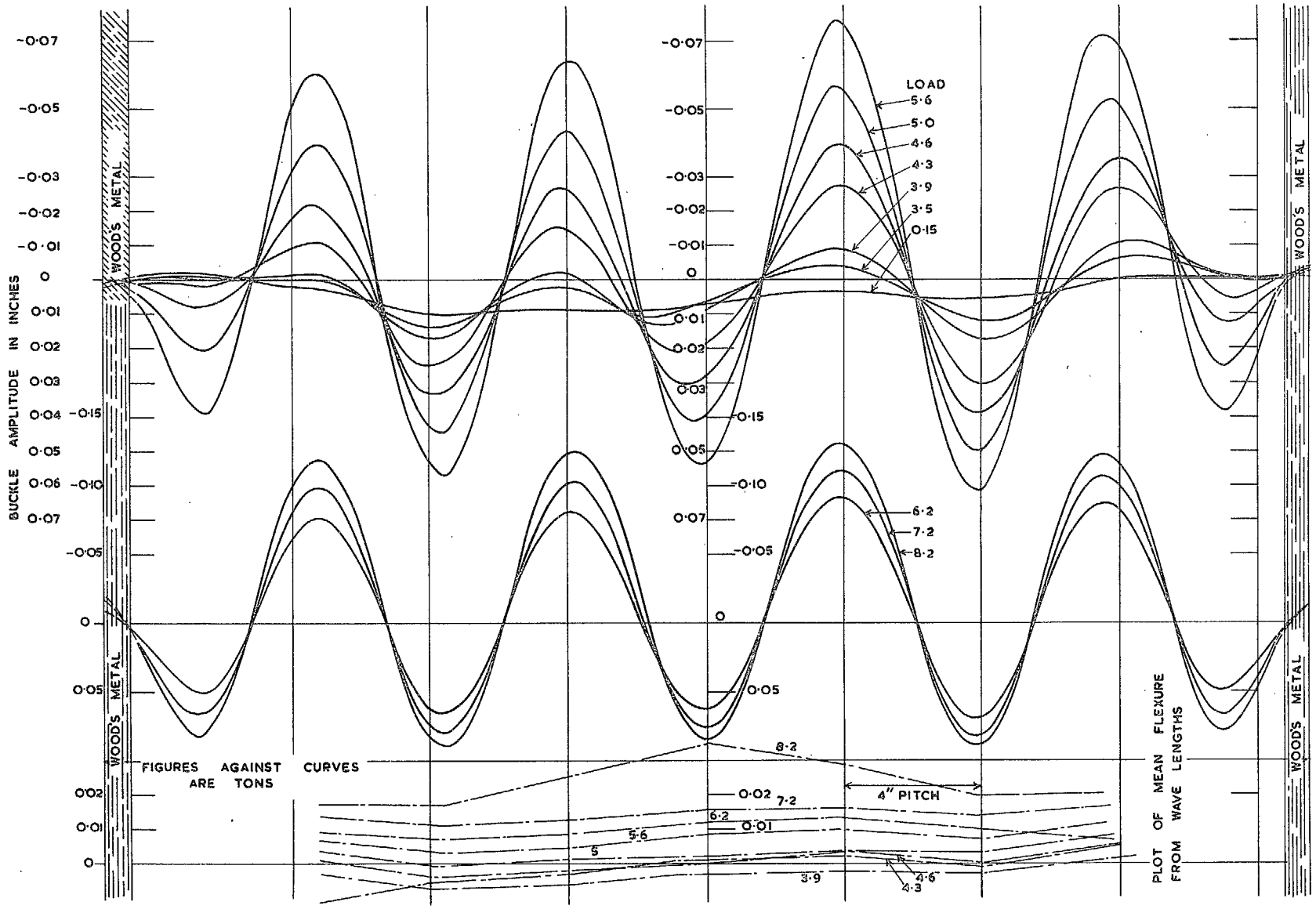

FIG 32 Panel B3A: Plot of Buckle Amplitude down ℄ of Panel

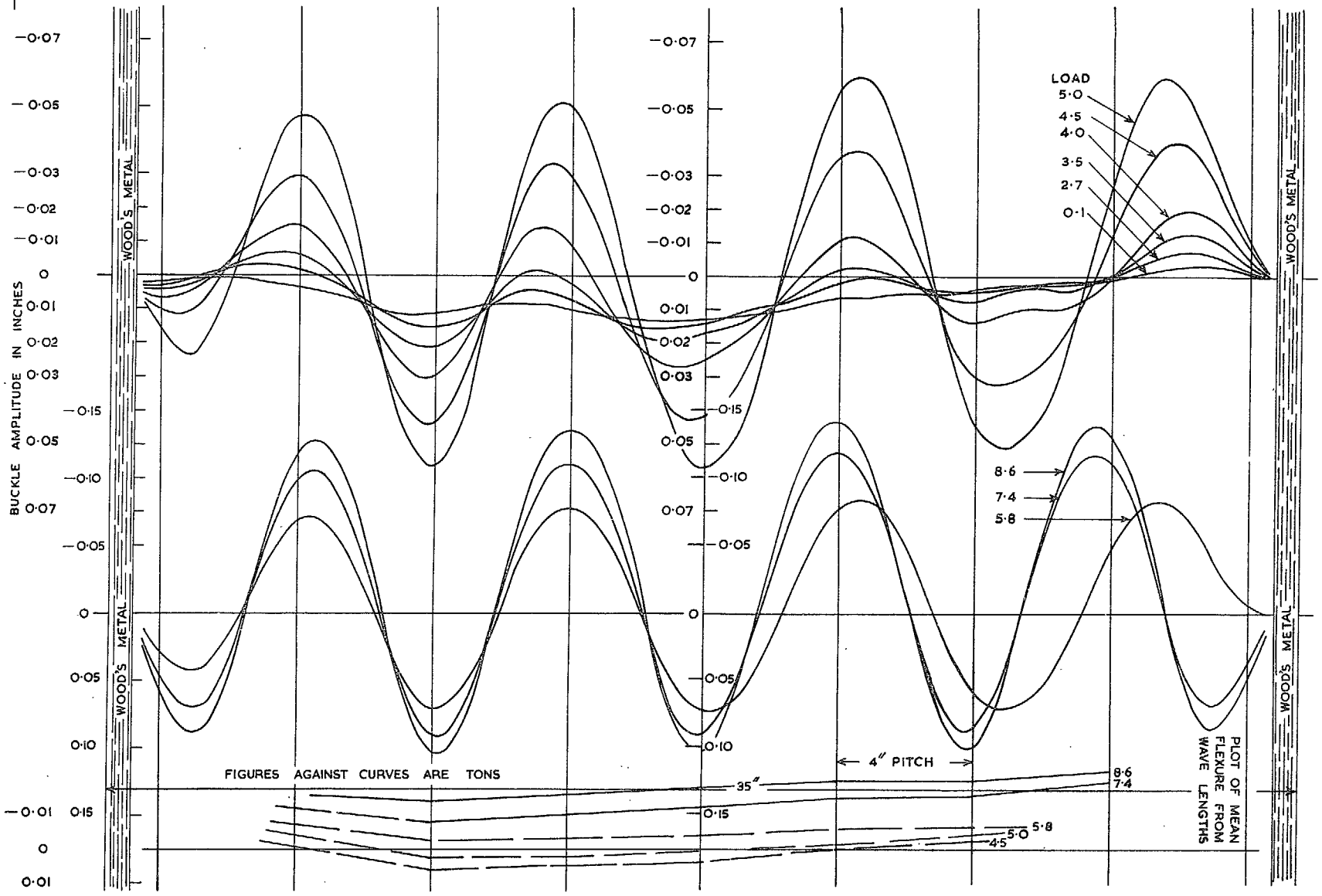

FIG. 33. Panel B3B: Plot of Buckle Amplitude down ℄ of Panel.

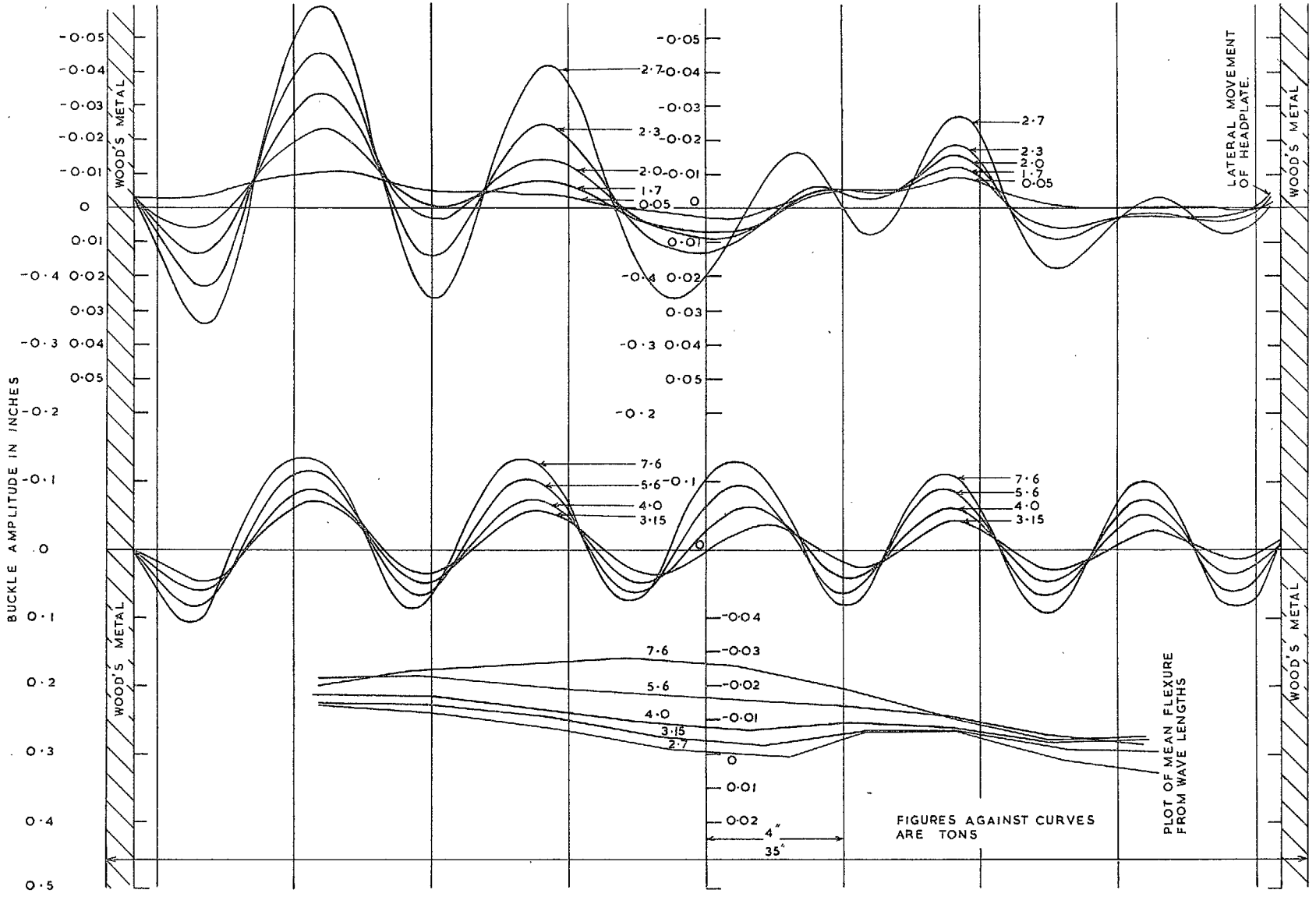

FIG. 34. Panel B4A Mat½ DTD 646. Plot of Wave Amplitude on Centre Line of Panel.

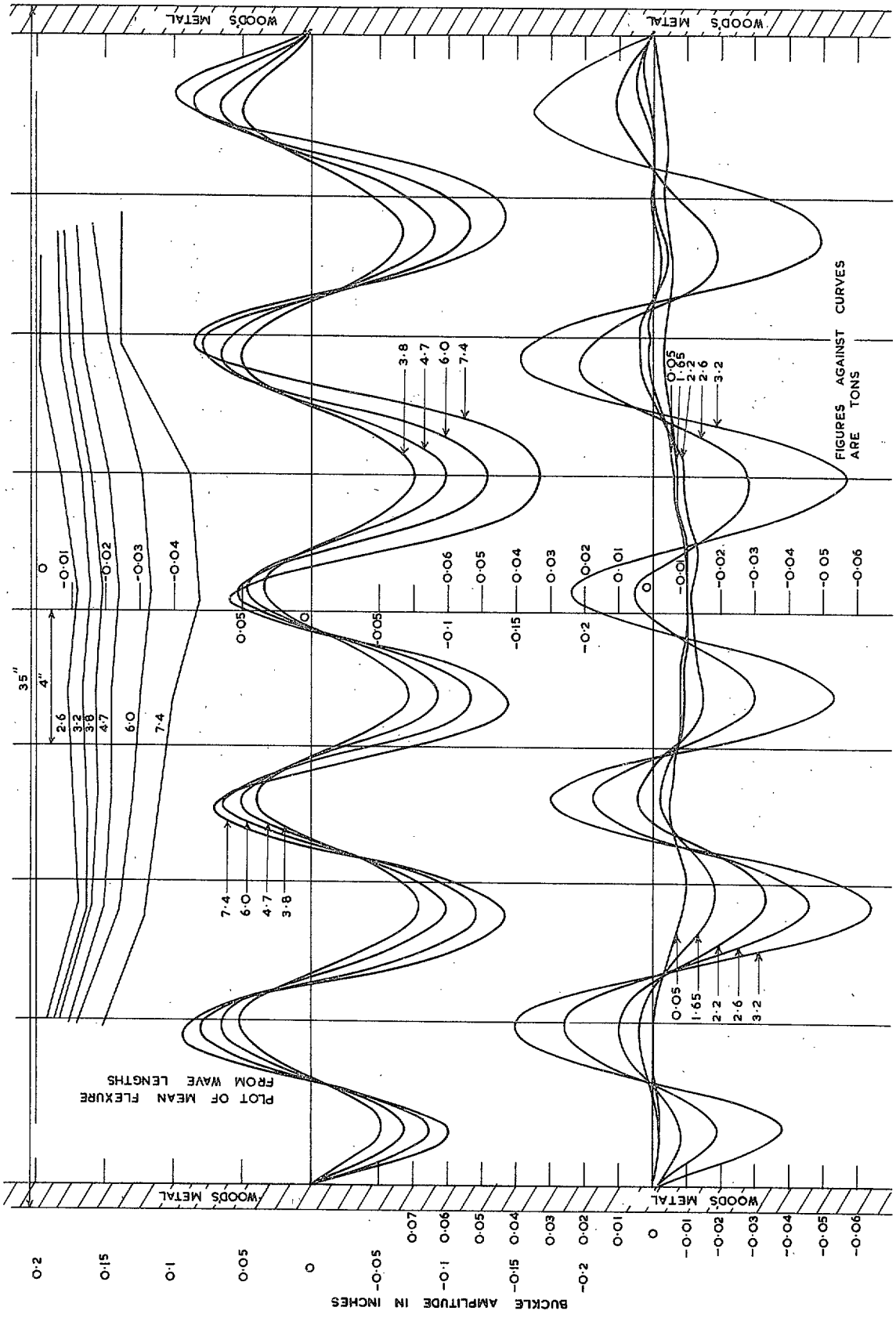

FIG. 35 Panel B4B. Mat^{l}. DTD 646. Plot of Wave Amplitude on Centre Line of Panel.

A8416 Wt.16 1,014 4/53 Gp.959 Fosh & Cross Ltd., Lond

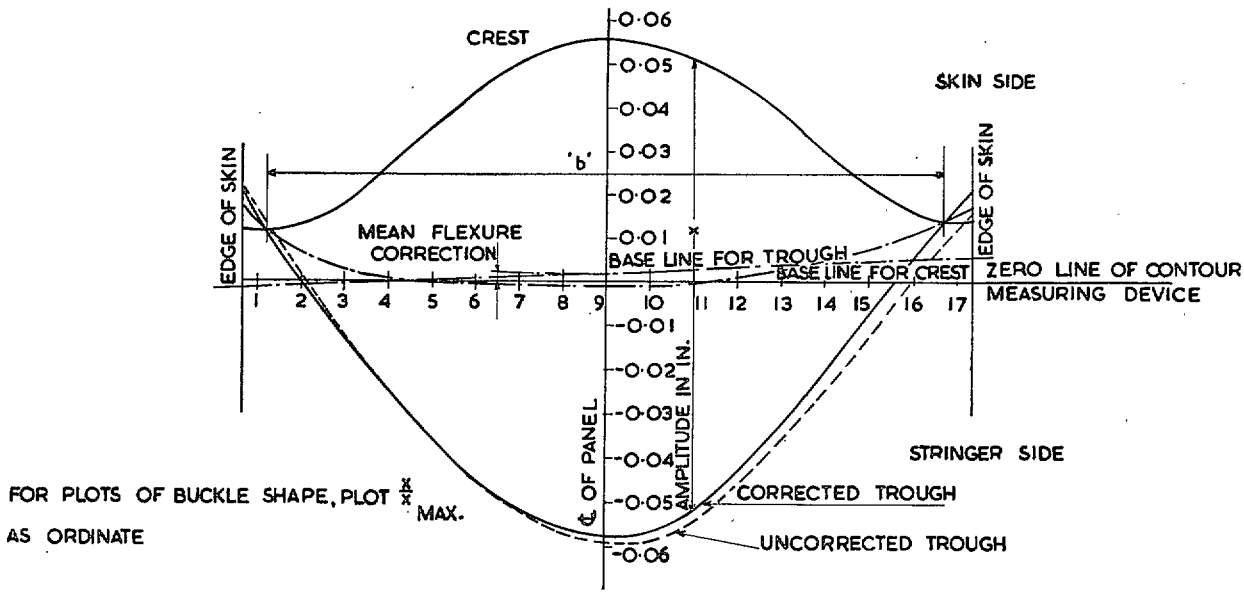

FIG. 36. Method used to find b, the distance between longitudinal skin nodal lines, and to obtain co-ordinates for the cross-sectional buckle shape. (As drawn for panel B.3B at five tons load.)

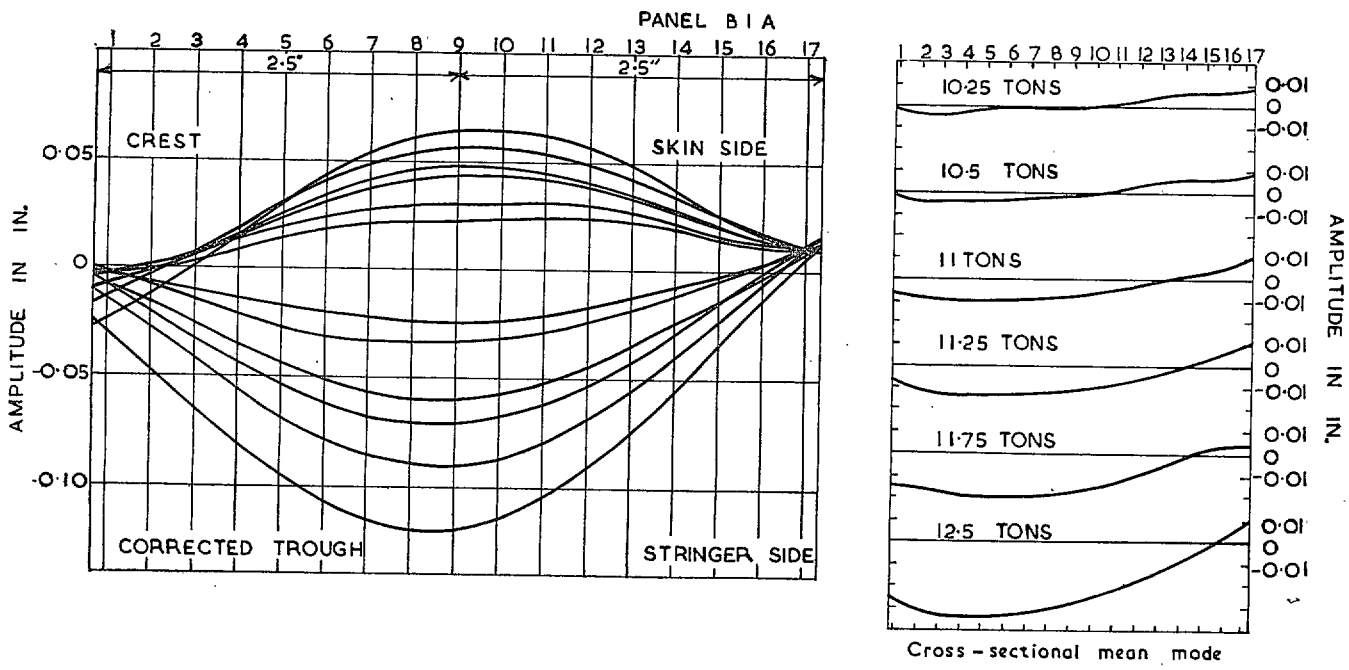

FIG. 37. Readings obtained on test of cross-sectional buckle shape.

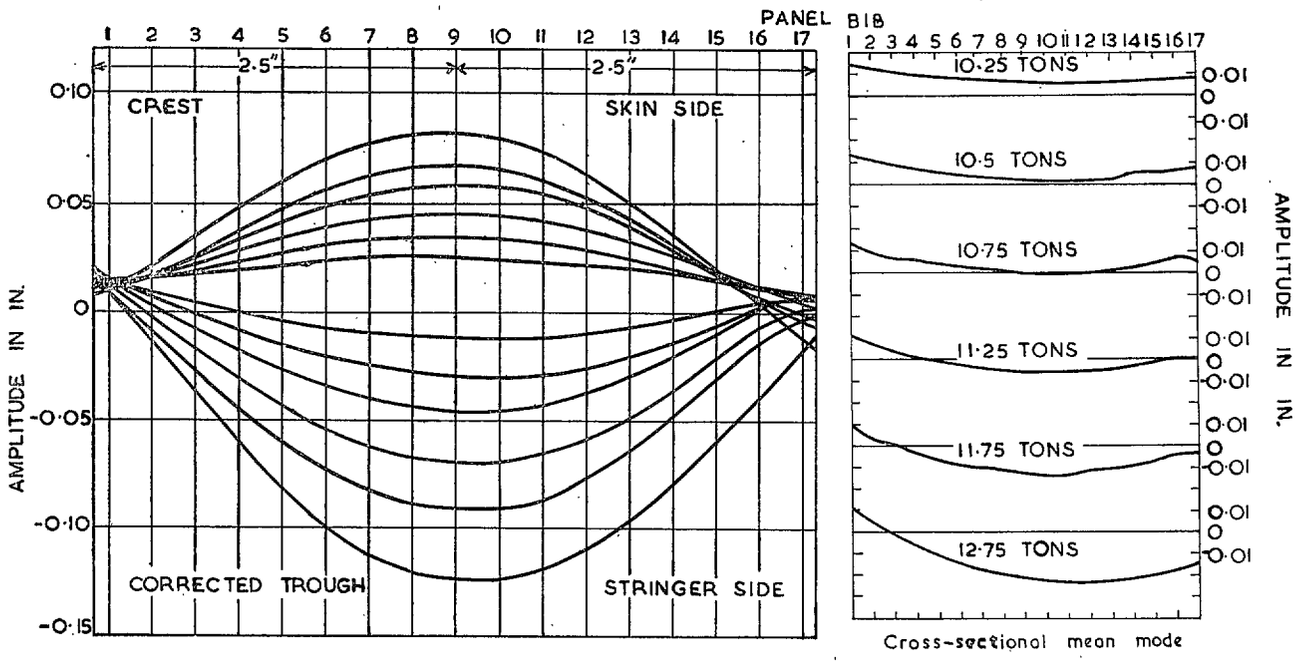

FIG. 38. Readings obtained on test of cross-sectional buckle shape.

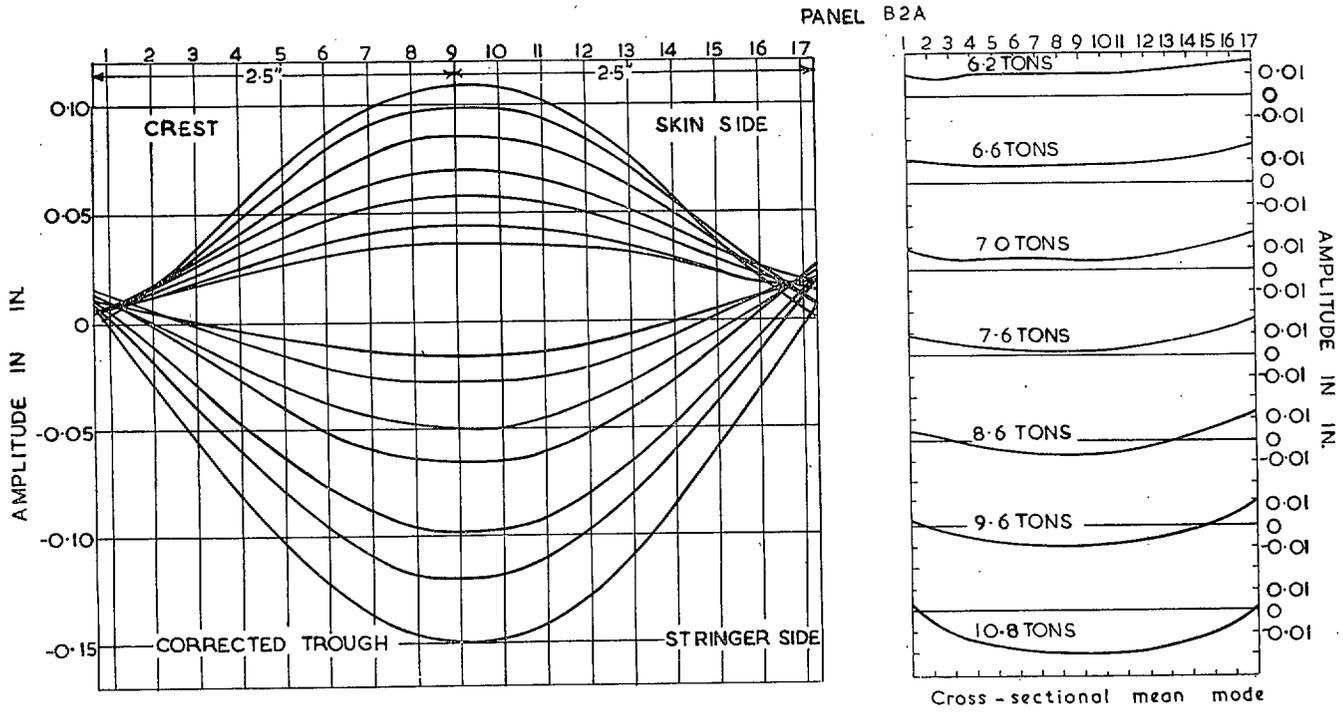

FIG. 39. Readings obtained on test of cross-sectional buckle shape.

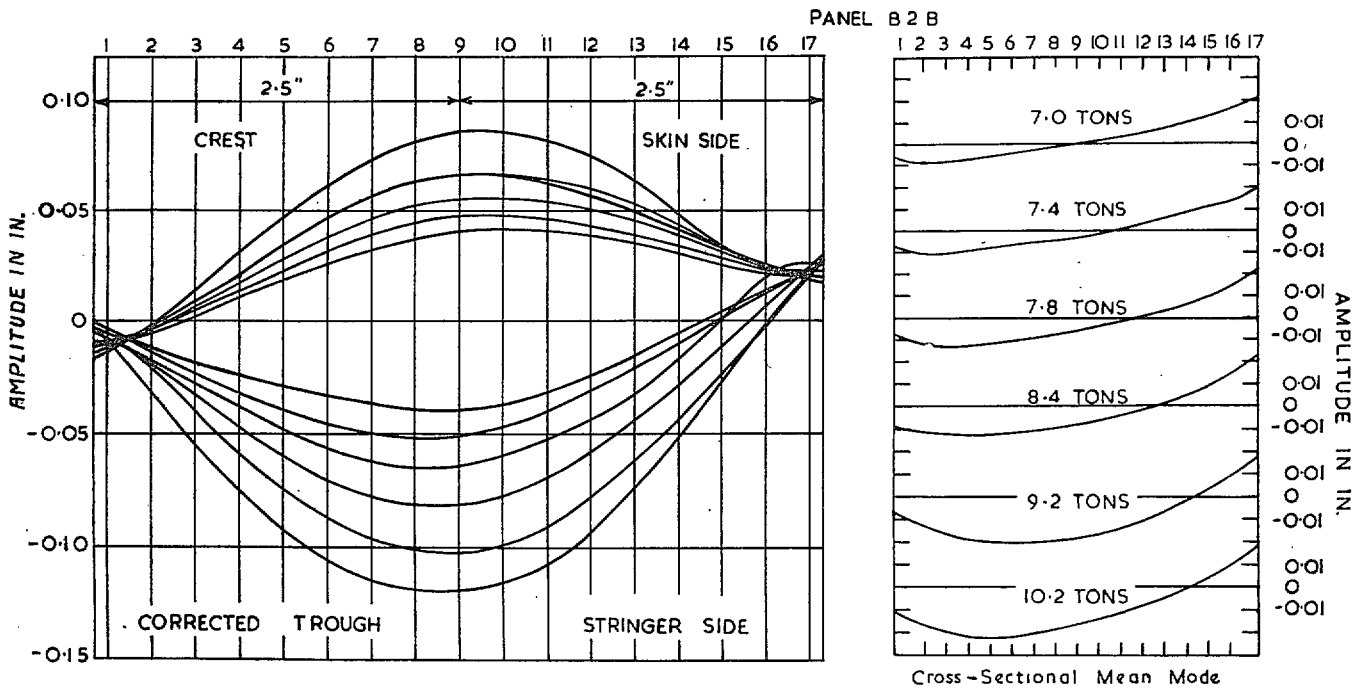

FIG. 40. Readings obtained on test of cross-sectional buckle shape.

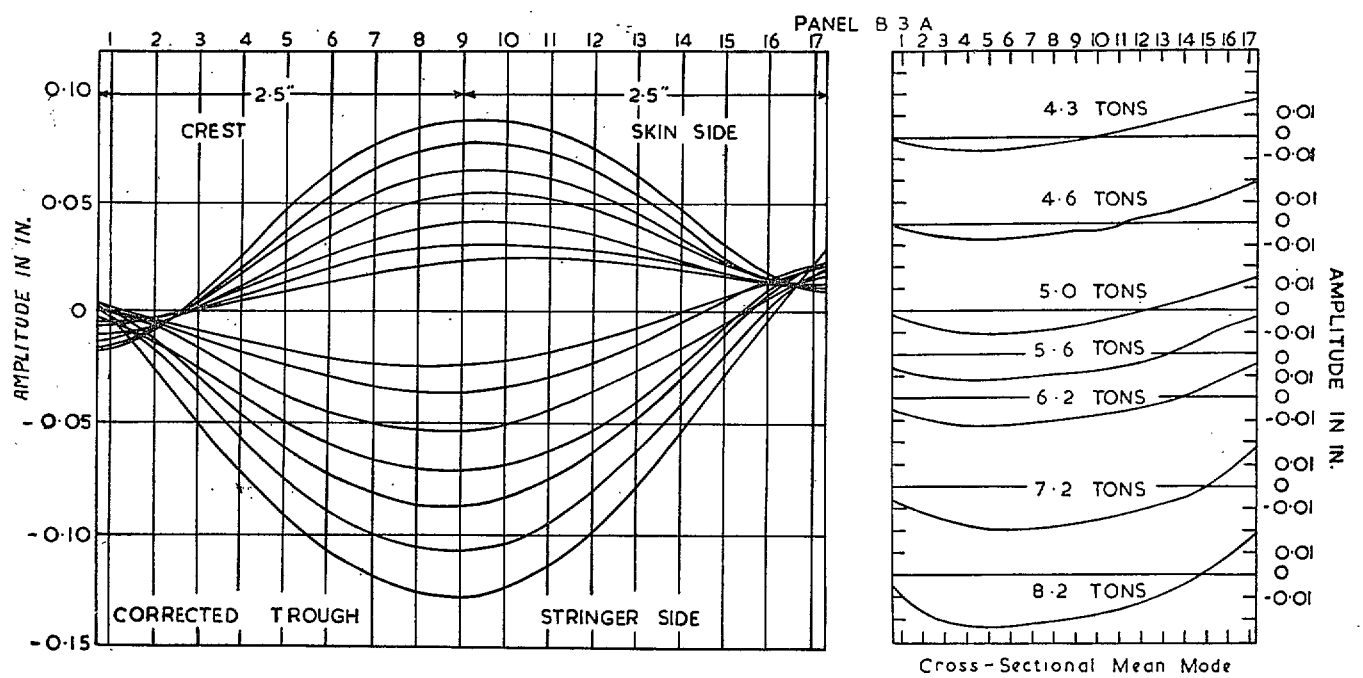

FIG. 41. Readings obtained on test of cross-sectional buckle shape.

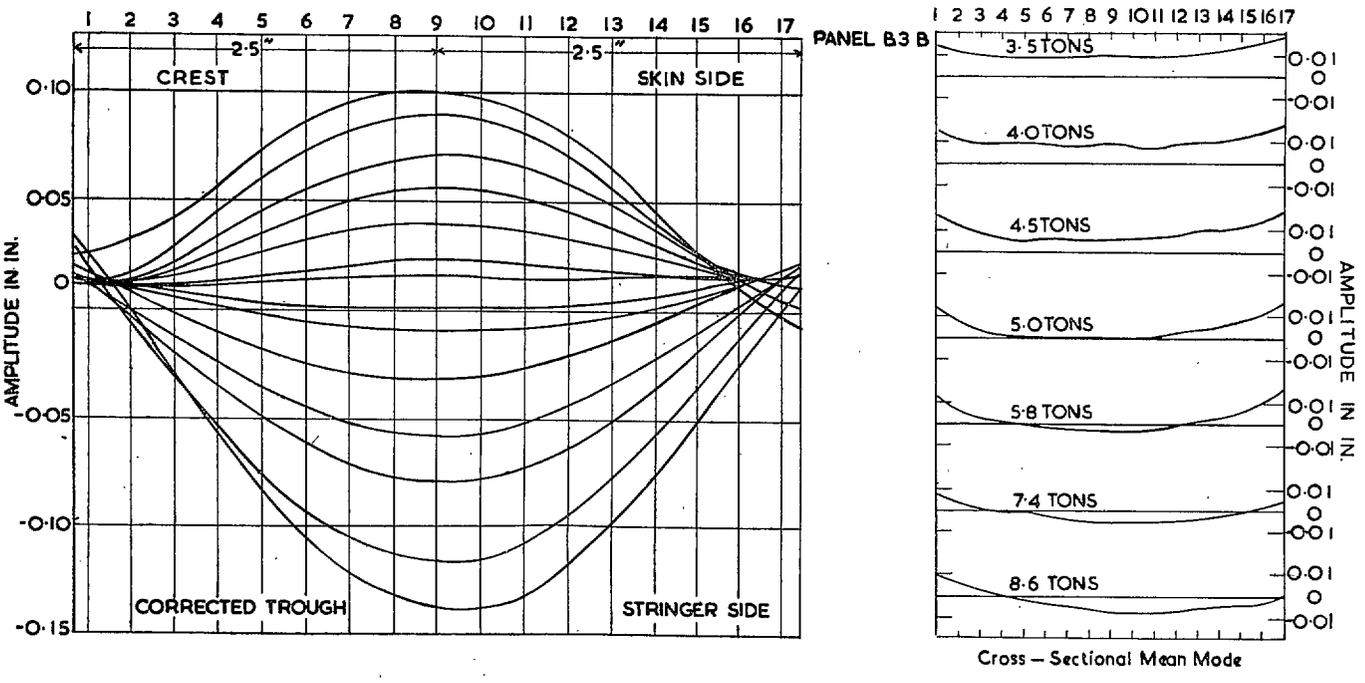

FIG. 42. Readings obtained on test of cross-sectional buckle shape.

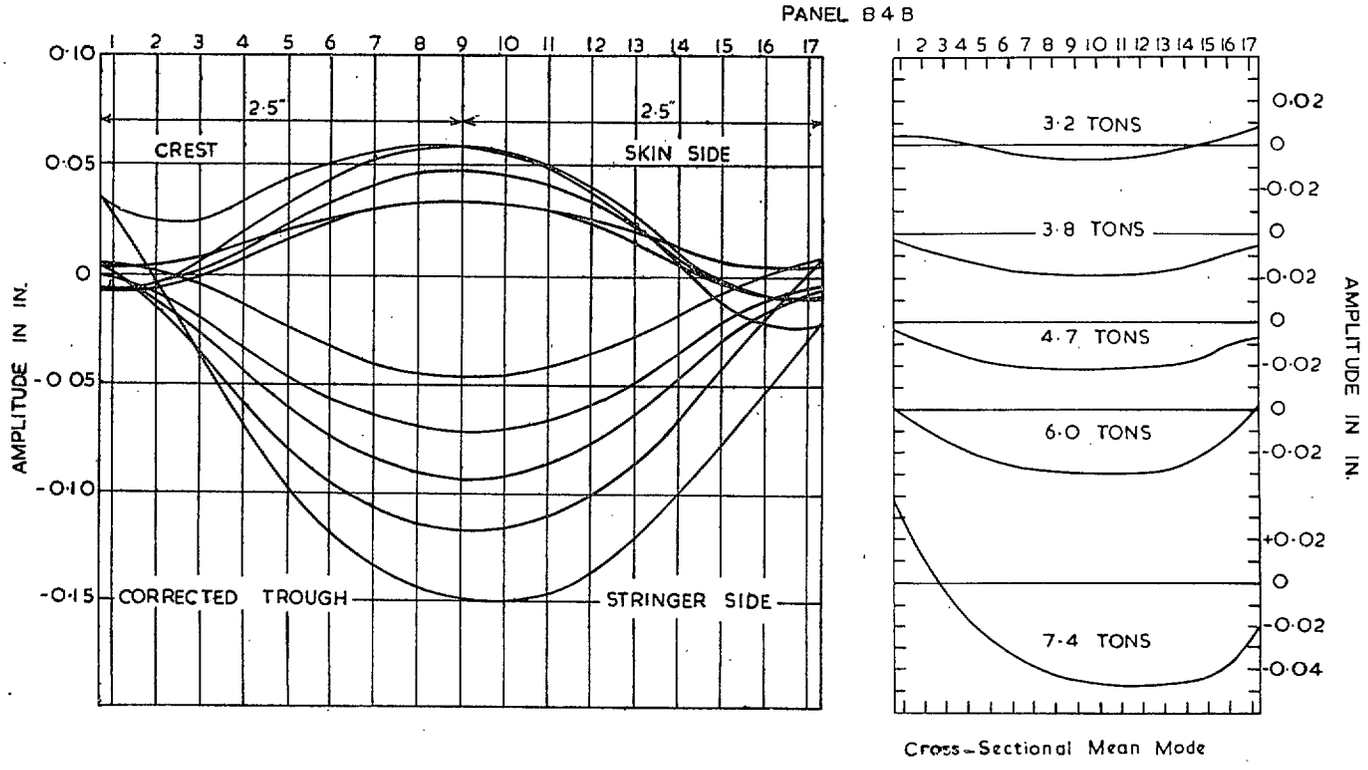

FIG. 43. Readings obtained on test of cross-sectional buckle shape.

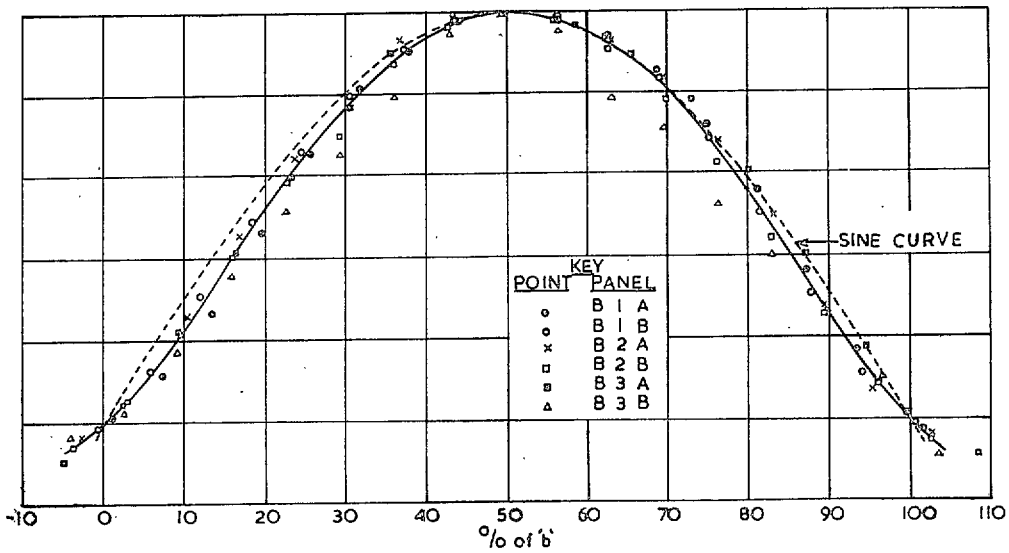

FIG. 44. Buckle shape at buckling strain.

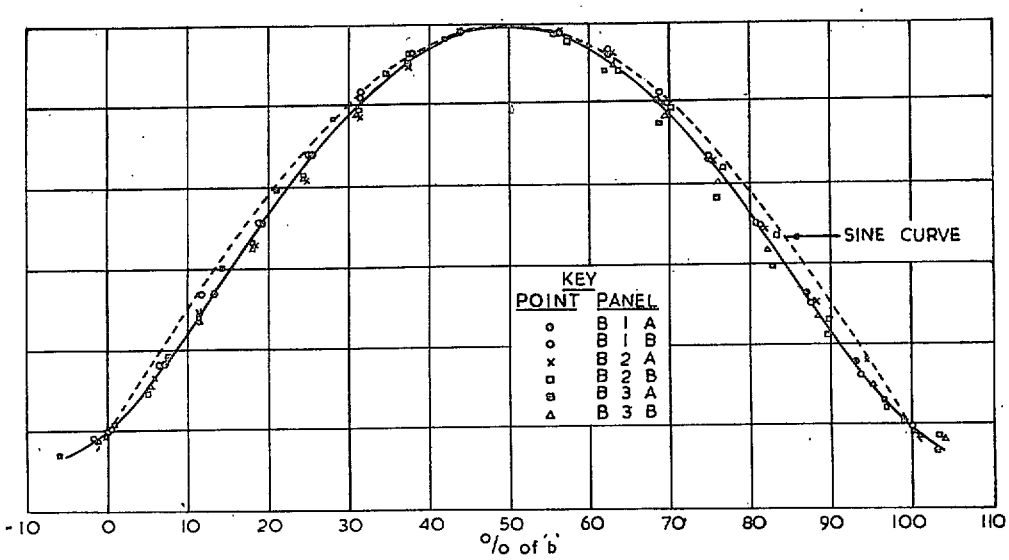

FIG. 45. Buckle shape at one-and-a-quarter times buckling strain.

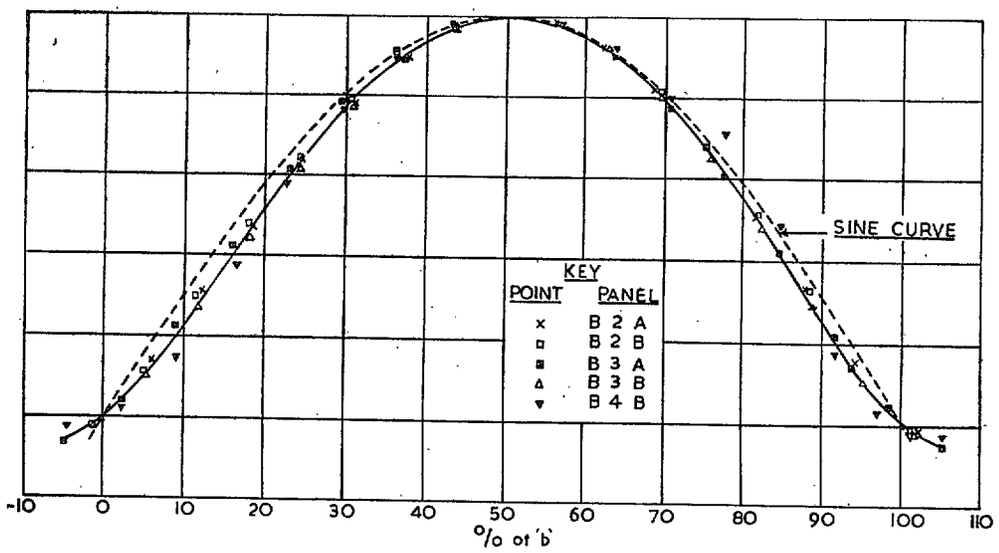

FIG. 46. Buckle shape at one-and-a-half times buckling strain.

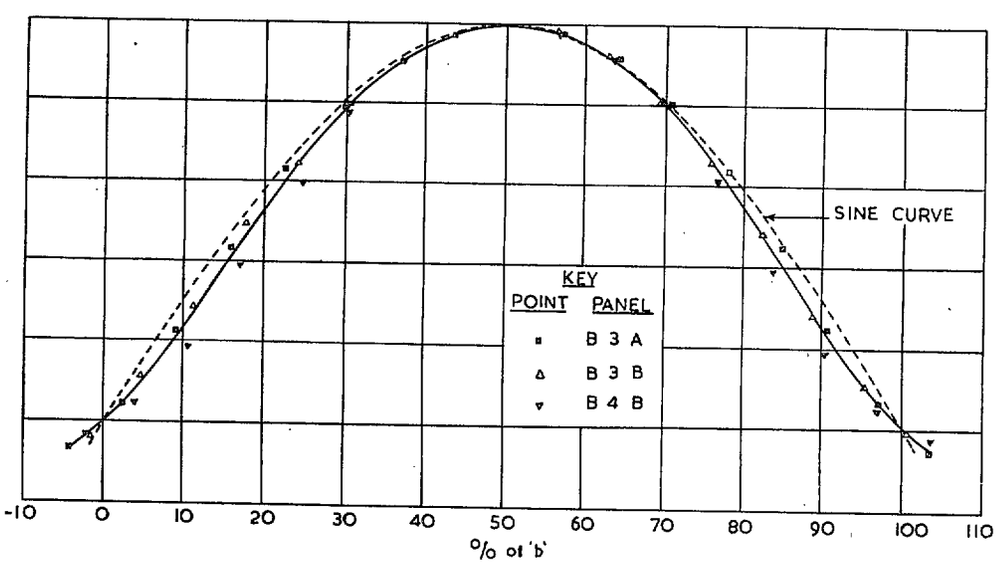

FIG. 47. Buckle shape at twice buckling strain.

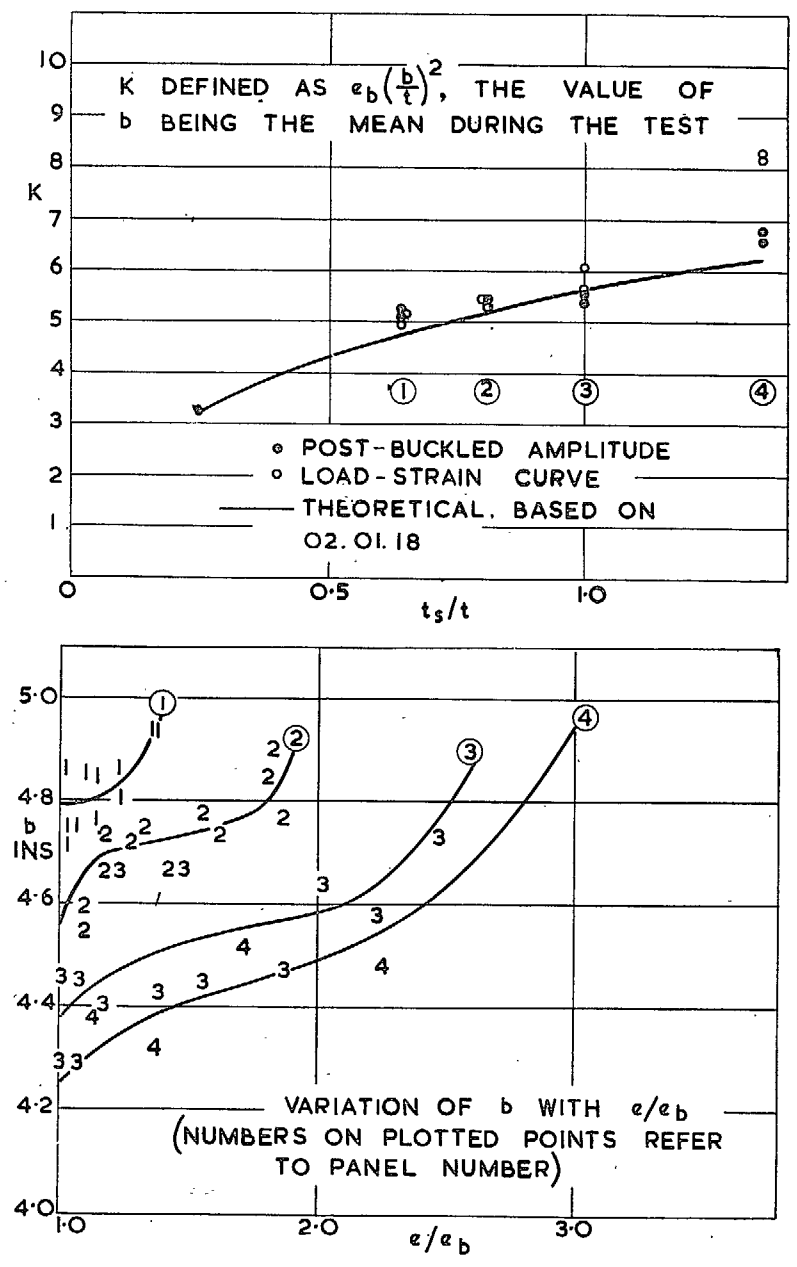

FIG. 48. Variation of K.
D.T.D. 646 panels with stringer edge supports.

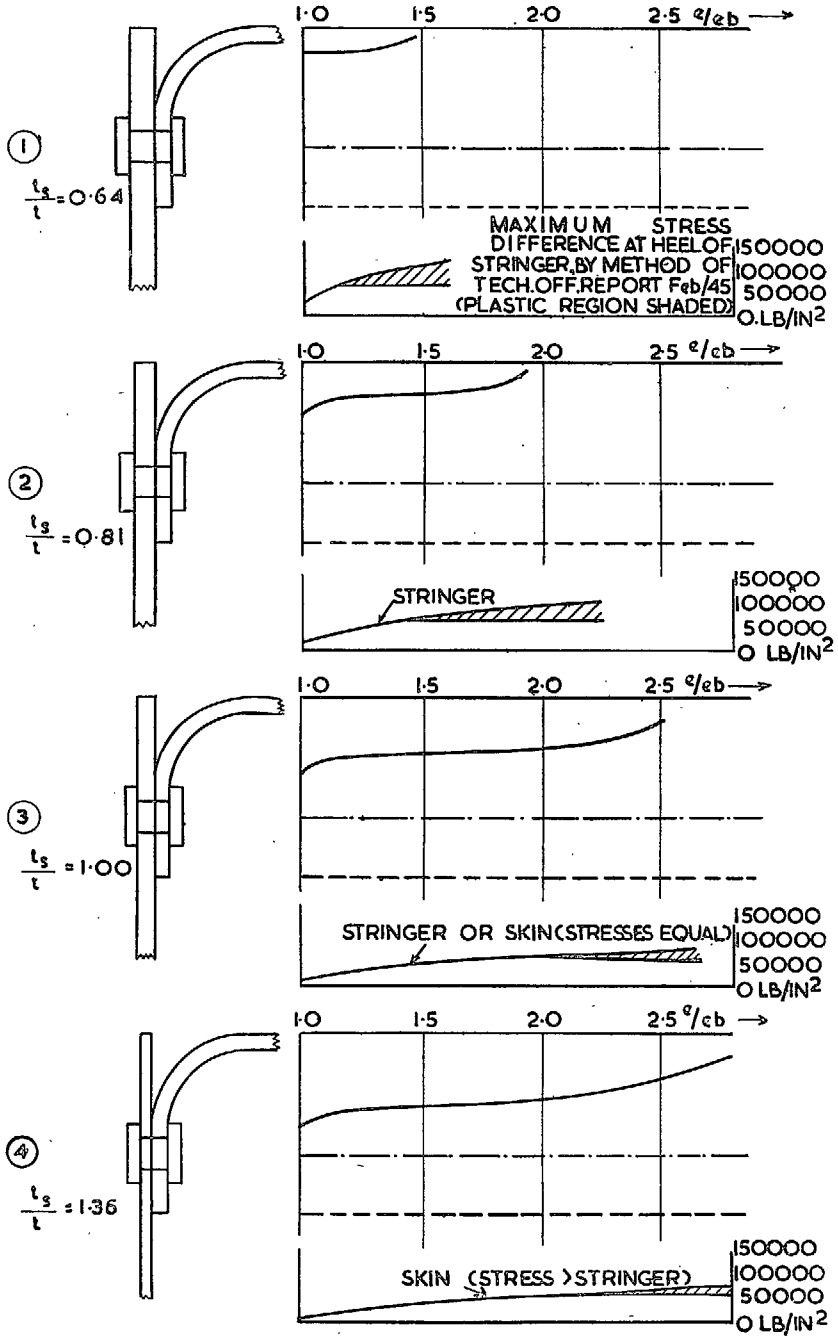

FIG. 49. Location of skin nodal line on stringer flange.

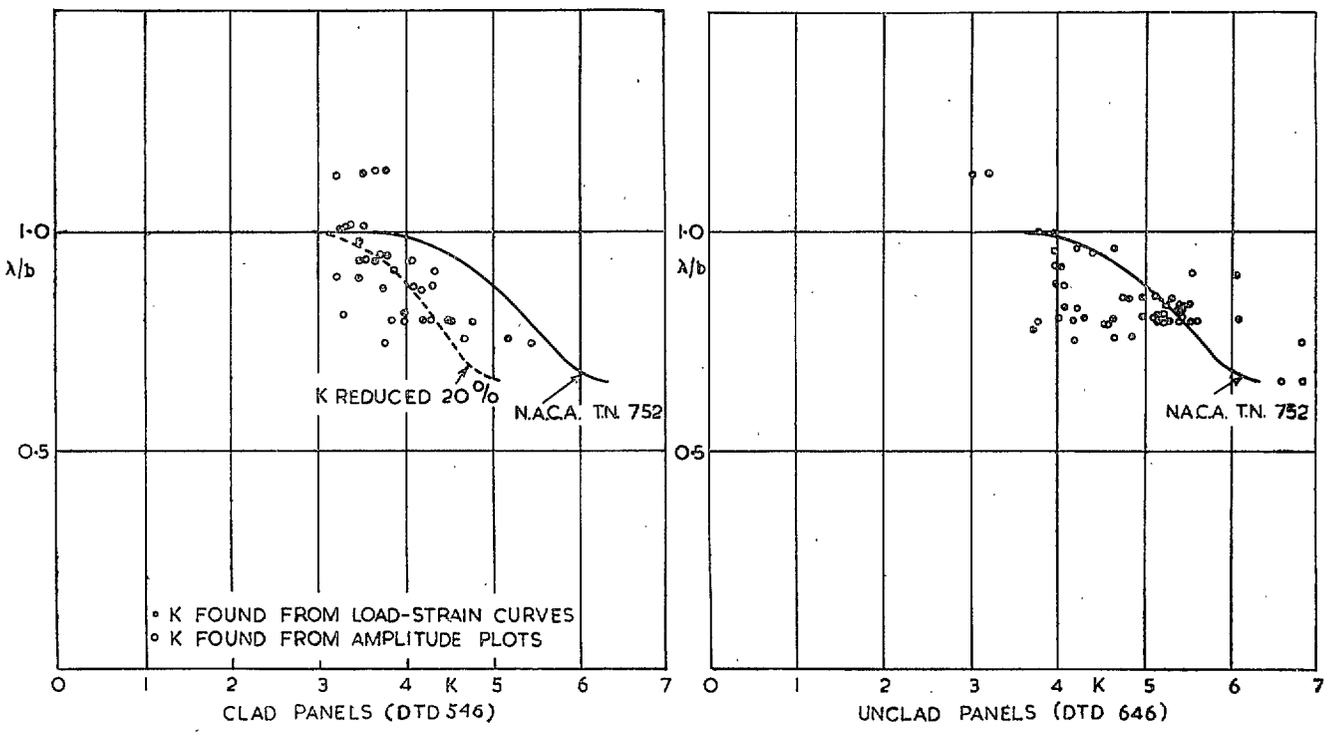

FIG. 50. Comparison of K and λ/b with results of N.A.C.A. T.N. 752.

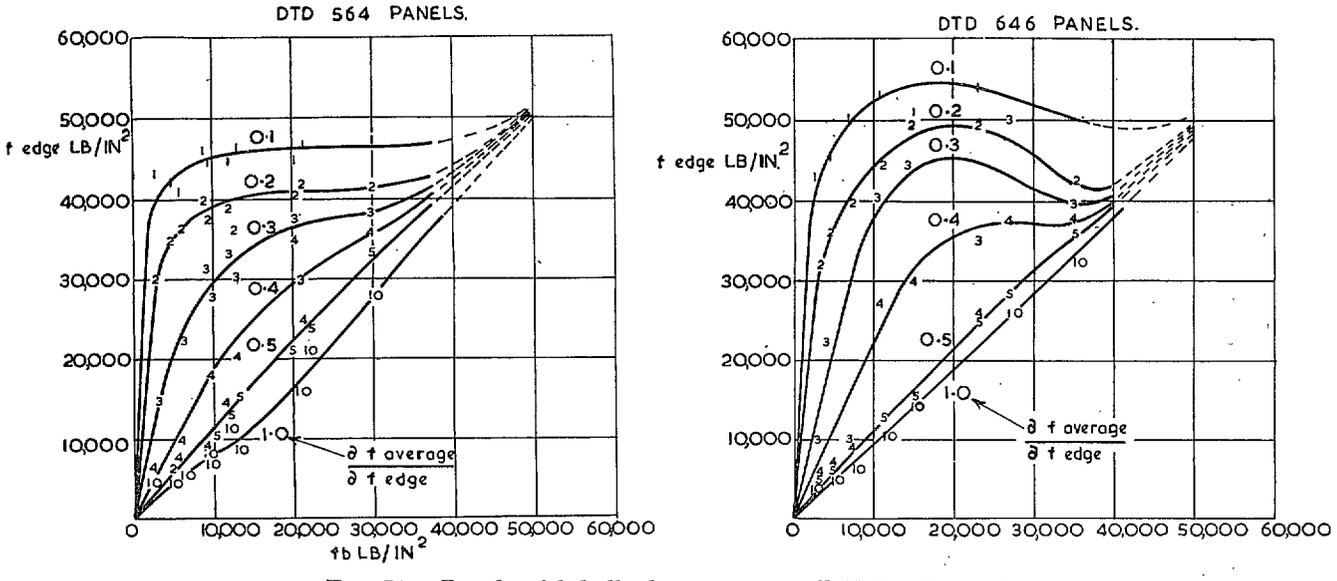

FIG. 51. Panels with ball edge supports. D.T.D. 546 panels.

Note: Numbers on plotted points give ten times the value of $df_{\text{average}}/df_{\text{edge}}$.

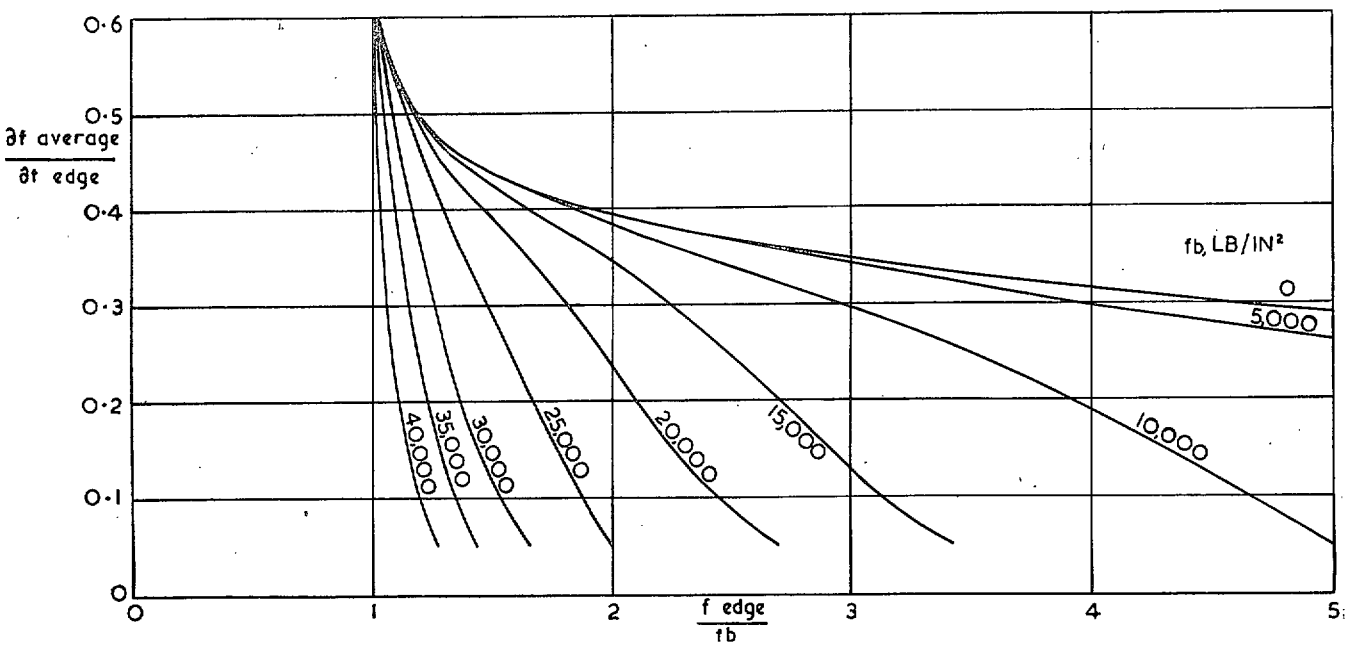

FIG. 52. D.T.D. 546 panels with ball edge supports. Curves of $\partial f_{\text{average}}/\partial f_{\text{edge}}$.

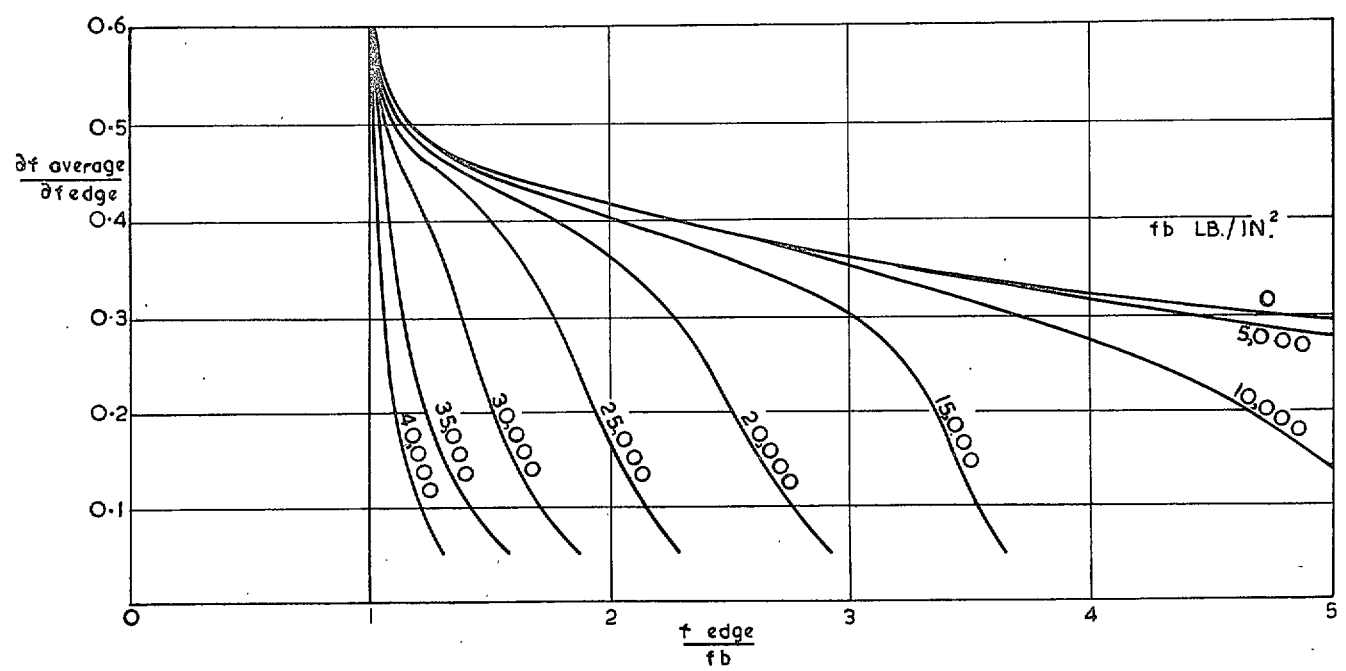

FIG. 53. D.T.D. 646 panels with ball edge supports. Curves of $\partial f_{\text{average}}/\partial f_{\text{edge}}$.
Note: Up to 52,000 lb/in.², $e = 0{\cdot}935 \times 10^{-7} f_{\text{edge}}$.

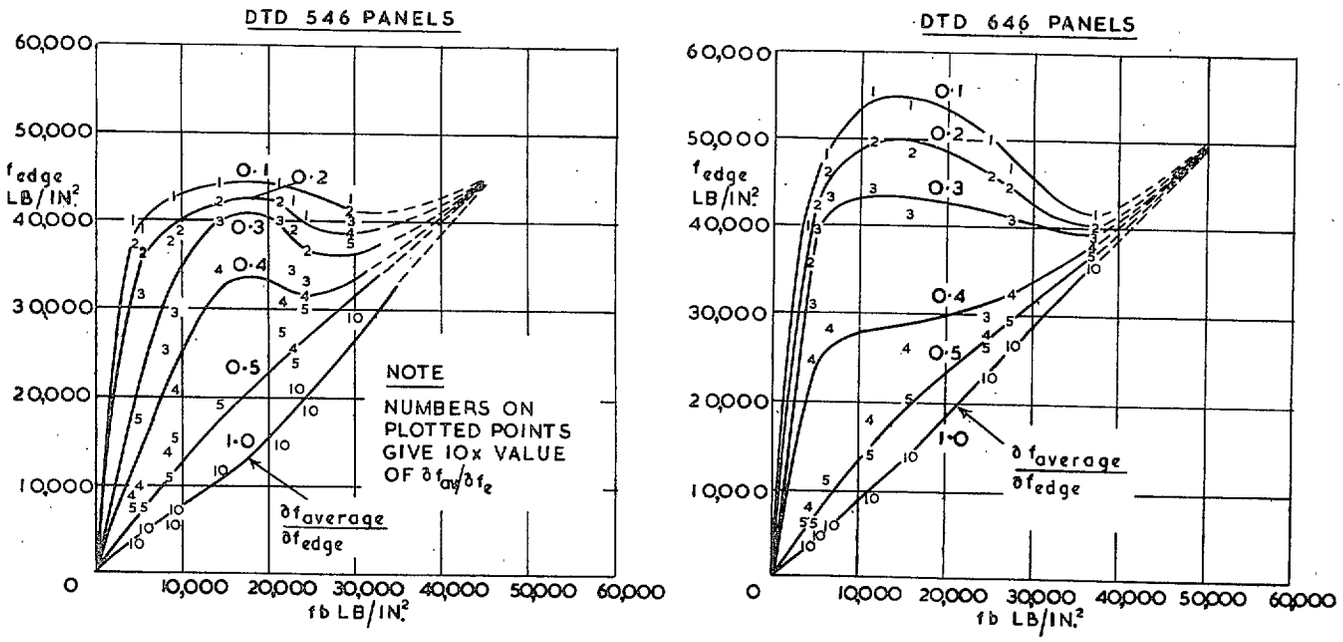

FIG. 54. Panels with roller edge supports. D.T.D. 546 panels.

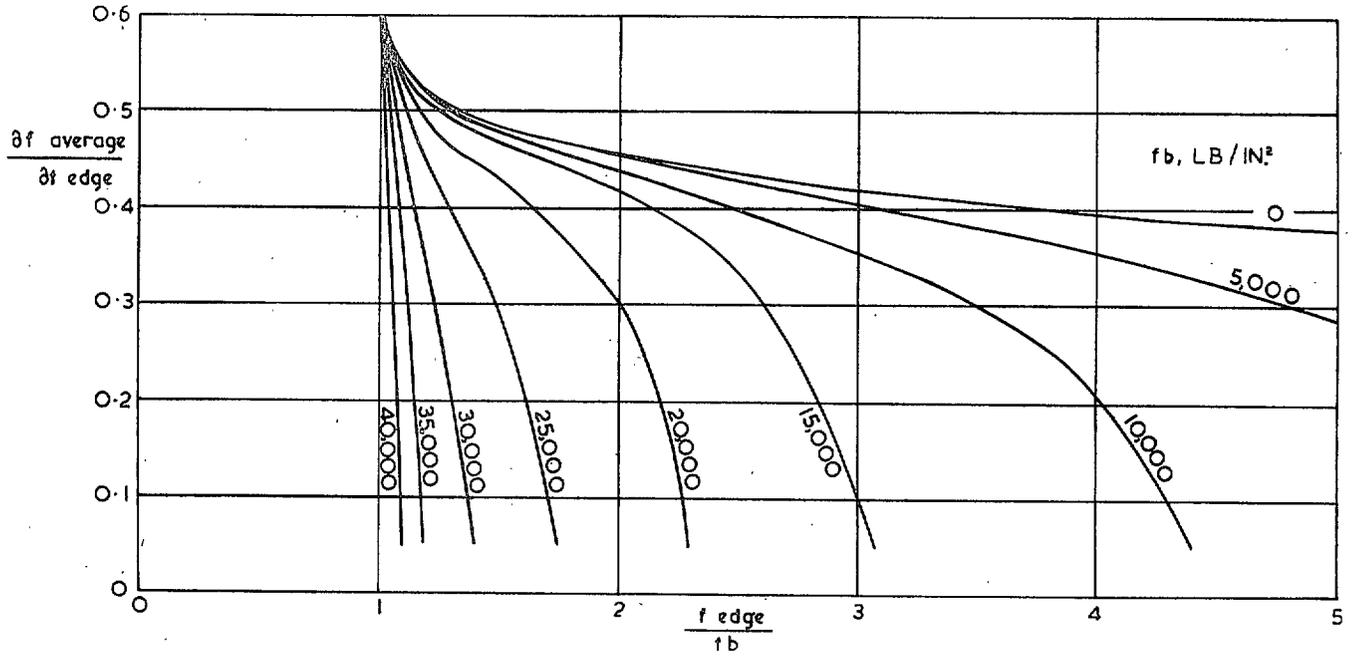

FIG. 55. D.T.D. 546 Panels with roller edge supports. Curves of $\partial f_{average}/\partial f_{edge}$.

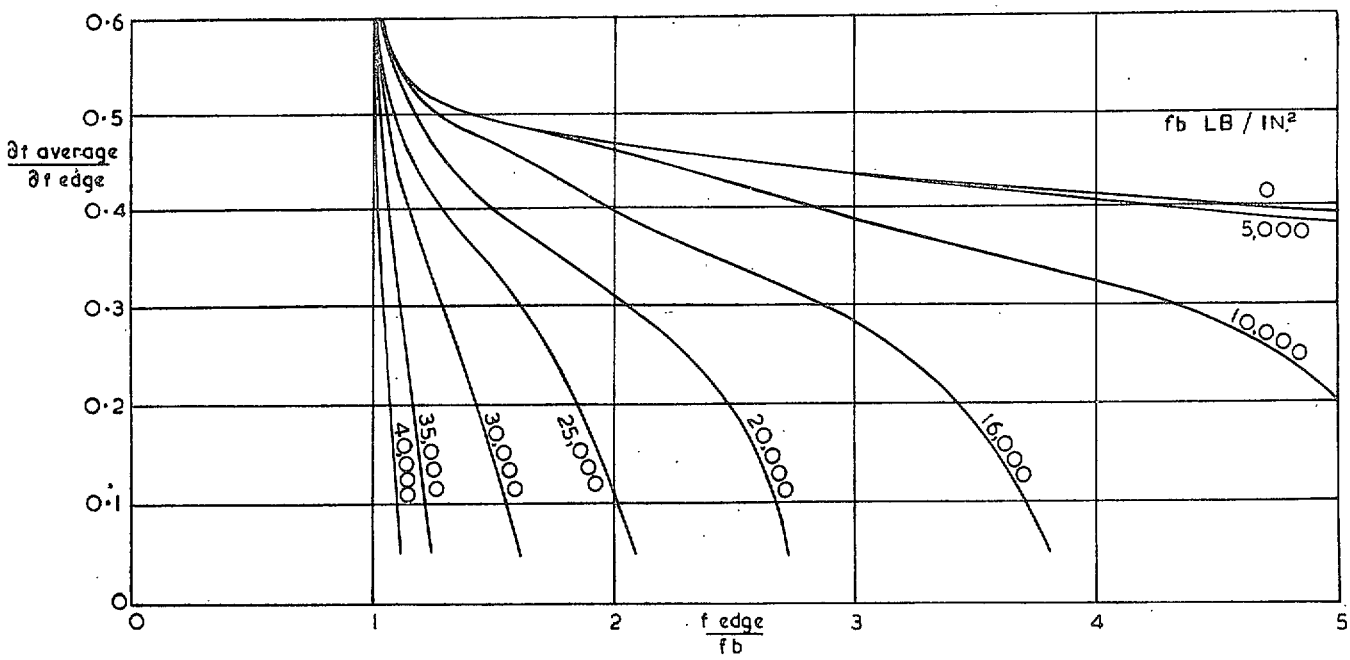

FIG. 56. D.T.D. 646 panels with roller edge supports. Curves of $\partial f_{average}/\partial f_{edge}$.

Note: Up to 52,000 lb/in.², $e = 0{\cdot}935 \times 10^{-7} f_{edge}$.

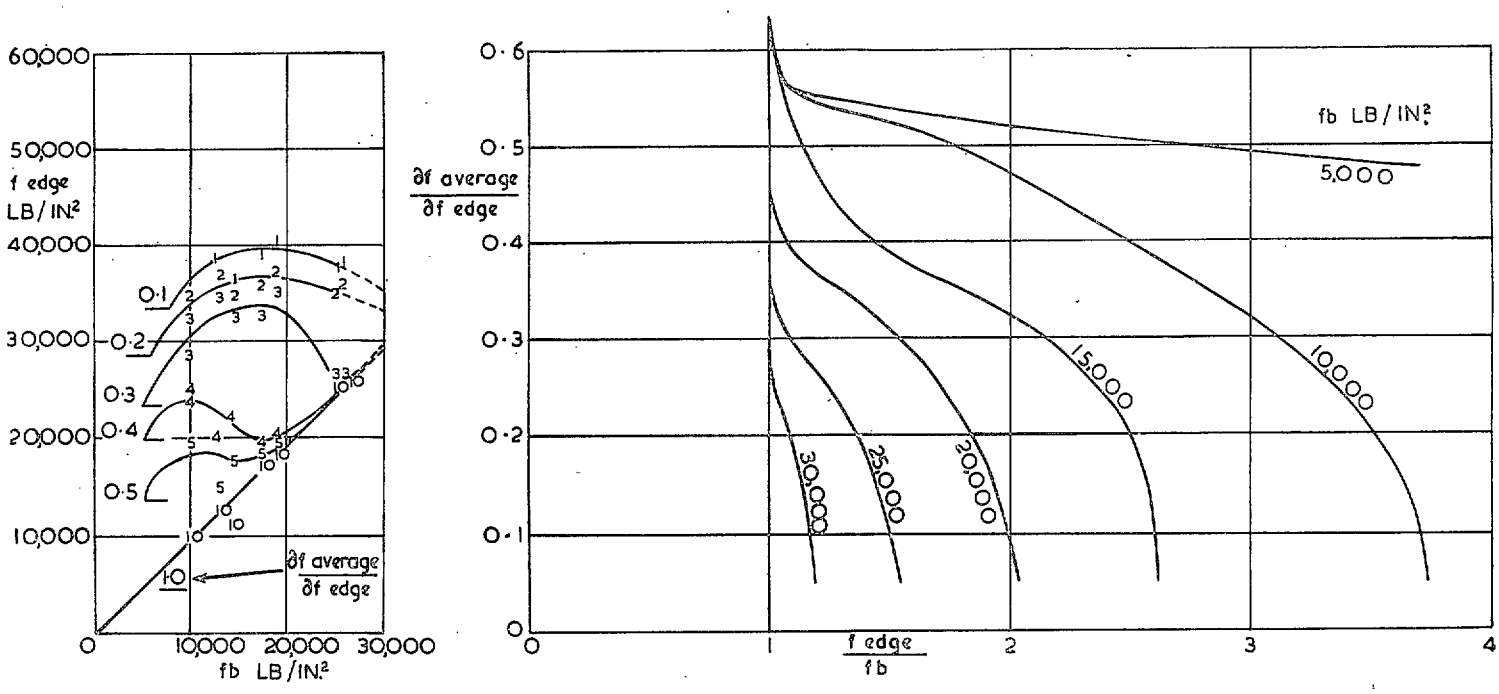

FIG. 57. D.T.D. 646 panels with stringer edge supports. Apparent skin $\partial f_{average}/\partial f_{edge}$ curves.

Note: Up to 52,000 lb/in.², $e = 0{\cdot}935 \times 10^{-7} f_{edge}$.

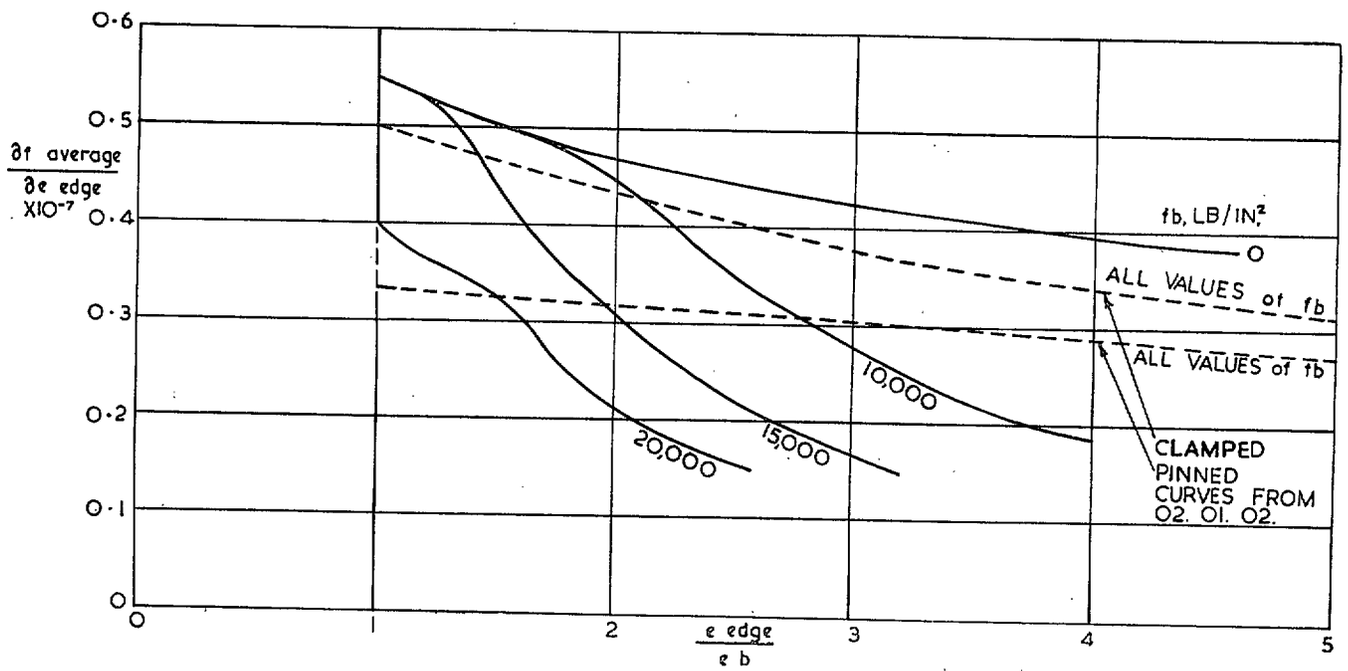

FIG. 58. Curves of $\partial f_{\text{average}}/\partial e_{\text{edge}}$ from Data Sheet 02.01.i (draft). 35–65 material. Practical edge conditions.

(25590) Wt. 16-680 K9 8/53 F. M. & S.

PRINTED IN GREAT BRITAIN

R. & M. No. 2652
(11,036, 11,037, 11,038)
A.R.C. Technical Report

Publications of the Aeronautical Research Council

ANNUAL TECHNICAL REPORTS OF THE AERONAUTICAL RESEARCH COUNCIL (BOUND VOLUMES)

1936 Vol. I. Aerodynamics General, Performance, Airscrews, Flutter and Spinning. 40*s.* (40*s.* 9*d.*)
Vol. II. Stability and Control, Structures, Seaplanes, Engines, etc. 50*s.* (50*s.* 10*d.*)

1937 Vol. I. Aerodynamics General, Performance, Airscrews, Flutter and Spinning. 40*s.* (40*s.* 10*d.*)
Vol. II. Stability and Control, Structures, Seaplanes, Engines, etc. 60*s.* (61*s.*)

1938 Vol. I. Aerodynamics General, Performance, Airscrews. 50*s.* (51*s.*)
Vol. II. Stability and Control, Flutter, Structures, Seaplanes, Wind Tunnels, Materials. 30*s.* (30*s.* 9*d.*)

1939 Vol. I. Aerodynamics General, Performance, Airscrews, Engines. 50*s.* (50*s.* 11*d.*)
Vol. II. Stability and Control, Flutter and Vibration, Instruments, Structures, Seaplanes, etc. 63*s.* (64*s.* 2*d.*)

1940 Aero and Hydrodynamics, Aerofoils, Airscrews, Engines, Flutter, Icing, Stability and Control, Structures, and a miscellaneous section. 50*s.* (51*s.*)

1941 Aero and Hydrodynamics, Aerofoils, Airscrews, Engines, Flutter, Stability and Control, Structures. 63*s.* (64*s.* 2*d.*)

1942 Vol. I. Aero and Hydrodynamics, Aerofoils, Airscrews, Engines. 75*s.* (76*s.* 3*d.*)
Vol. II. Noise, Parachutes, Stability and Control, Structures, Vibration, Wind Tunnels. 47*s.* 6*d.* (48*s.* 5*d.*)

1943 Vol. I. (In the press.)
Vol. II. (In the press.)

ANNUAL REPORTS OF THE AERONAUTICAL RESEARCH COUNCIL—

1933-34	1*s.* 6*d.* (1*s.* 8*d.*)	1937	2*s.* (2*s.* 2*d.*)
1934-35	1*s.* 6*d.* (1*s.* 8*d.*)	1938	1*s.* 6*d.* (1*s.* 8*d.*)
April 1, 1935 to Dec. 31, 1936.	4*s.* (4*s.* 4*d.*)	1939-48	3*s.* (3*s.* 2*d.*)

INDEX TO ALL REPORTS AND MEMORANDA PUBLISHED IN THE ANNUAL TECHNICAL REPORTS AND SEPARATELY—

April, 1950 - - - - - R. & M. No. 2600. 2*s.* 6*d.* (2*s.* 7½*d.*)

AUTHOR INDEX TO ALL REPORTS AND MEMORANDA OF THE AERONAUTICAL RESEARCH COUNCIL—

1909-1949 - - - - - R. & M. No. 2570. 15*s.* (15*s.* 3*d.*)

INDEXES TO THE TECHNICAL REPORTS OF THE AERONAUTICAL RESEARCH COUNCIL—

December 1, 1936—June 30, 1939.	R. & M. No. 1850.	1*s.* 3*d.* (1*s.* 4½*d.*)
July 1, 1939—June 30, 1945.	R. & M. No. 1950.	1*s.* (1*s.* 1½*d.*)
July 1, 1945—June 30, 1946.	R. & M. No. 2050.	1*s.* (1*s.* 1½*d.*)
July 1, 1946—December 31, 1946.	R. & M. No. 2150.	1*s.* 3*d.* (1*s.* 4½*d.*)
January 1, 1947—June 30, 1947.	R. & M. No. 2250.	1*s.* 3*d.* (1*s.* 4½*d.*)
July, 1951. - - - - -	R. & M. No. 2350.	1*s.* 9*d.* (1*s.* 10½*d.*)

Prices in brackets include postage.

Obtainable from

HER MAJESTY'S STATIONERY OFFICE

York House, Kingsway, London, W.C.2; 423 Oxford Street, London, W.1 (Post Orders: P.O. Box 569, London, S.E.1); 13a Castle Street, Edinburgh 2; 39 King Street, Manchester 2; 2 Edmund Street, Birmingham 3; 1 St. Andrew's Crescent, Cardiff; Tower Lane, Bristol 1; 80 Chichester Street, Belfast or through any bookseller.

S.O. Code No. 23-2652